PB91-212548

REPORT NO.
UCB/EERC-88/13
NOVEMBER 1988

EARTHQUAKE ENGINEERING RESEARCH CENTER

IMPLICATIONS OF RECORDED EARTHQUAKE GROUND MOTIONS ON SEISMIC DESIGN OF BUILDING STRUCTURES

by

CHIA-MING UANG
VITELMO V. BERTERO

Report to the National Science Foundation

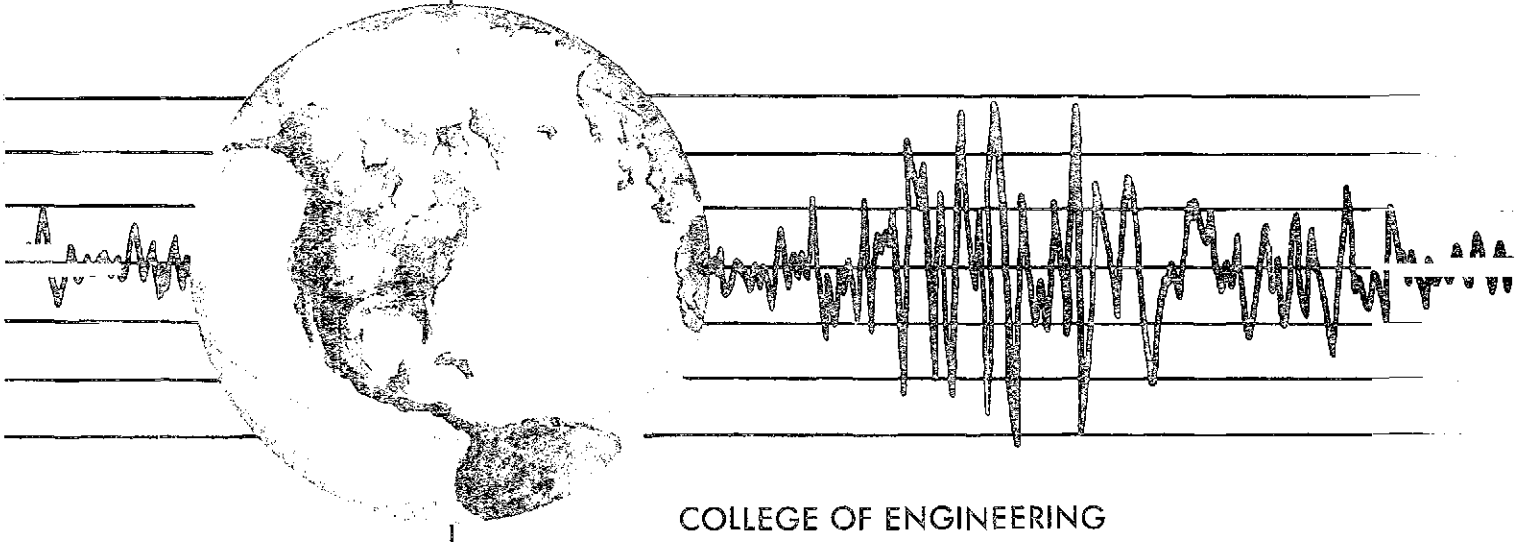

COLLEGE OF ENGINEERING

UNIVERSITY OF CALIFORNIA AT BERKELEY

For sale by the National Technical Information Service, U.S. Department of Commerce, Springfield, Virginia 22161

See back of report for up to date listing of EERC reports.

DISCLAIMER

PB91-212548

Implications of Recorded Earthquake Ground Motions on Seismic Design of Building Structures

California Univ., Richmond

Prepared for:

National Science Foundation, Washington, DC

Nov 88

PB91-212548

REPORT NO.
UCB/EERC-88/13
NOVEMBER 1988

EARTHQUAKE ENGINEERING RESEARCH CENTER

IMPLICATIONS OF RECORDED EARTHQUAKE GROUND MOTIONS ON SEISMIC DESIGN OF BUILDING STRUCTURES

by

CHIA-MING UANG
VITELMO V. BERTERO

Report to the National Science Foundation

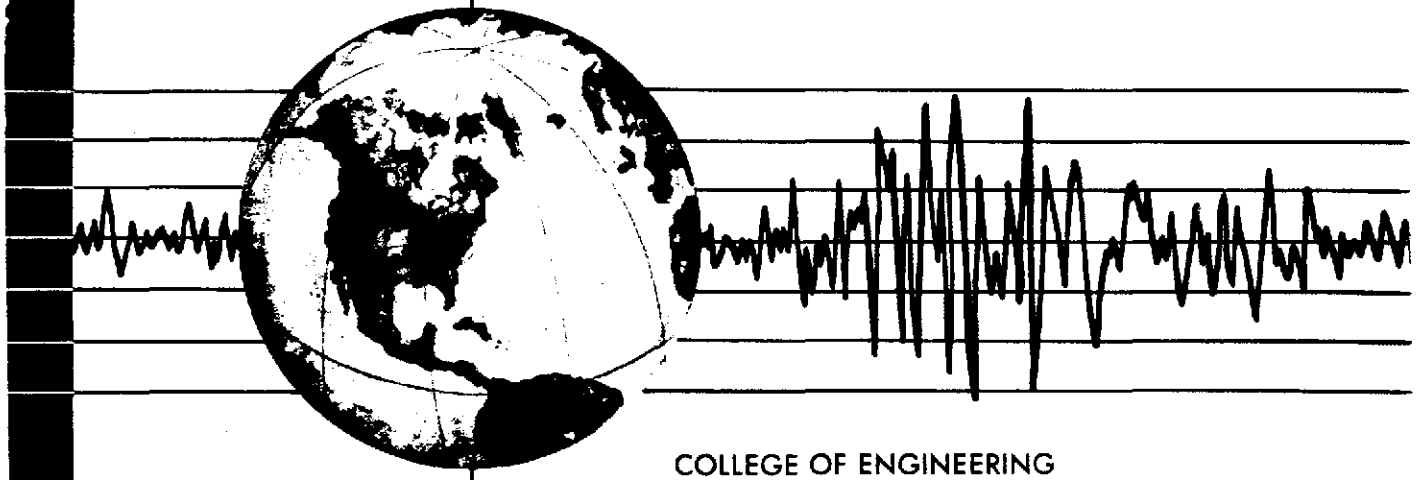

COLLEGE OF ENGINEERING

UNIVERSITY OF CALIFORNIA AT BERKELEY

For sale by the National Technical Information Service, U.S. Department of Commerce, Springfield, Virginia 22161

See back of report for up to date listing of EERC reports.

50272-101

REPORT DOCUMENTATION PAGE	1. REPORT NO. NSF/ENG-88049	2.	3. PB91-212548

4. Title and Subtitle

Implications of Recorded Earthquake Ground Motions on Seismic Design of Building Structures

5. Report Date November 1988

6.

7. Author(s)

C-M Uang and V.V. Bertero

8. Performing Organization Rept. No. UCB/EERC-88/13

9. Performing Organization Name and Address

Earthquake Engineering Research Center
University of California, Berkeley
1301 S 46th St.
Richmond, CA 94804

10. Project/Task/Work Unit No.

11. Contract(C) or Grant(G) No.

(C)

(G) ECE-8610870

12. Sponsoring Organization Name and Address

National Science Foundation
1800 G. St. NW
Washington, DC 20550

13. Type of Report & Period Covered

14.

15. Supplementary Notes

16. Abstract (Limit: 200 words)

This report presents the results obtained in studies that have been conducted to: (i) assess the reliability of the parameters that have been used to identify the damage potential of an earthquake at a given site; (ii) evaluate the reliability of ductility based earthquake-resistant design as the only engineering parameter to reflect the design criteria, the acceptable level or degree of damage and to reduce the yielding strength required on the basis of linear elastic response of structures to critical ground shakings; (iii) examine the role and importance of the main response quantities which include drift index, input energy, cumulative displacement ductility ratio, and number of yielding reversals in the formulation of design criteria; (iv) estimate the required overstrength for buildings that are designed to satisfy the ATC minimum required seismic forces and discuss their significance in relation to the response modification factor R; and (v) examine the actual seismic demands of structures that have been designed in accordance with the ATC recommended design provisions. Eight earthquake ground motions, including three recently recorded motions that caused significant building damage, were considered.

17. Document Analysis a. Descriptors

b. Identifiers/Open-Ended Terms

c. COSATI Field/Group

18. Availability Statement: Release Unlimited

19. Security Class (This Report) unclassified

20. Security Class (This Page) unclassified

21. No. of Pages 114

22. Price

(See ANSI-Z39.18) See Instructions on Reverse

OPTIONAL FORM 272 (4-77)
(Formerly NTIS-35)
Department of Commerce

IMPLICATIONS OF RECORDED EARTHQUAKE GROUND MOTIONS ON SEISMIC DESIGN OF BUILDING STRUCTURES

Chia-Ming Uang

Assistant Professor

Department of Civil Engineering

Northeastern University

360 Huntington Avenue

Boston, MA 02115

Vitelmo V. Bertero

Professor

Department of Civil Engineering

University of California, Berkeley

Berkeley, CA 94720

Report No. UCB/EERC-88/13

Earthquake Engineering Research Center

College of Engineering

University of California

Berkeley, California

November 1988

ABSTRACT

This report presents the results obtained in studies that have been conducted to: (i) assess the reliability of the parameters that have been used to identify the damage potential of an earthquake at a given site; (ii) evaluate the reliability of ductility based earthquake-resistant design as the only engineering parameter to reflect the design criteria, the acceptable level or degree of damage and to reduce the yielding strength required on the basis of linear elastic response of structures to critical ground shakings; (iii) examine the role and importance of the main response quantities which include drift index, input energy, hysteretic energy, cumulative displacement ductility ratio, and number of yielding reversals in the formulation of design criteria; (iv) estimate the required overstrength for buildings that are designed to satisfy the ATC minimum required seismic forces and discuss their significance in relation to the response modification factor R; and (v) examine the actual seismic demands of structures that have been designed in accordance with the ATC recommended design provisions. Eight earthquake ground motions, including three recently recorded motions that caused significant building damage, were considered.

The major conclusions drawn from these studies are as follows:

(1) Parameters used to specify the damage potential of an earthquake should take into consideration the effects of amplitude, frequency characteristics, and strong motion duration. The destructiveness factor P_D proposed by Araya *et al.* considers all these parameters; this factor appears to be the best in reflecting the severe building damage observed after the September 19, 1985 Mexico City earthquake.

(2) The damage potential of an earthquake may be underestimated by just considering independently the recorded components of the ground motion.

(3) The overstrength required, for constant displacement ductility, above the minimum strength specified by ATC for all of the ground motions considered in this study is not constant. The required overstrength varies with fundamental period; for several of the ground motions with small fundamental periods, a very large overstrength is required in order to survive the earthquake ground motion.

(4) For a constant displacement ductility ratio, the drift index calculated by assuming uniform inter-story drift over the height of a building tends to be critical for buildings with small fundamental periods. If a soft first story were to occur, the drift index becomes more critical as the building's fundamental period increases.

(5) Inelastic seismic resistance response spectra derived from linear elastic design response spectra for a constant displacement ductility ratio cannot reflect the high energy demand on buildings subjected to earthquakes with a long duration of strong motion. Using linear elastic pseudo-velocity response spectra may significantly underestimate the true input energy to the structures.

(6) The lack of reliable damage criteria imposes severe limitations on developing rational inelastic design response spectra. There is an urgent need to establish such criteria for all types of structural members with different materials and, then, for all types of structural systems.

ACKNOWLEDGEMENTS

This research is partially sponsored by the National Science Foundation, Grant No. CES-8810563 to the first author and Grant No. ECE-8610870 to the second author. Any opinions, discussions, findings, conclusions, and recommendations are those of the authors and do not necessarily reflect the views of the sponsor.

The authors wish to thank Dr. Mo-Jiann Huang of the Division of Mines and Geology, California Department of Conservation, who provided the processed records of the 1986 San Salvador Earthquake and Dr. Dennis Bernal of the Department of Civil Engineering, Northeastern University, who kindly reviewed the results presented in Chapter 3.

Dr. Andrew S. Whittaker reviewed this report on a number of occasions and his contributions are gratefully acknowledged. Dr. Beverley Bolt assisted in the editing of this report — her assistance is also gratefully appreciated.

TABLE OF CONTENTS

LIST OF TABLES

LIST OF FIGURES

I. INTRODUCTION

1.1. Statement of Problems

In earthquake-resistant design of building structures, the primary concern is to avoid collapse or structural and nonstructural damage that may jeopardize human lives during rare but severe ground shaking.[3] Although this design philosophy is well established and is generally accepted, its quantification in the form of design specifications is not an easy task. In particular, the difficulty in estimating (i) earthquake input, (ii) demand (strength, stiffness, and energy dissipation) on the structure, and (iii) supplied resistance to the structure, complicates the earthquake-resistant design of building structures.[14]

Earthquake ground motions that may occur at a given site are highly unpredictable. Recent recorded earthquakes, especially the September 19, 1985 Mexico City earthquake, demonstrate clearly that the data base of previously recorded earthquakes is not nearly adequate; an earthquake with frequency content, duration, and amplitude characteristics far beyond those previously recorded may strike our urban areas.

Since different earthquake ground motions cause different degrees of damage to engineered structures, it is logical for scientists and engineers to quantify their severity and damage potential. Although the Richter scale can be used to measure the size or the amount of total energy released during an earthquake, the Richter magnitude cannot be used to estimate damage away from the epicenter.[17, 25] The Modified Mercalli Intensity (MMI) is a subjective (as opposed to instrumental) index used to describe damage at a specific site. However, since the degree of earthquake damage in a building depends on design methods, construction materials, construction methods and so on, indiscriminate use of the MMI may be misleading.

The design of strong motion accelerographs in the United States in 1932 and their subsequent improvement has facilitated the collection of a large number of strong motion records.[26] On the basis of these instrumental records, researchers have proposed different parameters to express, usually through a simple index, the damage potential of the recorded ground motion to

structures located in the vicinity of the recording site. These parameters range from a simple instrumental peak value to a value resulting from a very complicated mathematical derivation. Questions that then arise include: how reliable are these parameters and how well do they correlate with the damage observed after an earthquake?

A structure may fail in different ways, depending upon the interaction between the dynamic characteristics of the external excitation and those of the structure itself. Therefore it is necessary to know: (i) what the dynamic characteristics that define the damage potential of a given ground motion are; (ii) what constitutes acceptable damage, that is, what are the damage criteria; and (iii) what are the desired dynamic characteristics of a building that will permit it to resist satisfactorily the demands imposed by seismic effect in combination with other loadings. The damage potential of the possible ground motions and damage criteria for both the structural members and the entire structural system are needed to establish reliable earthquake-resistant design criteria.

At present, displacement ductility ratio is probably the most widely used parameter to limit damage and also to express damage in terms of earthquake-resistant design criteria. The procedure for constructing inelastic design response spectra for a given ductility ratio is well established [32] and has been adopted by most current earthquake-resistant building codes. However, there are other response quantities, such as cumulative ductility, number of yielding reversals, incremental collapse, low-cycle fatigue, energy dissipation capacity and so on, which may also play an important role in structural failure during the earthquake.[5, 15, 22, 28, 29, 31] Unfortunately, very few studies have been performed to ascertain which are the most reliable parameters for formulating earthquake-resistant design criteria.

Current building codes[1-3] implicitly consider the overstrength of buildings in constructing inelastic design response spectra. Structural overstrength is inherent in the design process and its role in a building's surviving severe ground shaking has been demonstrated in recent experimental studies.[13, 39, 42] Although the designer does not quantify this overstrength and its contribution is not explicitly considered in formulating the seismic design forces, it is of the utmost importance to quantify the level of overstrength required for buildings designed to just satisfy the minimum strength requirements of current seismic regulations. This required overstrength should be compared with the actual overstrength of buildings that have been designed and

constructed in accordance with these building regulations.

1.2. Objectives and Scope

The objectives of the studies reported here are to: (i) assess the reliability of various parameters that have been used to identify the damage potential of an earthquake at a given site; (ii) evaluate the reliability of ductility based earthquake-resistant design (that is, of using the displacement ductility ratio as the engineering parameter to reflect the level or degree of damage and to develop design response spectra from linear elastic spectra); (iii) examine the role and importance of the other response quantities that include drift index, input energy, hysteretic energy, cumulative displacement ductility ratio, and number of yielding reversals in the formulation of design criteria; (iv) estimate the required overstrength for buildings that are designed to satisfy the ATC minimum required seismic forces and to discuss its significance in relation to the response modification factor R; and (v) examine the actual seismic demands of structures that have been designed in accordance with the ATC recommended design provisions.

Eight earthquakes were selected for this study. These earthquakes cover a wide range of characteristics with different amplitudes, durations, frequency content, epicentral distances, soil types, and so on. Three recently recorded destructive earthquakes — the March 3, 1985 Chilean earthquake, the September 19, 1985 Mexican earthquake, and the October 10, 1986 San Salvador earthquake — were included to cover the wide variability of the data base of earthquake records.

II. EARTHQUAKE GROUND MOTION CHARACTERISTICS AND DAMAGE POTENTIAL

2.1. Introductory Remarks

The parameters used to characterize the severity or damage potential of earthquake ground motion can be classified into the following six groups: [36]

(1) Peak instrumental values;

(2) Integration of records in the time domain;

(3) Frequency content by Fourier transforms or frequency characteristics by the zero-crossing method;[37]

(4) Parametric integration of the equation of motion of a single-degree-of-freedom (SDOF) system and subsequent analysis of the results;

(5) Parametric integration of the equation of motion of a SDOF system and subsequent integration in the frequency domain of intermediate results (e.g., linear elastic pseudo-velocity response spectra.)

(6) Parameters that combine the results derived from some of the above groups.

Some important parameters proposed by previous researchers in each group are discussed in the following section. The reliability of using these parameters is then evaluated.

Eight earthquake ground motions (Table 2.1) are used for this study; the selected records cover a broad range of the following main characteristics: Richter magnitude M_L, focal depth, epicentral distance, and geological condition at the site. Figures 2.1 through 2.8 show the acceleration time histories, Fourier amplitude spectra, and linear elastic response spectra for the eight earthquakes. Except for the San Salvador and Miyagi-Ken-Oki earthquakes, the records were obtained at free field stations and not at the foundation of a building. The importance of this observation will be discussed later.

2.2. Parameters Used to Characterize Earthquake Ground Motion Intensity

2.2.1. Group 1 — This group includes the following parameters:

(1) Peak ground acceleration (*PGA*);

(2) Peak ground velocity;

(3) Peak ground displacement.

The *PGA* of each record is listed in Table 2.2. Because it is easy to use and because the inertia forces depend directly on acceleration, peak ground acceleration is the parameter most widely used to describe the intensity and damage potential of an earthquake at a given site. The fact that peak ground acceleration is a poor parameter for this purpose has already been pointed out by many researchers, because the peak instrumental value might be associated with a short impulse of very high frequency. Peak ground acceleration may also be distorted by local irregular surface topography and other factors such as interaction with the response of large nearby structures. A well-known example is the Pacoima Dam record of the 1971 San Fernando earthquake (Fig. 2.5); its peak acceleration of 1.17g is possibly the largest peak acceleration ever recorded in the world. However, following deconvolution analysis,[34] the derived Pacoima Dam record (Fig. 2.6) had a peak acceleration of only 0.4g.

Structure damage observed after an earthquake has not been consistent with the associated peak ground acceleration recorded nearby. Although the peak ground acceleration of one of the horizontal components of the 1985 Mexico earthquake was only 0.17g, the extent of the building damage within that city was much more severe than that observed after the 1986 San Salvador earthquake with a peak ground acceleration exceeding 0.6g.

2.2.2. Group 2 — This group includes mean-square acceleration, root-mean-square acceleration, and Arias intensity.

Arias[8] defines an intensity coefficient as follows:

$$I_A = \frac{\pi}{2g} \int_0^{t_d} \ddot{v}_g^2(t) dt \tag{2.1}$$

where t_d and $\ddot{v}_g$ are the total duration and ground acceleration of an earthquake, respectively. The

coefficient I_A represents the sum of the total energies per unit mass stored in the oscillators of a population of undamped linear oscillators uniformly distributed as to their frequencies, at the end of the earthquake ground motion.[8] The calculated values of I_A are listed in Table 2.2, varying from 603 in/sec for CH to 97 in/sec for MX. The use of this parameter in conjunction with peak ground acceleration suggests that MX should have a much lower intensity than CH. Note that CH has a significantly higher value of I_A; this can be attributed to its long duration, high acceleration, and broad frequency content. Although MX has a long duration of strong motion shaking with respect to CH, it has very low *PGA* (0.17g versus 0.67g.)

Housner[24] proposed an "earthquake power" P_A as a measure of damage potential:

$$P_A = \frac{1}{t_{0.95}-t_{0.05}} \int_{t_{0.05}}^{t_{0.95}} \ddot{v}_g^2(t)\, dt \tag{2.2}$$

where $t_{0.05}$ and $t_{0.95}$ define the times at which 5 percent and 95 percent, respectively, of the value of the integration in Eq. 2.1 is achieved. P_A is basically the mean-square acceleration in the bracketed duration of $t_{0.05}$ and $t_{0.95}$. Because the integral in Eq. 2.2 is directly related to I_A, P_A is a measure of the average rate of energy input to the structure. The square root of P_A is defined as the root-mean-square acceleration in the bracketed duration:

$$RMS_A = \sqrt{P_A} = \left[\frac{1}{t_{0.95}-t_{0.05}} \int_{t_{0.05}}^{t_{0.95}} \ddot{v}_g^2(t)\, dt \right]^{1/2} . \tag{2.3}$$

The calculated P_A and RMS_A are shown in Table 2.2. The higher values of P_A and RMS_A suggest that short duration, impulsive earthquakes (SS, PD, DPD) should have a large damage potential.

2.2.3. Group 3 — The frequency content of an earthquake record can be identified by its Fourier transform:

$$F(\omega) = \int_0^{t_d} \ddot{v}_g\, e^{-i\omega\tau}\, d\tau = \int_0^{t_d} \ddot{v}_g\, (\cos\omega\tau - i\sin\omega\tau)\, d\tau . \tag{2.4}$$

The Fourier amplitude spectrum (*FAS*) is then expressed as:

$$FAS(\omega) = \left\{ \left[\int_0^{t_d} \ddot{v}_g \cos\omega\tau\, d\tau \right]^2 + \left[\int_0^{t_d} \ddot{v}_g \sin\omega\tau\, d\tau \right]^2 \right\}^{1/2} . \tag{2.5}$$

Figures 2.1 to 2.8 show such spectra for the eight earthquake records. MX and MO can be broadly classified as earthquakes with narrow-band frequency content, while the impulsive type of ground motions (SS, PD) exhibit broader band frequency content.

The Fourier amplitude spectrum is also a measure of the total energy of an undamped linear elastic SDOF system evaluated at the end (t_d) of an earthquake record; to be specific, the Fourier amplitude is the maximum relative velocity ($\dot{v}$) of an undamped SDOF system at the end of duration: [26]

$$|\dot{v}(t)|_{max} = \left\{\left[\int_0^{t_d} \ddot{v}_g \cos\omega\tau \, d\tau\right]^2\right\}^{1/2} + \left\{\left[\int_0^{t_d} \ddot{v}_g \sin\omega\tau \, d\tau\right]^2\right\}^{1/2} . \qquad (2.6)$$

The zero-crossing method was used by Saragoni[37] to characterize the frequency content of an earthquake record. He calculated the "intensity of zero crossings" (ν_0) by dividing the total number of zero-crossings of an acceleration record by the total duration. The calculated ν_0 values of the 8 records are listed in Table 2.3. Araya *et al.* [6] have shown that both the magnitude of the *PGA* and the value of ν_0 have significant influence on the ductility requirements of a simple elastic-perfectly plastic oscillator. However, examining only ν_0 for a particular earthquake record can be misleading — for example, MX has the lowest value of ν_0 yet MX produced severe damage.

2.2.4. Group 4 — This group includes linear elastic response spectra of various kinds, effective peak acceleration and velocity.

The linear elastic response spectra (LERS) of each earthquake are shown in Figs. 2.1 to 2.8; Pseudo-acceleration (S_{pa}) is associated with the maximum elastic force that can be developed in an elastic SDOF system; Figure 2.9a shows the pseudo-acceleration response spectra for the eight earthquake ground records considered in this study. For a 5 percent damping ratio, the maximum pseudo-acceleration of CH (= 2.4g) is more than twice that of MX (= 1.0g.) Since S_{pa} relates directly to the force that can be developed in a linear elastic SDOF system and since under quasi-static loading the larger the force the larger the damage, CH, SS, and PD should have high damage potential for structures with periods less than 0.5 second and MX should be very

destructive for long period structures ($T \approx 2$ sec.) However, under dynamic loading the potential for developing high forces in a linear elastic system is not a reliable index for measuring the damage potential for elastic-perfectly plastic systems.

The ATC [1,2] smoothed linear elastic design response spectra (LEDRS), C_sR, are expressed as:

$$C_sR = \frac{1.2A_vS}{T^{2/3}} \le 2.5A_a \quad \text{(soil type 1)} \tag{2.7}$$

$$\le 2.0A_a \quad \text{(soil type 3 when } A_a \ge 0.30\text{)}$$

where A_v and A_a are the effective peak velocity-related acceleration and effective peak acceleration, respectively, S is the soil type coefficient, and R is the response modification factor. For a typical office building located in an area of the highest seismicity, the ATC LEDRS for soil types 1 and 3 are shown in Fig. 2.9a. Although the ATC LEDRS are comparable to the LERS for EC and conservative for TF, they are non-conservative for: (i) short period structures ($T < 1$ sec) subjected to CH or SS; and (ii) long period structures ($T > 1.7$ sec) subjected to MX.

The maximum input energy, E_D, that is absorbed by an elastic SDOF system can be estimated from the linear elastic pseudo-velocity (S_{pv}) as follows:[22]

$$E_D = \frac{1}{2}m(S_{pv})^2 \tag{2.8}$$

Therefore S_{pv} ($= \sqrt{2E_D/m}$) is an index that can be used to express the damage potential of a ground motion from the energy perspective. Unlike S_{pa}, Fig. 2.9b shows that MX has the largest S_{pv}; the ratio of the maximum input energy between MX and CH for an elastic SDOF system is:

$$\frac{E_D^{MX}\ (T \approx 2.0 \text{ sec})}{E_D^{CH}\ (T \approx 0.5 \text{ sec})} \approx \left[\frac{120}{50}\right]^2 \approx 6\ . \tag{2.9}$$

The ATC linear elastic pseudo-velocity design spectra shown in Fig. 2.9b were calculated from the corresponding pseudo-acceleration design response spectra. If ground motions like those recorded during the 1985 Chile and Mexico and the 1986 San Salvador earthquakes could occur in the United States, then from the energy standpoint, the ATC spectra are non-unconservative for long period structures subjected to MX-type earthquake and for short period

structures subjected to CH or SS-type earthquake. For the intermediate period range of 1 second to 2 seconds, the input energy is maximized by the PD record. The ATC pseudo-velocity design spectra are similar to the EC spectra for periods less than 1 second and are conservative for longer periods. There is little energy associated with TF over the whole period range.

Realizing the shortcoming of using peak instrumental values, ATC[1,2] introduced the concept of effective peak acceleration. Although effective peak acceleration is a philosophically sound parameter for seismic hazard analysis, at present there is no standardized definition of this parameter. ATC defines the effective peak acceleration (*EPA*) and the effective peak velocity (*EPV*) as follows:

$$EPA = \frac{\bar{S}_{pa}}{2.5} \tag{2.10}$$

$$EPV = \frac{\bar{S}_{pv}}{2.5} \tag{2.11}$$

where $\bar{S}_{pa}$ is the mean pseudo-acceleration value in the period range of 0.1 to 0.5 second and $\bar{S}_{pv}$ is the pseudo-velocity value at a period of 1.0 second for the 5 percent damped LERS. The ATC definition was used to calculate the *EPA* and the *EPV* of the eight earthquake ground motions. The calculated values in Table 2.2 show that MX has the lowest *EPA* (= 0.08g) and that CH, SS, and PD have *EPA* values in excess of the *EPA* (= 0.4g) adopted by ATC as being appropriate for a region of high seismic risk. A problem arises in applying the ATC procedure to determine *EPV* for MX; the ATC definition will significantly underestimate *EPV* which is computed at a period of 1 second because the response to MX is concentrated at and around 2 seconds. A response spectrum shape similar to that of MX was not considered by ATC.

An instrumental intensity I_s given by the expression

$$I_s = \log_4(EPA \times EPV) + I_o \tag{2.12}$$

was proposed by Sandi,[36] where I_o is a constant. In the absence of more comprehensive analyses than those available to date, Sandi postulated a value equal to 8 for I_o if the units of EPA are m/sec^2 and of EPV are m/sec. Values of I_s calculated from the ATC values for *EPA* and *EPV* are listed in Table 2.2. The value of I_s for MX record is the lowest for the reason cited above.

On the basis of the results presented above and the extensive damage that resulted from MX, it is clear that more refined and reliable definitions of *EPA* and *EPV* than those used at present have to be developed.

2.2.5. Group 5 — This group includes the elastic response spectrum intensity (*SI*) proposed by Housner: [21]

$$SI(\xi) = \int_{0.1}^{2.5} S_{pv}(\xi,T)\, dT \quad . \tag{2.13}$$

For 5 percent damping, the calculated *SI* values in Table 2.2 show that the intensity of MX (= 111 in) is much higher than that of CH (= 78 in) or SS (= 87 in.) Using Housner's index, EC and TF are much less destructive than the other earthquakes. A comparison of the values of S_{pa} for CH and SS with that of MX shows that *SI* (or S_{pv}) and S_{pa} give completely different and contradicting indications of the ground motion intensity or damage potential.

To relate *SI* with S_{pa}, Eq. 2.13 can be rewritten as:

$$SI(\xi) = \int_{0.1}^{2.5} S_{pv}(\xi,T)\, dT = \frac{1}{2\pi}\int_{0.1}^{2.5} S_{pa}(\xi,T)\, T\, dT \tag{2.14}$$

which is the first moment area of S_{pa} (for $0.1 \le T \le 2.5$ sec) about the S_{pa} axis. Therefore Eq. 2.14 implies that *SI* is larger for ground motions with a significant amount of low frequency (or long period) content, and it explains why MX has a larger *SI* value than CH although its maximum S_{pa} is much lower than that of CH.

It should be noted that although the Arias intensity coefficient I_A (Eq. 2.1) accounts for earthquake *duration*, the I_A for MX is much lower than for CH. This is contradictory to what the *SI* value suggests and the reason for the lower value of I_A for the MX record may be explained by the following equality:[36]

$$I_A = \frac{\pi}{2g}\int_0^{t_d} \ddot{v}_g^2(t)\, dt = \frac{1}{2g}\int_0^{\infty} |F_{\ddot{v}_g}(\bar{\omega})|^2\, d\bar{\omega} \tag{2.15}$$

where $|F_{\ddot{v}_g}(\bar{\omega})|$ is the Fourier amplitude of $\ddot{v}_g(t)$. A comparison of the Fourier amplitude spectra in Figs. 2.1 and 2.3 explains why the I_A value for MX is low.

2.2.6. Group 6 — A destructiveness potential factor P_D that considers both the Arias intensity I_A and the intensity of zero crossings ν_0 was proposed by Araya and Saragoni:[7]

$$P_D = \frac{I_A}{\nu_0^2} \quad . \tag{2.16}$$

Araya *et al.* pointed out that in order to compare the destructiveness of different types of earthquake records, it is necessary to consider simultaneously the effect of their maximum ground acceleration, strong motion duration, and frequency content. The first two factors are considered in I_A, and the last one by the intensity of zero crossings (or characteristic frequency) ν_0. The calculated values of P_D for the eight earthquake records in Table 2.3 indicate that MX has extremely high destructiveness potential, consistent with the severe damage observed after that earthquake. The high value of P_D for MX is attributed to the low value of ν_0 (Table 2.3.) CH has a P_D value of about one-fifth that for MX, although the value of I_A for CH is six times greater than that for MX. The P_D value for MO, which caused significant structural damage, also suggests that it is more destructive than SS and PD. The values of P_D for EC and TF suggest that they have very low damage potential.

In order to judge whether a proposed parameter is reasonable, it is always necessary to correlate the values of the parameter with the observed damage in the vicinity of the recording sites for different earthquakes. Araya *et al.*[7] have shown that the proposed parameter P_D correlates very well with MMI values; however, it should be kept in mind that MMI values will depend on building technology, particularly on construction aspects (quality control of material, workmanship, etc.) For example, in addition to the collapse of many high-rise buildings during the 1986 San Salvador earthquake, many poorly constructed adobe-type houses also collapsed. The extensive damage to adobe-type construction may have contributed to a higher value of MMI (see Table 2.1.)

Park *et al.*[33] proposed the following "characteristics intensity" as a measure of the damage potential:

$$I_c = (RMS_A)^{1.5} (t_D)^{0.5} = (P_A)^{0.75} (t_D)^{0.5} \tag{2.17}$$

The values of I_c for each earthquake record in the bracketed strong motion duration (between $t_{0.05}$ and $t_{0.95}$) are shown in Table 2.2. This index implies that a damaging earthquake motion

should have large input power ($RMS_A = \sqrt{P_A}$), preferably together with long duration. The low value of I_c for MX is not consistent with the severe damage caused by this earthquake. The influence of frequency content is not considered in this index.

2.3. Earthquake Ground Motion Duration

It is well-known that the major disadvantage of using linear elastic response spectra is that the duration of ground motion is not considered. The ATC design spectra are constructed for a recorded ground motion duration of about 20 to 30 seconds.[1,2] The recorded CH and MX ground motions are much longer than 30 seconds (Figs. 2.1 and 2.3.) One commonly used definition of strong motion duration is that due to Trifunac and Brady:[38]

$$t_D = t_{0.95} - t_{0.05} \tag{2.18}$$

where $t_{0.95}$ and $t_{0.05}$ were defined in Section 2.2.2. For the CH and MX records, t_D is 35.8 seconds and 38.8 seconds, respectively (see Table 2.2), longer than the duration adopted by ATC; SS has a much shorter duration (4.3 sec.) Only EC and TF have t_D values comparable with that assumed by ATC. The ATC LEDRS are compatible with the characteristics of EC with regard to strong motion duration and linear elastic response spectra.

Because the mean-squared acceleration time history $E[\ddot{v}_g^2]$ tends to be a chi-squared distribution function:[37]

$$E[\ddot{v}_g^2] = \beta e^{-\alpha t} t^{\gamma} \tag{2.19}$$

where parameters α, β, and γ characterize the time evolution of acceleration amplitudes of each type of record, Araya *et al.* [7] defined the duration of strong motion (Δt_s) by the following formula:

$$\Delta t_s = \begin{cases} t_2^* - t_1^* = \dfrac{2\sqrt{\gamma}}{\alpha} & \text{for } \gamma > 1 \\ t_2^* = \dfrac{\gamma + \sqrt{\gamma}}{\alpha} & \text{for } \gamma \le 1 \end{cases} \tag{2.20}$$

In other words, the strong motion duration is defined as the time interval between the inflection points (at time t_1^* and t_2^*) of the chi-squared function (see Fig. 2.10.) The parameters α and γ are

calculated by solving the following equations:

$$\frac{\gamma + 1}{\alpha} = \frac{\int_0^{t_d} \tau \ddot{v}_g^2(\tau)\, d\tau}{\int_0^{t_d} \ddot{v}_g^2(\tau)\, d\tau} \tag{2.21a}$$

$$\frac{(\gamma + 1)(\gamma + 2)}{\alpha^2} = \frac{\int_0^{t_d} \tau^2 \ddot{v}_g^2(\tau)\, d\tau}{\int_0^{t_d} \ddot{v}_g^2(\tau)\, d\tau} . \tag{2.21b}$$

The value of t_1^* is equal to 0 for $\gamma \leq 1$. The calculated Δt_s for the eight earthquakes are listed in Table 2.3. The ratio of t_D to Δt_s is shown in Table 2.3. Except for EC, the ratios for all the records fall in the range 1.3 to 2.4. Different definitions of strong motion duration lead to very different values.

On the basis of a study of the influence of peak ground motion and intensity of zero crossings on the displacement ductility demand, Araya *et al.* [7] found that strong motion duration Δt_s plays a secondary role. This is true if displacement ductility is used as the only criterion to judge the structural damage. It will be demonstrated in the next chapter that duration plays a very important role when other factors such as energy demand or cumulative displacement ductility are used as the damage criterion. Several other definitions of strong motion duration have been proposed; [16,30,41] but an evaluation of all these definitions is outside the scope of this study.

2.4. Orthogonal Effect of Horizontal Earthquake Ground Motions

The above discussion considers only one significant (or major) component of the recorded horizontal ground motion. With two orthogonal recorded horizontal ground motions $\ddot{v}_{gx}(t)$ and $\ddot{v}_{gy}(t)$, the resultant acceleration in any direction, whose direction cosine is (λ,μ), is given by:[36]

$$\ddot{v}(t) = \lambda \ddot{v}_{gx}(t) + \mu \ddot{v}_{gy}(t) . \tag{2.22}$$

Therefore, the Arias intensity is

$$I_A = \lambda^2 I_{xx} + \mu^2 I_{yy} + 2\lambda\mu I_{xy} \tag{2.23}$$

where

$$I_{ij} = I_{ji} = \frac{\pi}{2g}\int_0^{t_d} \ddot{v}_{gi}(t)\,\ddot{v}_{gj}(t)\,dt \ .$$

The principal direction calculated by maximizing I_A is

$$\frac{\partial I_A}{\partial \lambda} = 0 \qquad \frac{\partial I_A}{\partial \mu} = 0 \tag{2.24}$$

which yields

$$\begin{bmatrix} I_{xx} & I_{xy} \\ I_{xy} & I_{yy} \end{bmatrix} \begin{bmatrix} \lambda \\ \mu \end{bmatrix} = \begin{bmatrix} 0 \\ 0 \end{bmatrix} \tag{2.25}$$

The principal direction may be obtained by solving this eigenvalue problem. Table 2.4 summarizes the peak ground acceleration and the Arias intensity coefficients in the principal directions for the first four earthquakes in Table 2.1. The corresponding pseudo-acceleration and pseudo-velocity response spectra are shown in Figs. 2.11a and 2.11b. Taking SS as an example, Table 2.4 shows that the peak acceleration is decreased after combination, but Figs. 2.11a and 2.11b show a significant increase of spectral quantities at a period of 0.7 second. This observation shows again that peak ground acceleration is a poor index by which to express the damage potential of a ground motion.

2.5. Concluding Remarks

The normalized intensity parameters for the eight earthquake records are shown in Fig. 2.12. For each set of parameters, the normalization was made by dividing the parameter values by the maximum value in that set. Since Araya's destructiveness parameter P_D agreed well with the observed MMI,[7] the earthquake records in Fig. 2.12 are ordered according to their P_D values.

Little correlation exists among these parameters. *PGA* and RMS_A are fairly close, noting that RMS_A is a measure of the average rate of input energy to an elastic system. Although I_A is also a measure of the energy input to an elastic system, it tends to overestimate the intensity of an earthquake with long duration, high acceleration and broad band frequency content (CH for example.) The spectral intensity *SI* is also a measure of the damage potential from an energy standpoint because S_{pv} reflects the energy demand of an elastic SDOF system. One obvious

disadvantage of the parameter *SI* (or S_{pv}) is that the duration is not considered and duration is very important for a structural system experiencing inelastic activity and yielding reversals.

After comparing the structure damage and the recorded ground motions for the 1966 Parkfield earthquake and the 1940 El Centro earthquake, Housner [23] concluded that neither S_{pv} nor *SI* was a reliable parameter for measuring the damage potential. It appears that considering recorded earthquake ground motion alone or examining the parameters derived from an elastic system subjected to an earthquake ground motion is insufficient to assess the damage potential of a ground motion.

In this study that considers some of the recently recorded severe earthquakes (e.g., MX, CH, and SS), it appears that Araya's destructiveness parameter P_D agrees with the observed damage much better than the other parameters. Of all the parameters evaluated, only Araya's destructive potential factor considers intensity, duration, and frequency content simultaneously. It is believed that this type of approach will give a more meaningful measurement of the damage potential of a given earthquake ground motion. Since damage involves nonlinear response (inelastic deformation), the only way to estimate damage and the actual behavior of a structure under severe earthquake excitation is to consider its inelastic behavior. Guided by this basic concept and the fact that the damage potential of any given earthquake ground shaking at the foundation of a structure depends upon the intensity, frequency content, duration, and the dynamic characteristics of the structure, the authors believe that one of the most reliable parameters for defining damage potential is *earthquake energy input.*

III. IDENTIFICATION OF RELIABLE PARAMETERS TO MEASURE THE DAMAGE POTENTIAL OF EARTHQUAKE GROUND MOTION

3.1. Introductory Remarks

Because of economic consideration, current design practices (codes) implicitly assume that buildings will undergo some inelastic deformation during severe earthquake shaking in order to dissipate the earthquake input energy. It was pointed out in the previous chapter that the ground motion record alone or elastic response quantities derived from it cannot characterize damage potential of an earthquake. Instead, response parameters based on the inelastic behavior of a structure have to be considered with the characteristics of the ground motion.

In current seismic regulations, displacement ductility ratio is generally used to reduce the design forces that would develop if the structure responds in the linear elastic range to a level that implicitly assumes some degree of inelastic behavior. The reliability of using just the displacement ductility ratio has been questioned, especially for structures subjected to near-field impulsive types of earthquake ground motions.[28] Other parameters have been proposed by previous researchers. In this chapter the reliability of using different parameters in constructing inelastic design response spectra (IDRS) is studied in the light of recently recorded earthquake ground motions. For simplicity only the SDOF system having linear elastic-perfectly plastic behavior is considered, and the earthquake records studied in the previous chapter are used. Most of these records were obtained at free field stations; the records that existed at the base of real buildings may differ from the free field motions, especially for buildings located at soft soil site.

3.2. Constant Displacement Ductility Ratio Response Spectra

Response spectra have been generated using the displacement ductility ratio (μ).[32,35] Limiting the maximum displacement can mitigate the adverse effects of geometric nonlinearities and non-structural component damage. The following basic equation of motion is the starting point for constructing the constant ductility ratio response spectra,

$$m\ddot{v}(t) + c\dot{v}(t) + f_s(t) = -m\ddot{v}_g(t) \tag{3.1}$$

where m = mass

c = viscous damping coefficient

f_s = restoring force

$v_t = v + v_g$ = absolute (or total) displacement of the mass

v = relative displacement of the mass with respect to the ground

v_g = earthquake ground displacement.

Equation 3.1 can be rewritten and normalized for a system with elastic-perfectly plastic (EPP) hysteretic behavior by defining:

$$C_y = \frac{R_y}{mg} \quad (R_y = \text{yielding resistance})$$

$$\eta = \frac{R_y}{m\ddot{v}_{g\,(max)}} = \frac{C_y}{\ddot{v}_{g\,(max)}/g}$$

$$\mu = \frac{v}{v_y} .$$

The normalized equation can be expressed as follows:

$$\ddot{\mu}(t) + 2\omega\xi\dot{\mu}(t) + \omega^2\rho(t) = -\frac{\omega^2}{\eta}\frac{\ddot{v}_g(t)}{\ddot{v}_{g\,(max)}} \tag{3.2}$$

where ω = natural angular frequency

ξ = viscous damping ratio

$$\rho = \frac{R(t)}{R_y} .$$

By specifying a yield force level (R_y or η) for a given earthquake ground motion to a viscous damped nonlinear SDOF system, the *constant strength* response spectrum can be generated with the computer program NONSPEC;[29] Fig. 3.1 shows such spectra. These spectra can be plotted three-dimensionally with period T as the x coordinate, η as the y coordinate, and μ as the z coordinate; Fig. 3.2(a) shows these three-dimensional profiles. Taking the CH record as an example,

the displacement ductility ratio spectrum for $\eta = 0.4$ in Fig. 3.1 corresponds to the curve on the vertical plane with $y = 0.4$ in Fig. 3.2(a). Similarly, other response quantities, such as cyclic ductility, cumulative ductility, number of yielding reversals, input energy, etc., can be plotted in this fashion (see Fig. 3.2b for the plot of input energy.)

The profiles in Fig. 3.2(a) show that much higher displacement ductility will be demanded for structures with small η values (or lower yielding resistances) in the short period range. This trend does not hold for the profiles of the total input energy in Fig. 3.2(b). In general, the profiles of the total input energy reflect the predominant exciting periods of the ground motion. The variation of the total input energy is very pronounced for MX; it reflects the fact that the input energy is much higher for structures with high yielding resistance and with natural periods close to the predominant exciting period of 2 seconds. In this region, the variation of the total input energy is more sensitive to the variation of structural natural period than to the variation of yielding resistance. Figure 3.2(b) also shows that EC has a very small input energy to structures.

For a given displacement ductility ratio, the method for constructing *constant ductility* response spectra from *constant strength* response spectra follows. For a given displacement ductility ratio $\bar{\mu}$, the constant displacement ductility ratio seismic resistance spectra can be constructed by drawing a contour line with $\mu = \bar{\mu}$ on the three-dimensional profiles shown in Fig. 3.2 (a) and projecting these contour lines onto the T–η plane. The curve generated by converting the η ordinate into the C_y ($= \eta \ddot{v}_{g(max)}/g$) ordinate defines the minimum seismic coefficient C_y needed to limit the ductility ratio to $\bar{\mu}$ for each earthquake record. Figure 3.3 shows the spectra corresponding to a displacement ductility ratio of 5. The implications of these spectra are discussed in Section 3.3.

3.3. Seismic Resistance Spectra (Yield Resistance or C_y Spectra)

3.3.1. Influence of Damping Ratios

Seismic response spectra have been constructed for three different values of damping ratio (0, 2, and 5 percent); Fig. 3.3 shows that the damping ratio has only a minor effect on the required yield strength. In the following discussion, emphasis is placed on a 5 percent damping

ratio, which is the value adopted by ATC for the construction of its elastic and inelastic design spectra. Note that the effect of damping ratio on C_y is negligible for impulsive types of earthquakes — SS, PD for example. Damping has its greatest effect on MX and this is attributed to its long duration, periodic (harmonic) nature.

3.3.2. Comparison of Seismic Resistance C_y and ATC Design Coefficient C_s

The ATC seismic inelastic design response spectra (IDRS) are expressed as follows:

$$C_s = \frac{1.2A_vS}{RT^{2/3}} \le \frac{2.5A_a}{R} \qquad \text{(soil type 1)} \tag{3.3}$$

$$\le \frac{2.0A_a}{R} \qquad \text{(soil type 3 when } A_a \ge 0.30\text{)}$$

where A_v and A_a are the effective peak velocity-related acceleration and effective peak acceleration, respectively, S is the soil type coefficient, and R is the response modification factor. Although ATC does not mention explicitly the ductility ratio adopted for each structural system, it does use a ''displacement amplification factor'' C_d to calculate the maximum lateral displacement from the displacement at the level of significant yielding. Therefore, C_d can be roughly treated as the level of displacement ductility ratio adopted by ATC. Taking a dual system with braced frame as an example, Table 3-B of the ATC seismic provisions gives values of 6 and 5 to R and C_d, respectively. Therefore C_s in Eq. 3.3 with $R = 6$ can be compared with the calculated seismic resistance (C_y) spectra with displacement ductility ratio of 5 for a dual system; Figure 3.4a shows such a comparison for soil type 1. A much higher demand than that specified by ATC is required for short period structures (T <1.0 second) subjected to CH, SS, PD, and DPD. The ATC IDRS is satisfactory for EC and TF. The ATC C_s spectrum corresponding to soil type 3 (soft soil) is plotted in Fig. 3.4b and compared with the C_y spectrum of MX to be consistent with the geology of Mexico City. MX has a comparable strength requirement to that of the ATC IDRS.

3.3.3. Evaluation of Overstrength Factor

Parameter R in Eq. 3.3 is an empirical seismic response modification factor intended to account for *damping*, *ductility*, and *overstrength* in a structure designed in accordance with the minimum requirements of ATC.[1,2] Since damping (5 percent) and ductility are considered in the construction of seismic resistance (C_y) spectra, the ratio between the required C_y and the C_s of ATC represents the required *overstrength factor*, Ω:

$$\Omega_{(req'd)} = \frac{C_y}{C_s} \tag{3.4}$$

Figure 3.4 shows the required overstrength factors for eight earthquake records. A structure with a period less than 1 second, whose design satisfies the seismic provisions of ATC, will not behave satisfactorily under CH, SS, PD, and DPD, unless it has been supplied with the overstrength factor shown in this figure. Note from Fig. 3.4b that a structure designed according to ATC is expected to survive MX from the strength point of view, even if it has very limited overstrength. The nonconservatism of the ATC IDRS in the short period range due to its constant response reduction factor over the whole period range has already been pointed out.[10,28]

Similar plots for special moment-resisting steel frames (R= 8, C_d= 5.5) are shown in Fig. 3.5. It is clear from this figure that in order to really take advantage of the *larger* ductility ratio (reflected in larger C_d and R values) of this structural system, a structure designed by ATC seismic provisions in general needs to be provided with higher overstrength.

Overstrength, inherent in the design process, results from higher material strength, strain hardening, strain rate effect, member over-size, code minimum requirements regarding proportioning and detailing, internal force redistribution (redundancy), effect of nonstructural elements, and so on. Since in practice overstrength is not quantified and is not explicitly accounted for in the current design process, the survival of an ATC-designed structure (especially in the short period range) cannot be guaranteed during severe earthquake shaking. Therefore, there is a need to *calibrate* the inherent (or supplied) overstrength of buildings designed and constructed in accordance with the ATC seismic provisions.

3.3.4. Influence of Ductility Level on Seismic Resistance C_y

The influence of displacement ductility ratio on C_y is shown in Fig. 3.6. In general the reduction of C_y by changing the displacement ductility ratio from 2 to 3 is significant, particularly for structures with natural periods close to the predominant periods of the ground motions. Taking MX as an example, the yield resistance is reduced from the elastic level by a factor of 4 for a structure with a natural period of 2 seconds if a ductility ratio of 2 is provided. However, the variation of C_y for a change in ductility from 4 to 6 is smaller than that from 2 to 3. This implies that for displacement ductility lower than a certain threshold, C_y is very sensitive to ductility ratio.

3.3.5. Evaluation of Drift Index

The major advantage of providing a larger ductility ratio to a structural system is to reduce the required yield resistance further. However, permitting a larger ductility ratio makes the story drift limitations more difficult to satisfy. Since the yielding displacement (v_y) for a SDOF system can be calculated as:

$$v_y = \frac{R_y}{k} = \frac{C_y mg}{k} = \frac{gC_y T^2}{4\pi^2} \tag{3.5}$$

where k is the elastic stiffness, the drift (or maximum displacement v_{max}) can be expressed as follows:

$$v_{max} = \mu v_y = \frac{g\mu C_y T^2}{4\pi^2} \ . \tag{3.6}$$

A relationship between T and H has to be established in order to calculate the drift index Θ ($= v_{max}/H$, where H is the story height.) The following empirical expression is based upon the measured response of 17 steel frames and 14 reinforced concrete frames during the 1971 San Fernando earthquake:[1,2]

$$T = \alpha H^{3/4} \tag{3.7}$$

where H = building height (in feet);

α = 0.049 (steel frame);

$= 0.035$ (reinforced concrete frame).

The values of α adopted in the ATC seismic provisions (0.035 for steel frames and 0.025 for reinforced concrete frames, see Fig. 3.7) are smaller than these more realistic values in order to provide a conservative (smaller) estimate of the fundamental period of vibration, and hence a larger base shear coefficient C_s. From Eq. 3.7, height H may be expressed as a function of T as follows:

$$H = \left[\frac{T}{\alpha}\right]^{4/3} . \tag{3.8}$$

The drift index (Θ) is therefore calculated by dividing Eq. 3.6 by Eq. 3.8:

$$\Theta = \frac{v_{max}}{H} = \frac{g\mu C_y \alpha^{4/3} T^{2/3}}{4\pi^2} . \tag{3.9}$$

Note that use of the conservative α values suggested by ATC will underestimate the drift index.

It should be noted that Eq. 3.9 was derived based on Eq. 3.7, which is the empirical equation for multi-story buildings. The drift index Θ calculated by v_{max}/H is valid for SDOF systems. To apply Eq. 3.9 to multi-story buildings, a uniform distribution of inter-story drift has to be assumed (see Fig. 3.8a.) The drift index calculated in this manner provides a lower bound estimate of drift index:

$$\Theta_l = \frac{v_{max}}{H} = \frac{g\mu C_y \alpha^{4/3} T^{2/3}}{4\pi^2} . \tag{3.10}$$

Figure 3.9a shows the variation of Θ_l with T for steel frames with displacement ductility ratios equal to 2 and 5. According to ATC, Θ should be limited to 0.01 for essential buildings (seismic hazard exposure group III) and to 0.015 for typical office buildings (seismic hazard exposure group I.) These two limits are also shown in the same figure. The following observations can be drawn from Fig. 3.9a:

(1) Since C_y decreases with increasing μ, particularly from $\mu = 2$ to $\mu = 3$ (see Fig. 3.6), drift index does not increase proportionally with the displacement ductility ratio. However, since Eq. 3.9 indicates that drift index is directly proportional to the product of μ and C_y, and C_y is practically independent of the ductility ratio for $\mu > 5$ when the period is larger than 1.0 second (see Fig. 3.6), it can be expected that the drift index is almost proportional

to μ for large displacement ductility ratio. For example, the drift index for $\mu = 10$ will be about twice that for $\mu = 5$ for period greater than 1.0 second.

(2) In most cases, for structures with small periods the drift index for a large ductility ratio is much higher than the drift index for a small ductility ratio.

(3) A smaller displacement ductility ratio does not necessarily imply a smaller drift index; that is, it is possible that the drift index for $\mu = 2$ is larger than the drift index for $\mu = 5$.

(4) The drift index tends to be constant in the longer period range ($T > 1.5$ sec) for a given displacement ductility ratio, consistent with the "constant displacement" region of the spectra.[32]

(5) The ATC drift limits will be exceeded for the CH, SS, and PD records with peak ground accelerations in excess of 0.5g, even if limited ductility ratio (2 to 3) is supplied.

Observed building failures during past earthquakes show that a soft story formation (partial collapse mechanism) is a common failure mode. In this case, Eq. 3.10 will significantly underestimate the maximum inter-story drift index. Experimental testing of buildings also demonstrates this phenomenon. Shaking table testing of a 0.3-scale six-story concentrically braced steel structure under severe earthquake excitation shows that v_{max}/H (roof drift index) was 0.9 percent while the maximum inter-story drift in the severely buckled fifth story was 1.9 percent.[39] The testing of a 0.3-scale six-story eccentrically braced steel structure shows that v_{max}/H was 0.7 percent while the the maximum inter-story drift in the first story, where the shear link experienced large inelastic deformation, was 1.3 percent.[42]

To estimate an upper bound for the drift index in a multi-story building, the formation of a soft bottom story is assumed (see Fig. 3.8b.) The upper bound to the drift index is calculated as:

$$\Theta_u = \frac{v_{max}}{\Delta H} = \frac{g\mu C_y T^2}{4\pi^2 \Delta H} \quad . \tag{3.11}$$

Assuming a first story height (ΔH) of 12 ft, the calculated Θ_u are shown in Fig. 3.9b. Comparing the results in Figs. 3.9a and 3.9b, the following observations can be made:

(1) A much higher drift index would occur if a soft story were to form in the bottom story.

(2) By assuming a *uniform* drift index along the height of a building, a larger drift index generally occurs in the *short* period range. On the other hand, a larger drift index would be demanded in the *long* period range if a *soft story* were to form.

Note the high demands on Θ_l and Θ_u for PD and that MX has a high demand on Θ_u but only a minor demand on Θ_l.

Alternatively, using the ATC drift index limit Θ_{max}, Eq. 3.9 may be used to calculate the upper bound of C_y beyond which the drift index limit is violated for a given displacement ductility ratio:

$$C_y^{drift} = \frac{4\pi^2 \Theta_{max}}{g \mu \alpha^{4/3} T^{2/3}} \geq C_y \quad . \tag{3.12}$$

For steel frames, Fig. 3.10 shows C_y and C_y^{drift} (with $\Theta = 0.015$) curves with displacement ductilities equal to 2 and 5, respectively. The drift index limit will be violated at period ranges for which C_y exceeds C_y^{drift}. This figure shows that drift limit usually will not control for long period structures (T> 1.5 sec.) The implication of this comparison of C_y and C_y^{drift} is that a constant, moderately large ductility ratio cannot be assigned throughout the period range. Taking the CH record as an example, Fig. 3.10 shows that drift limit will control in the period range from 0.1 to 0.7 second for a displacement ductility ratio of 5; the allowable displacement ductility ratio has to be reduced in this period range in order to satisfy the drift limitation. The ATC IDRS corresponding to $R = 6$, $C_d = 5$ and soil type 1 (with the exception of soil type 3 for MX) is also added to each plot in Fig. 3.10. Since the C_s of ATC is less than C_y^{drift} for $\mu = 5$, drift will not control, assuming that the inter-story drift is uniform along the height of a multi-story structure.

3.4. Input Energy Spectra

With the seismic resistance spectra (for a given displacement ductility ratio), the input energy spectra can be generated by the following integration:

$$E_I = -\int (m \ddot{v}_t) \, dv_g \tag{3.13}$$

where $\ddot{v}_t$ is the absolute acceleration of the SDOF system. For a unit mass, Fig. 3.11 shows the input energy spectra for displacement ductility ratios of 2, 4, and 6. The following observations can be drawn from this figure:

(1) The input energy for CH, EC, and TF is relatively insensitive to the level of displacement ductility ratio. On the other hand, the input energy for MO, PD, DPD and particularly for MX is sensitive to variations in displacement ductility ratio. It appears that the input energy for a long duration, harmonic type of earthquake will be more sensitive to variation in displacement ductility ratio between 2 and 4. For these earthquake ground motions (especially MX), Fig. 3.11 clearly shows that for a structure with a period at or close to the predominant period of the ground motion, the input energy decreases as C_y decreases whereas for a structure with period smaller than the predominant period of the earthquake ground motion, the input energy for decreasing C_y can be significantly larger than that for the elastic system .

(2) Frequently used earthquake records, such as TF and EC, have very small energy demand.

(3) MX, which appears to be non-destructive from the standpoint of demanded strength or seismic resistance (Fig. 3.4), has the largest energy demand for long period structures ($T > 1.5$ sec.) On the other hand, SS, which appears to be a very destructive earthquake for short period structures ($T < 1.0$ sec) from the standpoint of demanded strength, has a very small energy demand. Considering only the strength demand in seismic design may be misleading because the effects of duration, which are included in the calculation of the input energy, should be reflected in the design process.

(4) As noted in Section 2.2.4, linear elastic pseudo-velocity is an index that Housner [22] used to express the damage potential of an earthquake:

$$E_D = \frac{1}{2} m (S_{pv})^2 \quad . \tag{3.14}$$

Usually it is assumed that E_D is maximized by elastic response and therefore E_D can be used as the maximum input energy for an inelastic system. To verify this argument, the normalized input energy (E_I/m) spectra of Fig. 3.11 are re-plotted in Fig. 3.12 with the following ordinate:

$$V_I = \sqrt{\frac{2E_I}{m}} \quad . \tag{3.15}$$

V_I is defined as the *equivalent velocity* of the normalized input energy. For 5 percent

damping, a comparison of V_I and S_{pv} is shown in Fig. 3.12. From this figure, it is observed that S_{pv} may be a reasonable estimate of $\sqrt{2E_I/m}$ only for structures in the long period range ($T>1.0$ second) and subjected to impulsive types of earthquakes with just one major impulse (SS, PD, and DPD.) structures in the long period range ($T>1.0$ second). In general, S_{pv} can be used to obtain a lower bound to the input energy spectra and may significantly underestimate the true input energy for a structure with a period that is smaller than the predominant exciting period of the earthquake ground motion.

3.5. Hysteretic Energy Spectra

Input energy in a structural system is balanced (absorbed and dissipated) as follows:[40]

$$E_I = E_H + E_K + E_S + E_\xi \tag{3.16}$$

where E_H, E_K, E_S and E_ξ are the hysteretic energy, kinetic energy, elastic strain energy, and viscous damping energy. E_H is the portion of the input energy that relates directly to the damage to a structure and therefore it is more meaningful to generate hysteretic energy spectra for a constant displacement ductility ratio. The hysteretic energy can be expressed by the equivalent hysteretic velocity:

$$V_H = \sqrt{\frac{2E_H}{m}} \tag{3.17}$$

and is compared with the elastic pseudo-velocity (S_{pv}) in Fig. 3.13. A comparison of Figs. 3.12 and 3.13 shows that V_H is significantly lower than V_I for long duration earthquakes (CH, MX.) Hysteretic energy spectra are in general in close agreement with S_{pv}, except for the long duration strong motion earthquakes (CH and MX) and for structures having $T < 1.5$ seconds for CH, $T < 2.0$ seconds for MX. Similar conclusions to those made for the input energy spectra can also be drawn: MX has the largest hysteretic energy demand although its strength demand (reflected in the demanded C_y) is insignificant. TF and EC have the smallest hysteretic energy demand.

3.6. Cumulative Ductility Spectra

Cumulative ductility ratio (μ_a) is defined as the summation of the absolute values of all inelastic deformations normalized by yielding displacements. For an elastic-perfectly plastic model, the cumulative ductility ratio is directly related to the normalized hysteretic energy ductility (μ_H):[29]

$$\mu_H = \frac{E_H}{R_y v_y} + 1 \tag{3.18}$$

and Fig. 3.14 shows such spectra. Note that MX requires a structure to possess a very large cumulative ductility ratio, which is consistent with its high demand in hysteretic energy. However, the same argument does not apply for TF and EC for which relatively high cumulative ductility is associated with very low hysteretic energy demand for a constant displacement ductility ratio. This is attributed to the fact that, for a given period, TF and EC have very low C_y values (Figs. 3.3 and 3.5.) Cumulative ductility spectrum alone can be a misleading index to measure the severity of an earthquake ground motion since a large μ_a may be associated with very low C_y values, and hence a very low E_H value. Therefore if cumulative ductility spectra are used to compare the severity of different ground motions, these spectra should be compared for the same yield level C_y.

3.7. Number of Yielding Reversals Spectra

The number of yielding reversals (NYR) is defined as the number of times a structural system yields in one direction and subsequently yields in the opposite direction in the following cycle. For a given displacement ductility ratio, Fig. 3.15 shows that in general the number of yielding reversals is closely related and roughly proportional to the strong motion duration; long duration records (CH, MX) have a large number of yielding reversals while short duration impulse-type records (SS, PD, and DPD) have a very low number of yielding reversals. These NYR spectra indicate that low-cycle fatigue can be a problem for structures subjected to long duration earthquakes if they are designed for only the C_y resulting from the use of the assumed ductility ratio μ.

3.8. Effect of Damping on Constant Ductility Ratio Spectra

The damping ratio of a structure depends upon the structural material, connection types, stress levels, etc. Damping ratios for bare steel structures are generally considerably less than 2 percent whereas damping ratios in reinforced concrete structures can reach 5 percent when the structure is severely cracked. The presence of nonstructural components, particularly partitions, infills, and cladding elements can add a significant amount of damping to the structural system.

ATC [1,2] adopts a viscous damping ratio of 5 percent. Figure 3.16 shows the influence of damping ratio on the hysteretic energy spectra. The effect of a variation in viscous damping on E_H appears to be greatest for long duration earthquake motions (CH, MX) with the maximum variations occurring at periods in the vicinity of the predominant periods of the earthquake motions. Similar conclusions were also reported by other researchers.[43] From these results together with those of Fig. 3.3, it may be concluded that damping ratio has a minor effect on response spectra with a constant ductility ratio. Considering the insensitivity of constant ductility ratio response spectra to damping ratio, it appears that a 5 percent damping ratio is reasonable for real building structures with a moderate amount of light nonstructural elements.

3.9. Comments on Constant Displacement Ductility Response Spectra

Traditionally, displacement ductility ratio is used as: (i) the main parameter to measure the degree of damage (permanent deformation) substained by a structure during its response to an earthquake ground motion; and (ii) the most reliable index to represent damage in the derivation of seismic inelastic design response spectra. Various response spectra based on a constant lateral displacement ductility ratio have been constructed and analyzed in this chapter. The important conclusions drawn from these studies are as follows:

(1) Structures with short period (say $T < 1.0$ sec) designed for the yielding strengths required by ATC must possess significant overstrength to survive earthquakes similar to the records considered in this study, particularly CH, MX, SS, and PD. There is a need to calibrate the inherently supplied overstrength of structures designed by codes.

(2) Although a significant reduction of the required linear elastic strength can be achieved through the use of a small displacement ductility ratio (2 to 3), this reduction does not

increase proportionally with increasing displacement ductility ratio (Fig. 3.6.)

(3) Estimates of upper and lower bounds for the drift index for multi-story buildings have been derived for a constant displacement ductility ratio. The lower bound for the drift index (corresponding to a uniform drift index distribution) may control the design of structures in the short period range. The upper bound for the drift index (corresponding to the formation of a soft bottom story) becomes increasingly critical with increasing period.

(4) An upper bound has been derived for C_y on the basis of constant displacement ductility and code drift limits. Drift limit usually does not control the design for long period structures ($T > 1.5$ sec) if soft story mechanisms can be avoided. For short period structures subjected to earthquakes with severe acceleration pulses (i.e., pulses with large peak ground acceleration, say in excess of 0.4g, and long duration) the ductility ratio that can be used should be limited. In this case, the use of a large ductility ratio to reduce seismic design forces leads to excessive drift indices. The use of a constant displacement ductility ratio to construct design spectra cannot be justified from the viewpoint of drift control.

(5) One significant disadvantage of seismic resistance (C_y) spectra is that the effect of strong motion duration is not considered. The energy demands associated with a long duration earthquake record may be very large and a design based only on C_y may not be conservative. A study of this conventional way of constructing an inelastic design response spectrum suggests that other controlling factors must be considered.

(6) While the linear elastic pseudo-velocity spectra S_{pv} can be used to obtain a lower bound to the equivalent input energy V_I spectra, they may significantly underestimate the true energy input.

(7) Although the equivalent hysteretic energy V_H spectra are in general in close agreement with the S_{pv} spectra, the S_{pv} spectra may significantly underestimate the V_H spectra in the case of long duration strong ground shaking such as CH and MX.

(8) While a variation in the value of damping ratio affects the response of linear elastic structures considerably, this variation has only minor effects on the required yielding strength C_y as well as on the hysteretic energy of yielding structures.

3.10. Possible Parameters to Construct Inelastic Spectra

In the previous sections all the inelastic response spectra were calculated on the basis of a constant displacement ductility ratio. The use of displacement ductility as a damage criterion is reasonable from two perspectives: (i) it not only allows the structural damage to be controlled, but it also allows damage to deformation-sensitive nonstructural components to be controlled; and (ii) it allows the undesirable effects of geometric nonlinearities to be controlled. However, using seismic resistance spectra (C_y spectra) based on a constant ductility ratio for design purposes may be inadequate because other failure modes may control. Damage criteria should ideally reflect the following important parameters:

(1) The energy dissipation capacity of both the structural members and the entire structural systems;

(2) Cyclic ductility demand due to repeated bursts of large energy input in an earthquake record.

Use of these parameters to establish damage criteria requires identification of the acceptable levels of hysteretic energy dissipation capacity and cyclic ductility of structural elements, structural systems, and of entire soil-foundation-superstructure and non-structural component system.

The high hysteretic energy demanded by MX (Fig. 3.13), based on a constant ductility ratio, is a good example to demonstrate the need for establishing damage criteria that include energy dissipation demand.

Previous researchers [5,22] have proposed that the energy dissipation capacity of a structure under cyclic excitation be estimated directly from its response under monotonic loading. The energy dissipation capacity of a structure under monotonic loading is usually well defined.[12,20] Other researchers have found that energy dissipation capacity is not constant and varies with the amplitudes of the inelastic deformation and loading or deformation paths as shown by the following results obtained by Bertero *et al.*;[9] Fig. 3.17 shows results of steel beams tested under yielding reversals. By ignoring strain hardening and Bauschinger effects, the moment-curvature curve under cyclic loading can be idealized as shown in Fig. 3.18; these two factors tend to compensate each other from the standpoint of energy dissipation. The dissipated energy per unit length, e_d, is the area enclosed by the hysteresis loop:

$$e_d = \int M_p d\phi_p = 2M_p (2\phi_p) = 4M_p \phi_p \simeq 4M_p \bar{\phi} \tag{3.19}$$

where M_p is the plastic moment, ϕ_p is the plastic curvature, and $\bar{\phi}$ is the controlling (constant) curvature, which, from Fig. 3.18, is the sum of ϕ_p and the yielding curvature ϕ_y. Plastic curvature ϕ_p is approximated by $\bar{\phi}$ in Eq. 3.19; this is a reasonable assumption when the controlling curvature, $\bar{\phi}$, is much larger than the yielding curvature, ϕ_y. By letting

$$\bar{\phi} = \frac{\bar{\varepsilon}}{d/2}$$

where $\bar{\varepsilon}$ is the controlling strain at beam flange, and d is the beam depth, the total energy dissipated per unit length in n cycles (n is the number of cycles required to rupture the beam) is

$$e_d = 4 M_p n \bar{\varepsilon} (\frac{2}{d}) = \frac{8M_p}{d} (n \bar{\varepsilon}) \ . \tag{3.20}$$

Figure 3.17 also shows the $n\bar{\varepsilon}$ versus $\bar{\varepsilon}$ curve. From this curve it is obvious that the larger the amplitudes of the cyclic deformations to which the beam is subjected, the smaller the total energy dissipation capacity $e_d L_p$ will be, where L_p is the average plastic hinge length.

Similar conclusions can be drawn from the behavior of reinforced concrete structures. Figure 3.19 shows the hysteretic behavior of two identical shear wall structures tested under monotonic and cyclic loading.[11] Although Wall 3 has a larger ductility ratio, the total energy dissipation capacity of Wall 3 is only 60 percent of that of Wall 1. These experimental results demonstrate that energy dissipation capacity is not constant but is dependent on loading or deformation paths or both. From analysis of available results it appears that for properly designed and detailed structures the energy dissipation capacity under monotonic loading is a lower limit of the energy dissipation capacity under cyclic loading. Nevertheless, the use of this lower limit could be too conservative for earthquake-resistant design, particularly if the ductility ratio is limited to low values with respect to the ductility ratio reached under monotonic loading.

From a study of the cyclic behavior of shear links, Kasai[27] also concluded that the energy dissipation capacity of a link is not constant. Instead, he found that cyclic ductility is the controlling damage criterion for shear links.

Since the hysteretic dissipation capacity of a structural member (or a structural system) is not constant, an energy-based design that assumes a constant energy supply cannot be justified.

Realizing the limitation of using constant displacement ductility or constant hysteretic energy dissipation as a damage criterion, Park *et al.*[33] proposed a damage index (D_e) that combined these two factors:

$$D_e = \frac{v_{max}}{v_u} + \frac{\beta}{R_y v_y} \int dE_H \tag{3.21}$$

where

v_{max} = maximum deformation under an earthquake;

v_u = ultimate deformation capacity under monotonic loading;

v_y = yield deformation;

R_y = yield strength;

$\int dE_H$ = cumulative hysteretic energy;

β = non-negative parameter.

Appropriate parameters for this proposed damage index were evaluated on the basis of a statistical study of available monotonic and cyclic test data of reinforced concrete beams and columns. To calculate the overall damage index (D_T) at structure level, Park used the following formula:

$$D_T = \frac{\sum D_e^i E_H^i}{\sum E_H^i} \tag{3.22}$$

where D_e^i is the damage index of the i-th member, and the hysteretic energy E_H^i of the i-th member is used as the weighting factor. Nine reinforced concrete buildings that were moderately or severely damaged during the 1971 San Fernando earthquake and the 1978 Miyagi-Ken-Oki earthquake were analyzed and the results were then calibrated with the corresponding damage. Park concluded that an overall damage index D_T of less than 0.4 represents repairable damage and a D_T value larger than 1.0 represents total collapse. Since the maximum displacement and dissipating energy are closely related, the rationale of the linear combination of the displacement term and energy term in Eq. 3.21 has been questioned.[19]

A similar approach was also proposed by Chen, [18] who used a parameter defined as:

$$N = \frac{E_H}{R_y(v_u - v_y)} \tag{3.23}$$

and the displacement ductility ratio μ to establish a damage criterion. After calibrating the analytical prediction of eight reinforced concrete building frames damaged during the 1976 Tangshang earthquake, the following damage criterion was proposed (see Fig. 3.20):

$$(\mu - 0.676)(N - 0.676) = 1.403 \ . \tag{3.24}$$

3.11. Concluding Remarks

(1) It appears that the best index for selecting critical earthquake ground shaking for a structure designed for a code specified C_y is to construct the input energy and the hysteretic energy spectra corresponding to all of the types of earthquake ground motions that can occur (or have been recorded) at the site in question.

(2) Conventional ductility response spectra based on constant displacement ductility have been constructed. The implication of these spectra, especially those of recent destructive earthquakes, is that the use of inelastic design spectra based on constant displacement ductility ratio as a damage criterion is nonconservative because these spectra cannot reflect high energy dissipation demand for long duration earthquakes. An energy design method based just on the computed input energy or the hysteretic energy cannot be justified because the energy dissipation capacity of a structure (or a member) is dependent on loading or deformation path or both.

(3) The energy dissipation capacity under monotonic loading is a lower limit to the energy dissipation capacity under generalized cyclic loading.

(4) Damage criteria based on the simultaneous consideration of ductility ratio and hysteretic energy (or its alternatives such as N in Eq. 3.23) is a promising approach for rational earthquake-resistant design of building structures. It is believed that *calibration* of these results to the observed damage to buildings during earthquakes, especially some of the recently recorded destructive earthquakes, is a sound way to establish realistic damage criteria. The effects of nonstructural components and workmanship should be taken into

account when interpreting the results of these studies.

(5) A high degree of scatter in the calculated D values was reported.[33] More reliable damage criteria for both the reinforced concrete and steel members need to be established.

IV. EVALUATION OF DAMAGE POTENTIAL FOR STRUCTURES DESIGNED ACCORDING TO ATC DESIGN SPECTRA

4.1. Introductory Remarks

An evaluation of the damage potential for some recently recorded earthquake ground motions in terms of different response quantities was presented in the previous chapter. In this chapter, the damage potential to structures that just satisfy the minimum strength requirements of ATC are evaluated. For simplicity only the *elastic-perfectly plastic SDOF system* is considered.

4.2. ATC Inelastic Design Response Spectra

The ATC IDRS are expressed as follows (see Eq. 3.3):

$$C_s = \frac{1.2A_vS}{RT^{2/3}} \le \frac{2.5A_a}{R} \quad \text{(soil type 1)} \tag{4.1}$$

$$\le \frac{2.0A_a}{R} \quad \text{(soil type 3 when } A_a \ge 0.30\text{)}$$

In the following discussion, only a *dual system* with $R = 6$, $C_d = 5$ is considered.[1,2] This type of system has been shown to exhibit moderate ductility. The earthquake ground motions studied in the previous two chapters are used in this chapter. Except for MX, to which the soil type is assigned as type 3, soil type 1 is assumed for all other earthquake ground motions. Five percent viscous damping is assumed in these analyses. Furthermore, DPD was not considered in the following study since: (i) DPD is derived from PD by deconvolution; (ii) the response spectra of DPD and PD are similar; and (iii) DP has a greater damage potential than DPD.

4.3. Displacement Ductility Demand

Displacement ductility ratios, calculated by assuming that C_y is equal to C_s, are shown in Fig. 4.1. As discussed in Section 3.3.2, the value of C_d (= 5) can be roughly treated as the level of displacement ductility ratio accepted by ATC; this level is shown in Fig. 4.1. The following

observations can be made:

(1) In general the displacement ductility ratio demand is much higher than the C_d value in the shorter period range ($T < 0.5$ sec.) In this period range, the ductility demand is closely related to the peak ground acceleration; high ductility demand is associated with high value of peak ground acceleration. Note that MX ($PGA = 0.17$g) does not demand high displacement ductility in the vicinity of the 2 second period mark.

(2) If a structure, designed to just satisfy the minimum strength requirement (C_s) of ATC, is to respond within the acceptable range of ductility ratio C_d, significant overstrength is required. A larger degree of overstrength is required in the shorter period range and this is consistent with the results shown in Fig. 3.4. If overstrength is nonexistent, the excessive deflection that is reflected in the large ductility ratio will cause non-structural component damage and induce significant P-Δ effects.

4.4. Drift Index Demand

Figure 4.2 shows the lower bound drift index demand calculated by Eq. 3.10. The limiting drift index of 1.5 percent specified by ATC is exceeded for structures with short periods ($T < 0.5$ sec) subjected to earthquakes with large peak ground accelerations (CH, SS, and PD.)

Equation 3.11 is used to estimate the upper bound to the maximum inter-story drift for multi-story buildings; the formation of a soft bottom story is assumed in this equation. The results are shown in Fig. 4.3 for an assumed typical value of 12 ft for ΔH. While large values of Θ_l are demanded for structures with a *uniform* drift distribution over the height in the *shorter* period range, large values of Θ_u would be demanded in the *longer* period range if a *soft bottom story* were to form. As is the case with Θ_l, a large Θ_u demand is associated with earthquakes with large peak ground accelerations (CH, SS and PD). The only exception is the periodic-type MX for which Θ_l is generally low but for which high values of Θ_u are demanded in the long period range.

4.5. Input Energy Demand

Total input energy spectra for structures designed according to ATC seismic provisions are shown in Fig. 4.4. All but MX tend to maximize the input energy in the vicinity of 0.5 second. The shapes and magnitudes of these energy demands are similar to those constructed in Fig. 3.11 for constant displacement ductility ratios of 4 and 6.

The input energy demands are converted into equivalent velocity V_I by Eq. 3.15 for comparison with the ATC design spectra. Two figures are presented separately in Fig. 4.5 because the MX response calculation is based on soil type 3 whereas the calculation of the responses to the other earthquakes is based on soil type 1. Although SS demands a high ductility ratio (see Fig. 4.1), its peak input energy demand is smaller than that of MO. Harmonic ground acceleration can input a large amount of energy into a structure especially when the ground acceleration has a long duration of strong motion shaking (MX). Since part of the input energy is dissipated in the form of viscous damped energy, it is more meaningful to examine the hysteretic energy demand.

4.6. Hysteretic Energy Demand

The equivalent velocities of the hysteretic energy demand are shown in Fig. 4.6. By *assuming* that an ATC-designed structure can only supply the following hysteretic energy

$$E_H = \frac{m}{2}(S_{pv})^2 = \frac{m}{2}(\frac{2\pi}{T}C_s R)^2 \tag{4.2}$$

it follows that the structure (i) will not survive MX if its period lies between 1.0 and 2.5 seconds; and (ii) will not survive CH, PD, SS and MO if its period is less than 1.0 second. Proper structural detailing is important, especially at critical regions of the members and at their joints, in order to dissipate energy through member inelastic deformation.

4.7. Cumulative Displacement Ductility Demand

Figure 4.7 shows the cumulative displacement ductility demand as a function of period for all the earthquake records investigated in this chapter. The cumulative displacement ductility ratio demand, μ_a, is larger than 100 for CH, PD, and SS in the period range between 0.1 and 0.5

second.

4.8. Yielding Reversal Demand

Figure 4.8 shows the number of yielding reversals (NYR) for structures designed for the ATC's specified yielding resistance. MX demands an NYR of the order of 50 in the vicinity of the predominant period (T≈ 2.0 seconds) of the ground motion while PD demands the same order of NYR for very short period structures (T ≤ 0.2 second.) For structures subjected to CH, the NYR is significant for natural periods less than 1.0 second. Considering the high cumulative displacement ductility demand of CH in this region (Fig. 4.7), low-cycle fatigue may play an important role in building damage, especially for buildings with natural periods less than 0.5 second. A high NYR demand is generally associated with: (i) long durations of strong motion shaking; and (ii) instances where the fundamental period of a structure is close to the predominant period of the ground motion.

4.9. Concluding Remarks

The following conclusions are based on a study of the performance of a dual system which was assumed to just satisfy the minimum strength requirements of ATC and was subjected to severe earthquake shaking using the records listed in Table 2.1.

(1) A structure designed according to the ATC seismic provisions will demand a very high displacement ductility ratio if its fundamental period is less than 0.5 second. For such a structure to perform satisfactorily during severe earthquake shaking, it must have an overstrength of the order shown in Fig. 3.4.

(2) A lower drift index bound (Θ_l) that assumes a uniform inter-story drift index distribution over the height of a multi-story building and an upper drift index bound (Θ_u) that assumes the formation of a soft bottom story were presented in Figs. 4.2 and 4.3. Excessive Θ_l is demanded for structures with short periods and excessive Θ_u demand is the tendency with larger periods. These results emphasize the importance of avoiding soft stories in a building.

(3) A large amount of input energy is generally associated with: (i) earthquake ground motions with large ground accelerations; or (ii) harmonic-type time histories of long duration; or (iii) both.

(4) NYR demand is high for: (i) a structure with a fundamental period close to the predominant period of the ground motion; or (ii) long strong motion duration; or (iii) both.

(5) In order to assess reliably the damage potential to a building that has been designed in accordance with current seismic regulations, the demands of displacement ductility ratio, cumulative ductility ratio, NYRs, and inter-story drift index must be estimated.

Overstrength is generally inherent in a building designed to meet the requirements of current seismic provisions and the greater the building's overstrength, the smaller the response. That is, the response demand (drift index, ductility and so on) will be reduced with increasing strength.

V. CONCLUSIONS AND RECOMMENDATIONS

5.1. Conclusions

This report has presented the results of studies that have been conducted to: (i) assess the reliability of parameters that have been used to identify the damage potential of an earthquake at a given site; (ii) evaluate the reliability of ductility based earthquake-resistant design, that is, of using the displacement ductility ratio as the engineering parameter to : (a) reflect the level or degree of damage; and (b) develop design response spectra from linear elastic spectra, for the critical ground motions; (iii) examine the role of other response quantities which include drift index, input energy, hysteretic energy, cumulative displacement ductility ratio and number of yielding reversals in the formulation of design criteria; (iv) estimate the required overstrength for buildings that are designed to satisfy ATC minimum required seismic forces and to discuss their significance in relation to the response modification factor R; and (v) examine the actual seismic demands of structures that have been designed in accordance with the ATC design provisions. A summary of the main conclusions of these studies are as follows:

(1) The different parameters proposed by previous researchers to specify the damage potential (or intensity) of a given earthquake ground motion do not correlate well. The inadequacy of most of these parameters in judging intensity arises from the fact that they do not consider all of the important dynamic characteristics of a ground motion such as: amplitude, frequency content, strong motion duration, and the sequence of the severe acceleration pulses (if any) and so on. Correlation between the intensity parameters and observed building damage is essential to verify their adequacy. Of the parameters reviewed in this report, the destructiveness potential factor P_D proposed by Araya *et al.* correlates best with observed damage. This factor accounts for the magnitude, duration, and frequency characteristics of the earthquake ground motion.

(2) A large percentage of the strong motion records have been obtained in the free field. The response of, or damage to, a building depends on the characteristics of the earthquake

shaking at it's foundation — foundation excitation can be quite different from the free field excitation.

(3) Only one component of the recorded earthquake ground motion is commonly used by earthquake engineering researchers. The damage potential may be much higher if the acceleration time histories in the ground motion's principal directions are analyzed in lieu of the recorded components. This effect should be included in correlation studies with damaged buildings.

(4) For a given level of displacement ductility ratio, the input energy or hysteretic energy spectra are insensitive to variations in damping ratio. While the linear elastic pseudo-velocity response spectra (S_{pv}) provide a lower bound to the input energy equivalent velocity spectra, they may significantly underestimate the actual input energy. Although hysteretic energy equivalent velocity spectra are generally in close agreement with the S_{pv} spectra, they may underestimate the actual hysteretic energy demand for structures subjected to long duration ground shaking (MX, CH.)

(5) A large overstrength is necessary for short period structures that are designed for the minimum strength requirements of ATC.

(6) An upper bound was derived for the required seismic resistance (C_y) for: (a) constant displacement ductility ratio; and (b) code-based drift limits. It was observed that if soft story formation is avoided for short period structures, the acceptable ductility ratio is limited by the maximum acceptable inter-story drift rather than by the yielding strength requirement.

(7) By extrapolating the drift index results for a SDOF to a multi-story building, lower and upper bounds to the inter-story drift index can be developed. When a uniform inter-story drift index distribution is assumed over the height of a building, the lower bound drift index (Θ_l - Eq. 3.10) tends to be critical for short periods. If a soft first story is assumed, the upper bound drift index (Θ_u - Eq. 3.11) is critical for larger periods. The upper bound results emphasize the importance of avoiding soft-story response in the lower levels of a building.

(8) The energy dissipation (hysteretic) capacity of a structure subjected to earthquake ground motion cannot be estimated directly from its response to monotonic loading. Monotonic

test results will give a lower bound to the energy dissipation capacity of an element (building) under generalized loading.

(9) Damage criteria for earthquake-resistant design cannot be based on limiting the displacement ductility ratio alone.

(10) Damage criteria based on the simultaneous consideration of ductility ratio, hysteretic energy (including cumulative ductility ratio and NYR) are promising for defining rational earthquake-resistant design procedures.

5.2. Recommendations

(1) Strong motion instrument arrays should be installed in and around different kinds of structures to establish the three dimensional relationships between free field motion, foundation level earthquake motion, and building response.

(2) Using displacement ductility ratio as the only parameter to construct rational inelastic design response spectra cannot be justified. Rational design spectra can be constructed only after reliable damage criteria have been established. Damage criteria of structural members, entire structure, and of whole soil-foundation-superstructure and non-structural component system for different materials have to be established. These damage criteria should reflect the effect of deformation path, ductility ratio, number of yielding reversals, energy dissipation capacity and so on.

(3) All of the previous studies on developing inelastic design response spectra ignore the contribution of overstrength. As a result of very limited information on building overstrength, *empirical* response reduction factors have been used to generate inelastic design response spectra.[1-4] In this report, the required overstrength factors for structures designed for ATC minimum strength requirements, subjected to different earthquake ground motions, have been derived. There is an urgent need to calibrate the actual overstrength of different structural systems. Rational response reduction (or modification) factors can be established only after: (a) actual overstrength factors; and (b) ductility reduction factors; have been explicitly quantified.

(4) There is an urgent need for integrated analytical and experimental studies of the stiffness, strength, stability, and energy dissipation capacity of real buildings which have been designed in accordance with current seismic regulations, when they are subjected to realistic earthquake ground motions.

REFERENCES

1. Applied Technology Council, *Tentative Provisions for the Development of Seismic Regulations for Buildings*, U.S. National Bureau of Standards, Special Publication 510, 1978.
2. Building Seismic Safety Council, *NEHRP Recommended Provisions for the Development of Seismic Regulations for New Buildings*, Washington, D.C., 1984.
3. *Recommended Lateral Force Requirements and Commentary*, Seismology Committee, Structural Engineers Association of California, San Francisco, California, 1987.
4. *Uniform Building Code*, International Conference of Building Officials, Whittier, California, 1988.
5. Akiyama, H., *Earthquake Resistant Limit-State Design for Buildings*, University of Tokyo Press, 1985.
6. Araya, R. and Saragoni, G. R., "Capacity of Strong Ground Motion to Cause Structural Damage," *Proceedings of the Seventh World Conference on Earthquake Engineering*, pp. 483-490, Istanbul, Turkey, 1980.
7. Araya, R. and Saragoni, G. R., "Earthquake Accelerogram Destructiveness Potential Factor," *Proceedings of the Eighth World Conference on Earthquake Engineering*, pp. 835-842, Earthquake Engineering Research Institute, San Francisco, CA, 1985.
8. Arias, A., "A Measure of Earthquake Intensity," in *Seismic Design for Nuclear Power Plants*, ed. R.J. Hansen, pp. 438-469, Massachusetts Institute of Technology Press, Cambridge, Mass., 1970.
9. Bertero, V. V. and Popov, E. P., "Effect of Large Alternating Strains on Steel Beams," *Proceedings*, vol. 91, no. ST1, pp. 1-12, ASCE, February, 1965.
10. Bertero, V. V., "Establishment of Design Earthquakes - Evaluation of Present Methods," *Proceedings of the International Symposium on Earthquake Structural Engineering*, pp. 551-580, St. Louis, Mo., August, 1976.
11. Bertero, V. V., Popov, E. P., Wang, T. Y., and Vallenas, J. M., "Seismic Design Implications of Hysteretic Behavior of Reinforced Concrete Structural Walls," *Proceedings of the Sixth World Conference on Earthquake Engineering*, pp. 10-19, New Delhi, India, January, 1977.

12. Bertero, V. V., "Strength and Deformation Capacities of Buildings under Extreme Environments," in *Structural Engineering and Structural Mechanics*, ed. K.S. Pister, pp. 188-237, Prentice-Hall Inc., 1980.

13. Bertero, V. V., Aktan, A. E., Charney, F. A., and Sause, R., "Earthquake Simulation Tests and Associated Studies of a 1/5th-scale Model of a 7-Story R/C Frame-Wall Test Structure," *Report No. UCB/EERC-84/05*, Earthquake Engineering Research Center, University of California, Berkeley, California, June 1984.

14. Bertero, V. V., "Implications of Recent Earthquakes and Research on Earthquake-Resistant Design and Construction of Buildings," *Report No. UCB/EERC-86/03*, Earthquake Engineering Research Center, University of California, Berkeley, California, March 1986.

15. Blume, J. A., "A Reserve Energy Technique for the Earthquake Design and Rating of Structures in the Inelastic Range," *Proceedings of the Second World Conference on Earthquake Engineering*, pp. 1061-1083, Tokyo, Japan, 1960.

16. Bolt, B. A., "Duration of Strong Ground Motion," *Proceedings of the Fifth World Conference on Earthquake Engineering*, pp. 1304-1313, Rome, Italy, 1973.

17. Bolt, B. A., *Earthquakes*, W. H. Freeman and Company, New York, 1988.

18. Chen, Y. and Gong, S., "Double Control Damage Index of Structural Ductility and Dissipated Energy During Earthquake," *Journal of Building Structure*, pp. 35-48, Beijing, China, January, 1986.

19. Chung, Y. S., Meyer, C., and Shinozuka, M., "Seismic Damage Assessment of Reinforced Concrete Members," *NCEER-87-0022*, National Center for Earthquake Engineering Research, State University of New York, Buffalo, New York, October, 1987.

20. Galambos, T. V., "Deformation and Energy Absorption Capacity of Steel Structure in the Inelastic Range," *AISI Bulletin No. 8*, March, 1968.

21. Housner, G. W., "Spectrum Intensities of Strong Motion Earthquakes," *Proceedings of the Symposium of Earthquake and Blast Effects on Structures*, pp. 21-36, EERI, Los Angeles, California, 1952.

22. Housner, G. W., "Limit Design of Structures to Resist Earthquake," *Proceedings of the First World Conference on Earthquake Engineering*, pp. 5-1 to 5-13, Berkeley, California, 1956.

23. Housner, G. W., "Earthquake Research Needs for Nuclear Power Plants," *Journal of the Power Division*, vol. 97, No. PO1, pp. 77-91, ASCE, January, 1971.

24. Housner, G. W., "Measures of Severity of Earthquake Ground Shaking," *Proceedings of the U.S. National Conference on Earthquake Engineering*, pp. 25-33, EERI, Ann Arbor, Michigan, June, 1975.

25. Housner, G. W. and Jennings, P. C., *Earthquake Design Criteria*, EERI, Berkeley, California, 1982.

26. Hudson, D. E., *Reading and Interpretating Strong Motion Accelerograms*, EERI, Berkeley, California, 1979.

27. Kasai, K., "A Study of Seismically Resistant Eccentrically Braced Steel Frame Systems," *Report No. UCB/EERC-86/01*, Earthquake Engineering Research Center, University of California, Berkeley, California, January, 1986.

28. Mahin, S. and Bertero, V. V., "An Evaluation of Inelastic Seismic Design Spectra," *Journal of the Structural Division*, vol. 107, no. ST9, pp. 1177-1195, ASCE, September, 1981.

29. Mahin, S. A. and Lin, J., "Construction of Inelastic Response Spectrum for Single Degree of Freedom System," *Report No. UCB/EERC-83/17*, Earthquake Engineering Research Center, University of California, Berkeley, March, 1983.

30. McCann, N. W. and Shah, H. C., "Determining Strong-Motion Duration of Earthquakes," *Bulletin of the Seismological Society of America*, vol. 69, no. 4, pp. 1253-1265, 1979.

31. McKevitt, W. E., Anderson, D. L., Nathan, N. D., and Cherry, S., "Towards a Simple Energy Method for Seismic Design of Structures," *Proceedings of the Second U. S. National Conference on Earthquake Engineering*, pp. 383-392, EERI, 1979.

32. Newmark, N. M. and Hall, W. J., "Procedures and Criteria for Earthquake Resistant Design," *Building Science Series No. 46*, pp. 209-236, Building Practices for Disaster Mitigation, National Bureau of Standards, February, 1973.

33. Park, Y. J., Ang, A. H.-S., and Wen, Y. K., "Seismic Damage Analysis and Damage-Limiting Design of Reinforced Concrete Buildings," *Structural Research Series No. 516*, University of Illinois, Urbana, Illinois, October, 1984.

34. Reimer, R. B., "Deconvolution of Seismic Response for Linear Systems," *Report No. UCB/EERC-73/10*, Earthquake Engineering Research Center, University of California, Berkeley, California, October 1973.

35. Riddle, R. and Newmark, N. M., "Statistical Analysis of the Response of Nonlinear Systems Subjected to Earthquake," *Structural Research Series No. 468*, University of Illinois, Urbana, Illinois, August, 1979.

36. Sandi, H., "Engineering Aspects and Possible Refinements of the Concept of Seismic Intensity," *12th Regional Seminar on Earthquake Engineering*, Halkidiki, Grace, September 1985.

37. Saragoni, G. R., "The αβγ Method for the Characterization of Earthquake Accelerograms," *Proceedings of the Sixth World Conference on Earthquake Engineering*, pp. 357-361, New Delhi, India, 1977.

38. Trifunac, M. D. and Brady, A. G., "A Study on the Duration of Strong Earthquake Ground Motion," *Bulletin of the Seismological Society of America*, vol. 65, no. 3, pp. 581-626, June, 1975.

39. Uang, C.-M and Bertero, V. V., "Earthquake Simulation Tests and Associated Studies of a 0.3-Scale Model of a 6-Story Concentrically Braced Steel Structure," *Report No. UCB/EERC-86/10*, Earthquake Engineering Research Center, University of California, Berkeley, California, December 1986.

40. Uang, C.-M and Bertero, V. V., "Use of Energy as a Design Criterion in Earthquake Resistant Design," *Report No. UCB/EERC-88/18*, Earthquake Engineering Research Center, University of California, Berkeley, California, November, 1988.

41. Vanmarcke, E. M. and Lai, S. P., "Strong-Motion Duration and rms Amplitude of Earthquake Records," *Bulletin of the Seismological Society of America*, vol. 70, no. 4, pp. 1293-1307, April, 1980.

42. Whittaker, A. S., Uang, C.-M, and Bertero, V. V., "Earthquake Simulation Tests and Associated Studies of a 0.3-Scale Model of a 6-Story Eccentrically Braced Steel Structure," *Report No. UCB/EERC-87/02*, Earthquake Engineering Research Center, University of California, Berkeley, California, June 1987.

43. Zahrah, T. F. and Hall, W. J., "Seismic Energy Absorption in Simple Structures," *Structural Research Series No. 501*, University of Illinois, Urbana, Illinois, July, 1982.

No.	Earthquake	Record	Abbr.	Comp.	Focal Depth (km)	M_L	MMI	Geology	Epicentral Distance (km)
1	Chile March 3, 1985	Llolleo	CH	N10E	6.7	7.8	VIII	Sandstone and volcanic rock	4.5
2	Imperial Valley May 18, 1940	El Centro	EC	N00E	16.0	6.3	VII-VIII	30m stiff clay volcanic rock	9.3
3	Mexico City September 19, 1985	SCT	MX	E00W	4.2-5.0	8.1	VIII-IX	Soft lacustrine clay	350
4	San Salvador October 10, 1986	CIG	SS	E00W	8.0	5.4	VIII-IX	Fluviatile pumice	9.0
5	San Fernando February 9, 1971	Pacoima Dam	PD	S16E	13.0 to surface	6.6	IX-X	Highly jointed diorite gneiss	9.1
6	San Fernando February 9, 1971	Derived Pacoima Dam	DPD	S16E	13.0 to surface	6.6	IX-X	Highly jointed diorite gneiss	9.1
7	Kern County July 21, 1952	Taft	TF	N21E	16.0	7.7	VII	Alluvium	43
8	Miyagi-Ken-Oki June 12, 1978	Tohuku Sendai City	MO	N00E	30.0	7.4	VII-VIII	Alluvium	100

Table 2.1 Earthquake Data

Earthquake	PGA	I_A	P_A	RMS_A	ATC		I_s	$SI(\xi=5\%)$	t_D	I_c
	(g)	(g·sec)	(10^{-2}·g^2)	(10^{-1}·g)	EPA(g)	EPV(in/s)		(g·sec^2)	(sec)	(g$^{1.5}$·sec$^{0.5}$)
CH	0.67	1.56	2.49	1.58	0.57	16	8.6	0.20	35.8	0.38
EC	0.35	0.19	0.44	0.65	0.28	12	7.9	0.14	24.4	0.08
MX	0.17	0.25	0.37	0.60	0.08	6	6.5	0.29	38.8	0.09
SS	0.69	0.25	3.38	1.84	0.54	17	8.6	0.23	4.3	0.16
PD	1.17	0.85	7.30	2.69	0.80	24	9.1	0.36	6.7	0.36
DPD	0.40	0.26	2.46	1.58	0.27	24	8.3	0.31	6.1	0.16
TF	0.16	0.06	0.10	0.31	0.14	5	6.7	0.06	30.5	0.03
MO	0.26	0.21	0.88	0.93	0.17	16	7.7	0.18	13.7	0.105

Table 2.2 Comparison of Earthquake Ground Motion Parameters

Earthquake	ν_0 (1/sec)	P_D (in/sec^3)	Δt_s (sec)	$\frac{t_D}{\Delta t_s}$
CH	8.21	8.94	22.37	1.6
EC	6.67	1.62	3.65	6.6
MX	1.42	48.35	30.26	1.3
SS	5.21	3.61	2.04	2.2
PD	9.15	3.93	4.37	1.5
DPD	12.61	0.64	4.33	1.4
TF	6.20	0.57	12.53	2.4
MO	4.00	5.06	7.90	1.7

Table 2.3 Comparison of Saragoni's Parameters

Earthquake	Component	PGA (g)	I_A (in/sec)
Chile (CH)	N10E	0.67	603
	S80E	0.40	274
	N06E	0.67	605
El Centro (EC)	N00E	0.35	72
	N90E	0.21	51
	S23E	0.35	76
Mexico (MX)	N90E	0.17	96
	N00E	0.10	52
	N62E	0.19	114
San Salvador (SS)	N90E	0.69	98
	N00E	0.42	66
	N57E	0.67	120

Table 2.4 Comparison of Earthquake Ground Motion Parameters in Orthogonal and Principal Directions

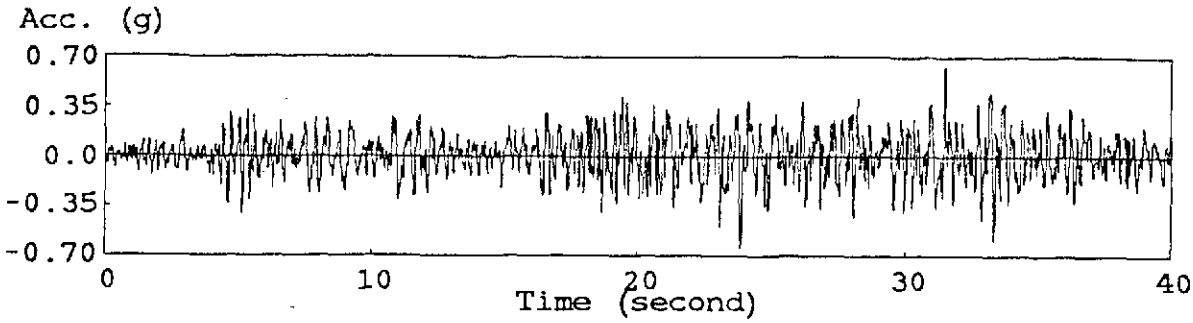

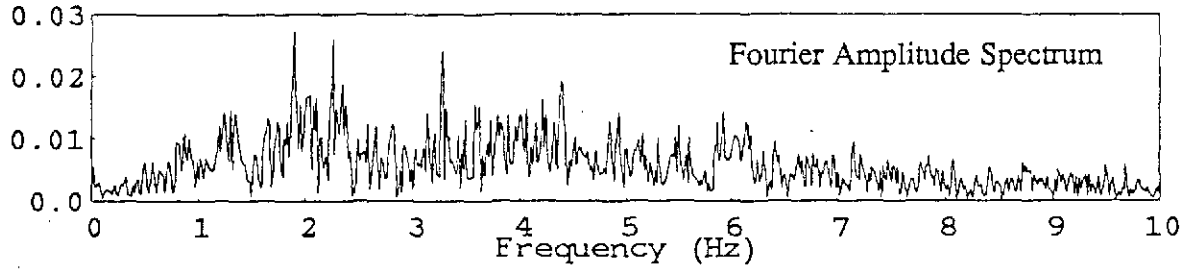

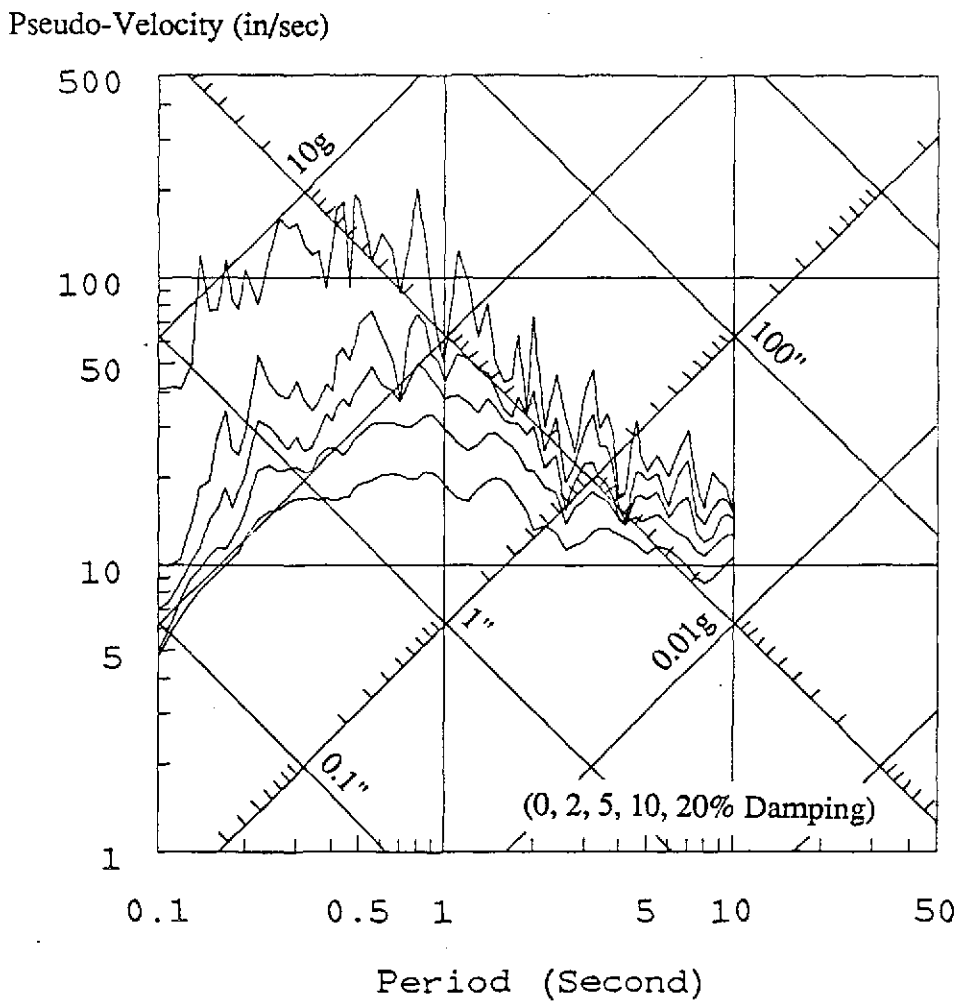

Fig. 2.1 1985 Chile Earthquake Ground Motion (Llolleo, N10E)

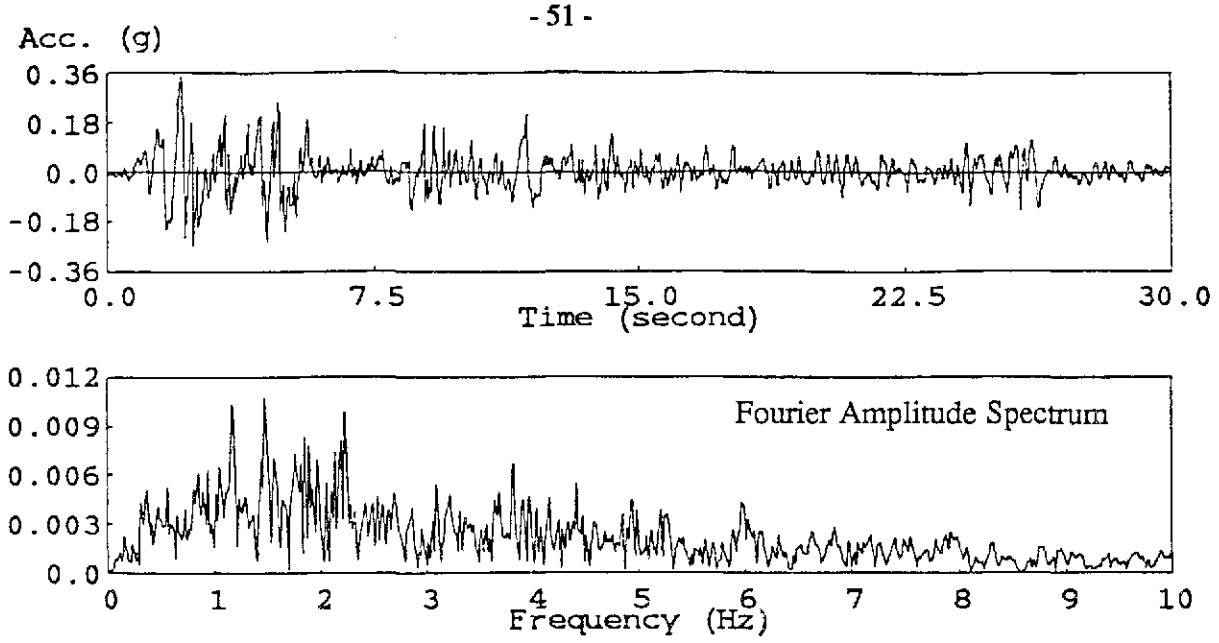

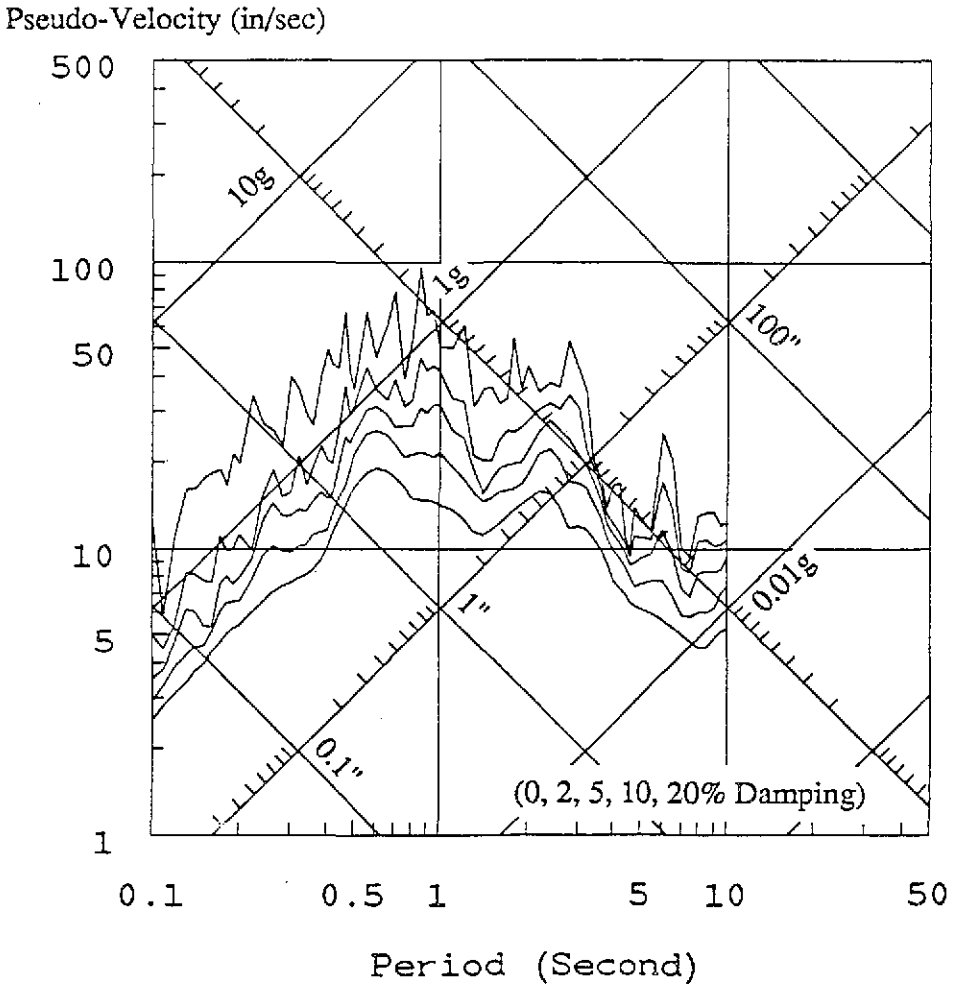

Fig. 2.2 1940 Imperial Valley Earthquake Ground Motion (El Centro, N00E)

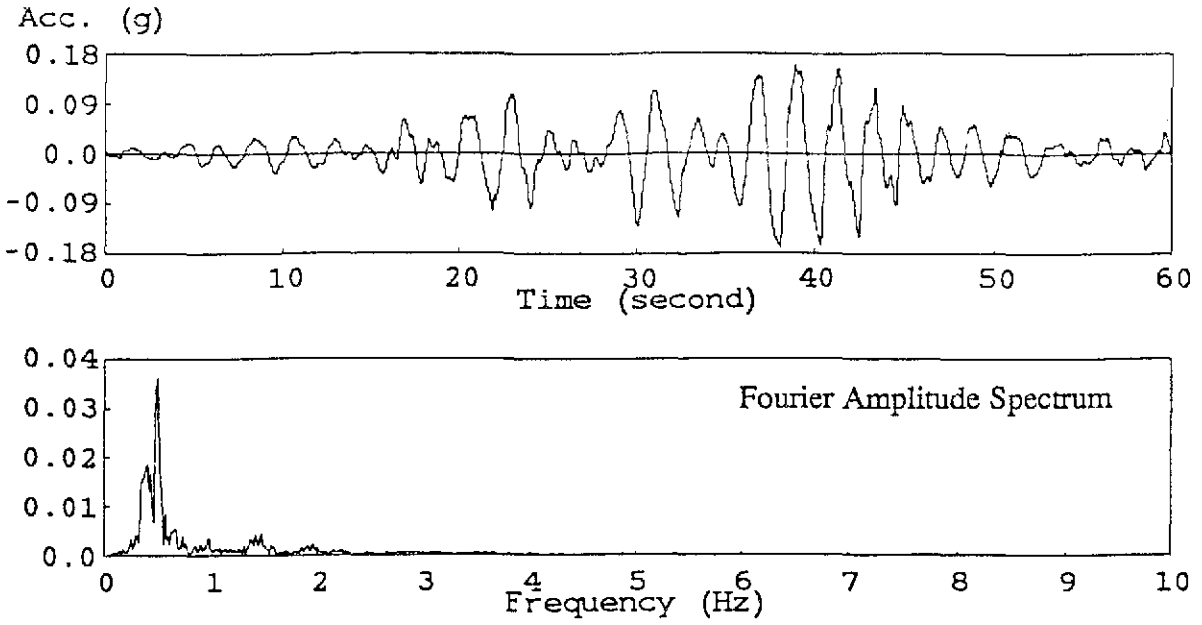

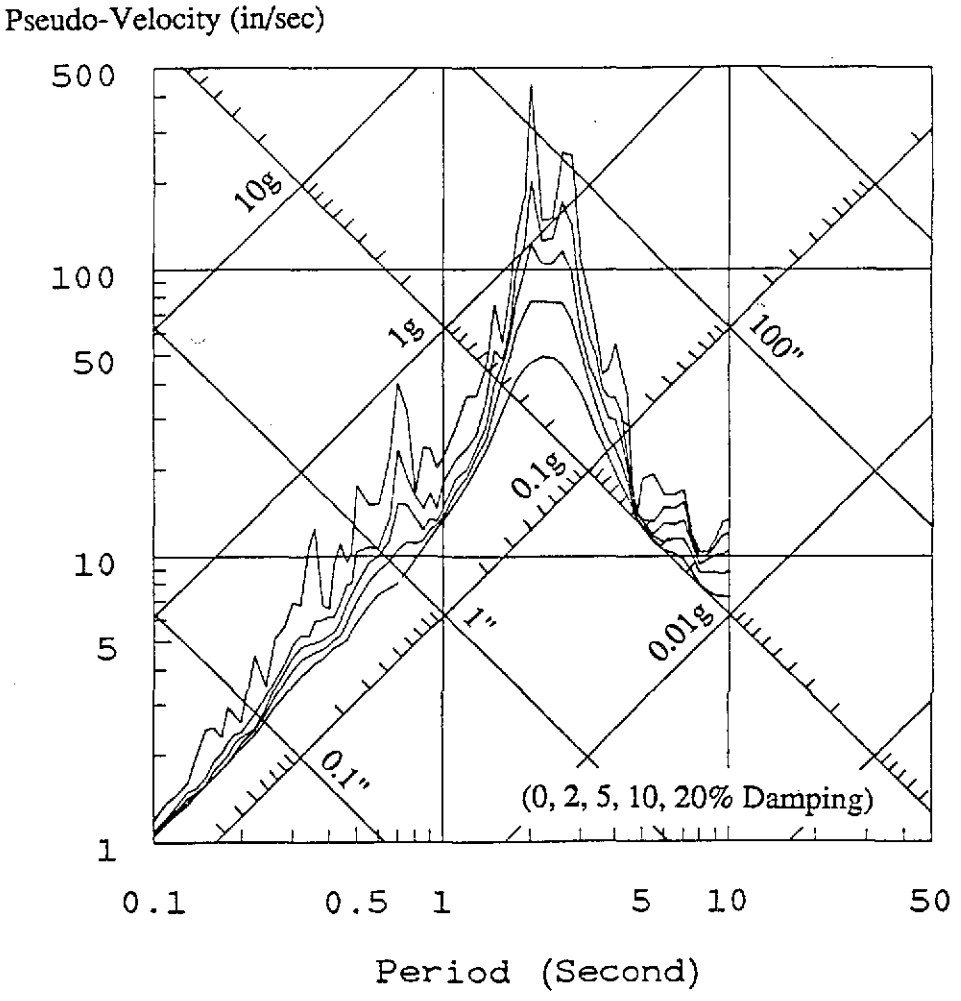

Fig. 2.3 1985 Mexico City Earthquake Ground Motion (SCT, E00W)

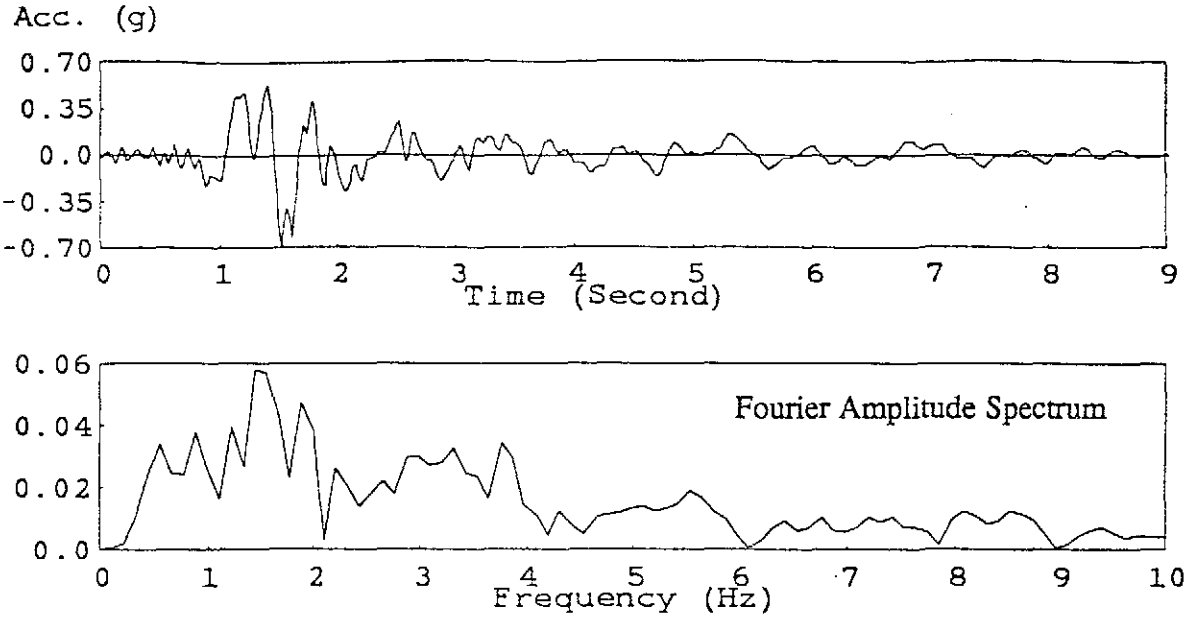

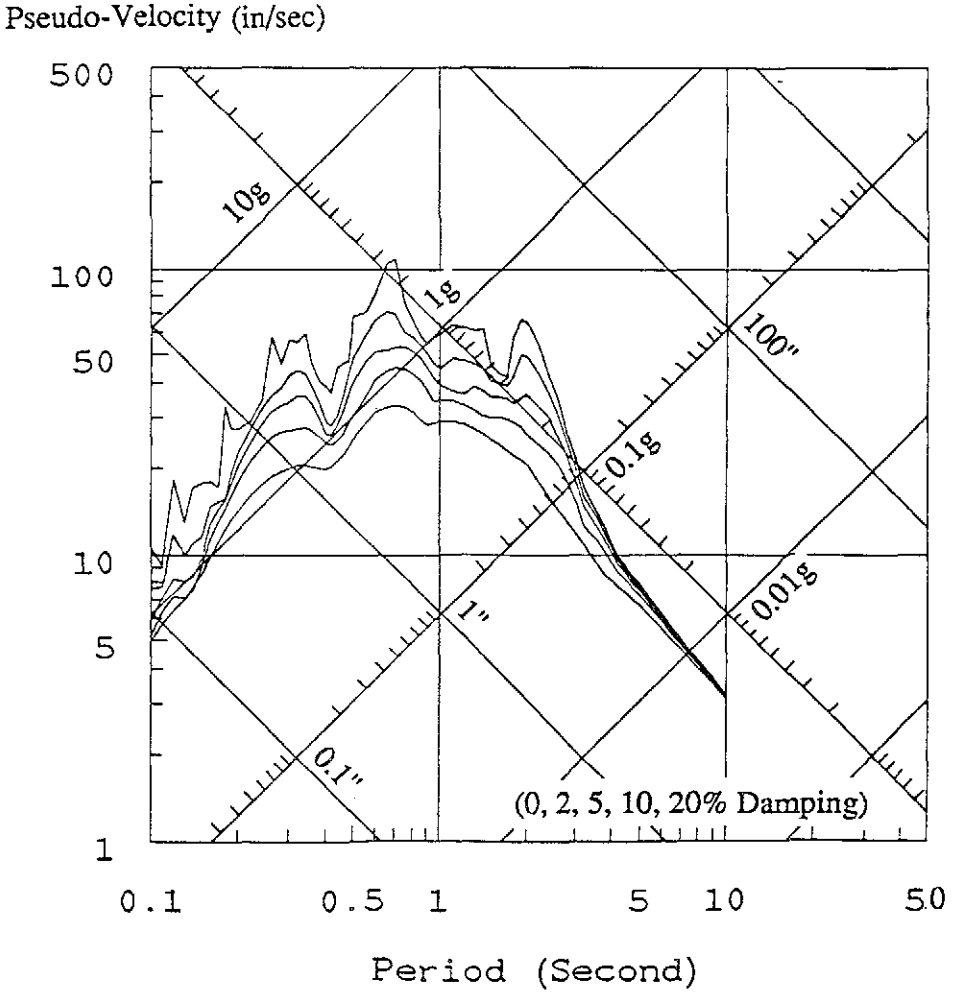

Fig. 2.4 1986 San Salvador Earthquake Ground Motion (CIG, E00W)

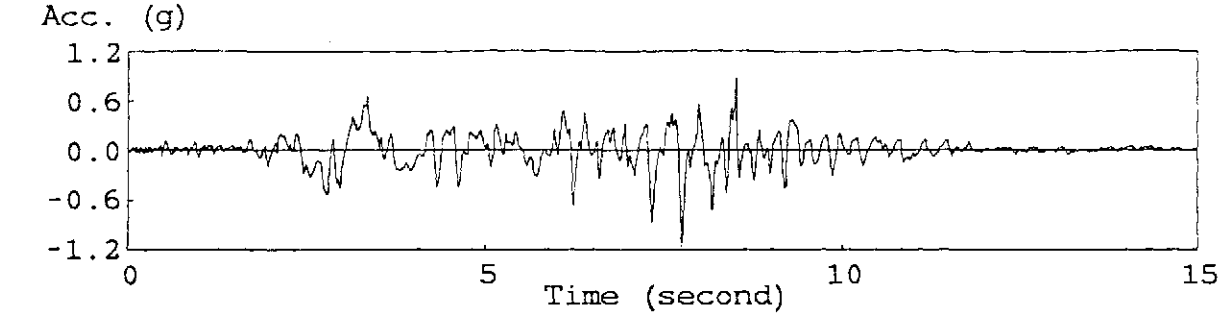

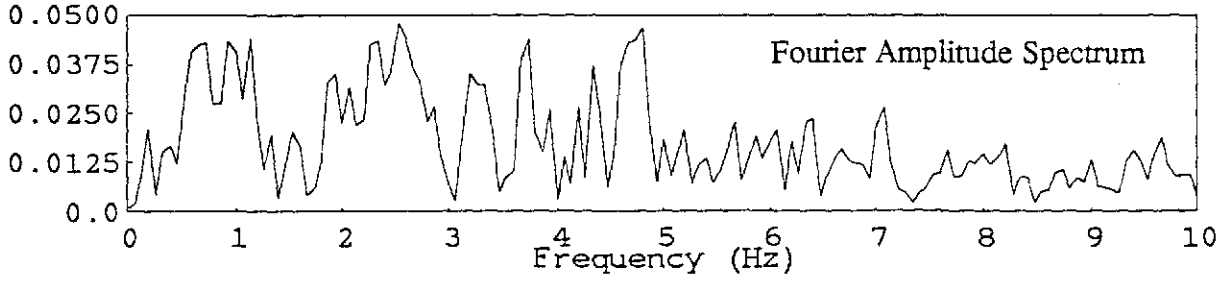

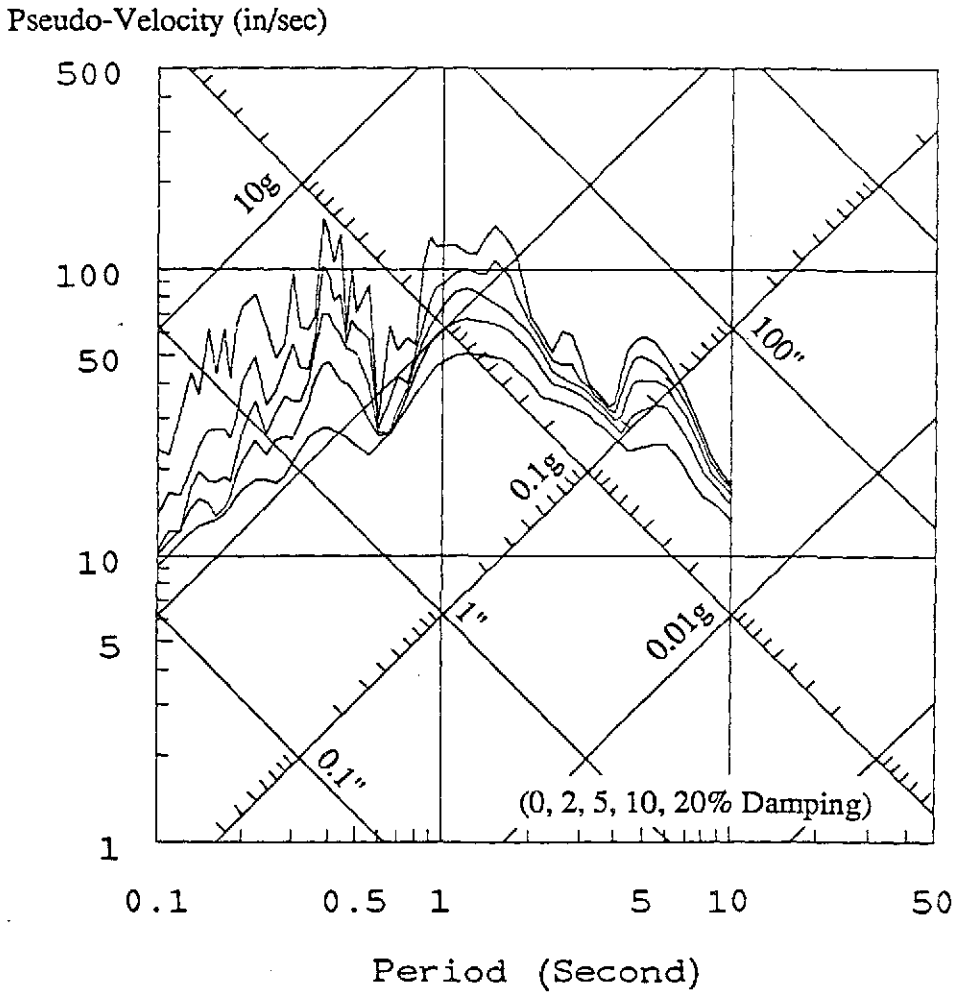

Fig. 2.5 1971 San Fernando Earthquake Ground Motion (Pacoima Dam, S16E)

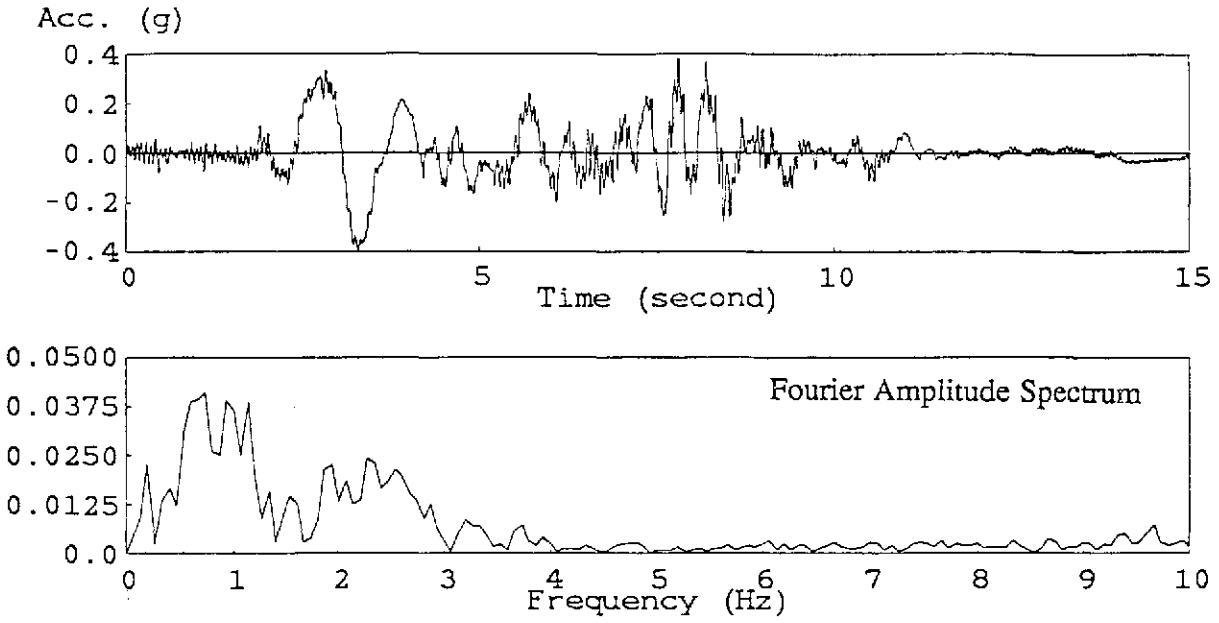

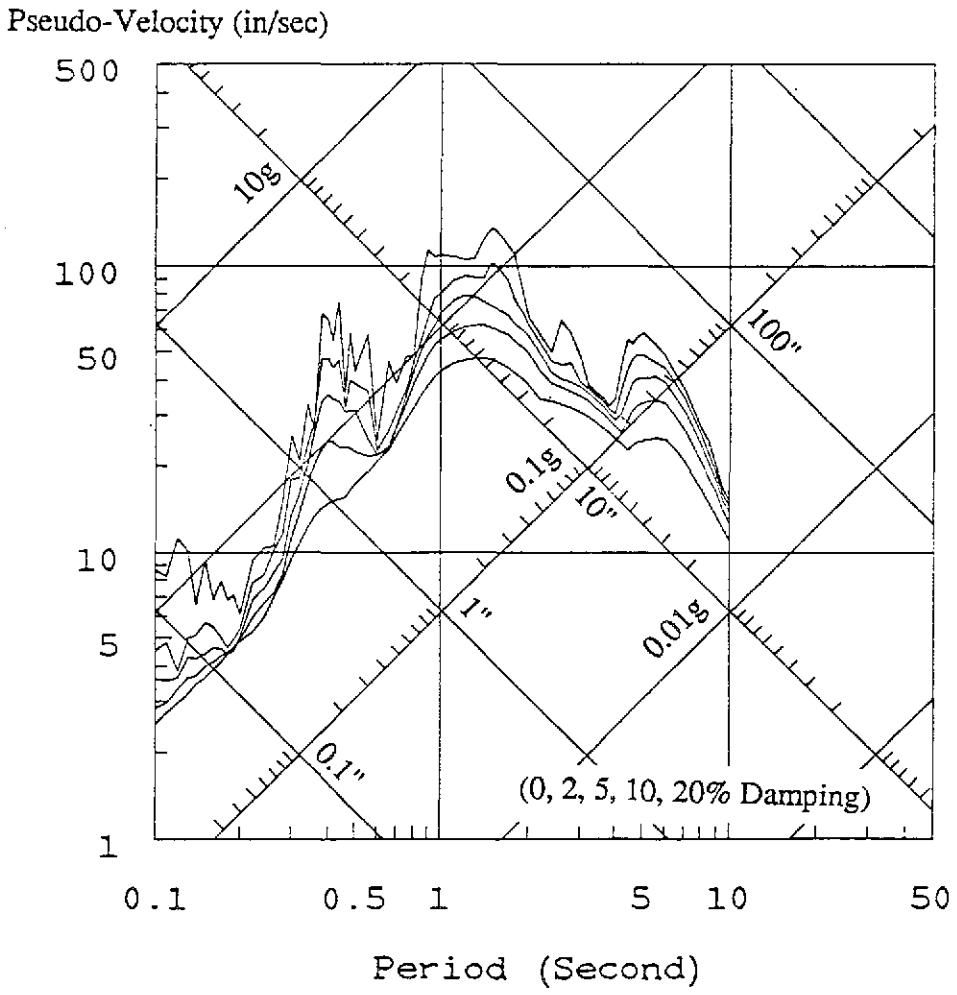

Fig. 2.6 1971 San Fernando Earthquake Ground Motion (Derived Pacoima Dam, S16E)

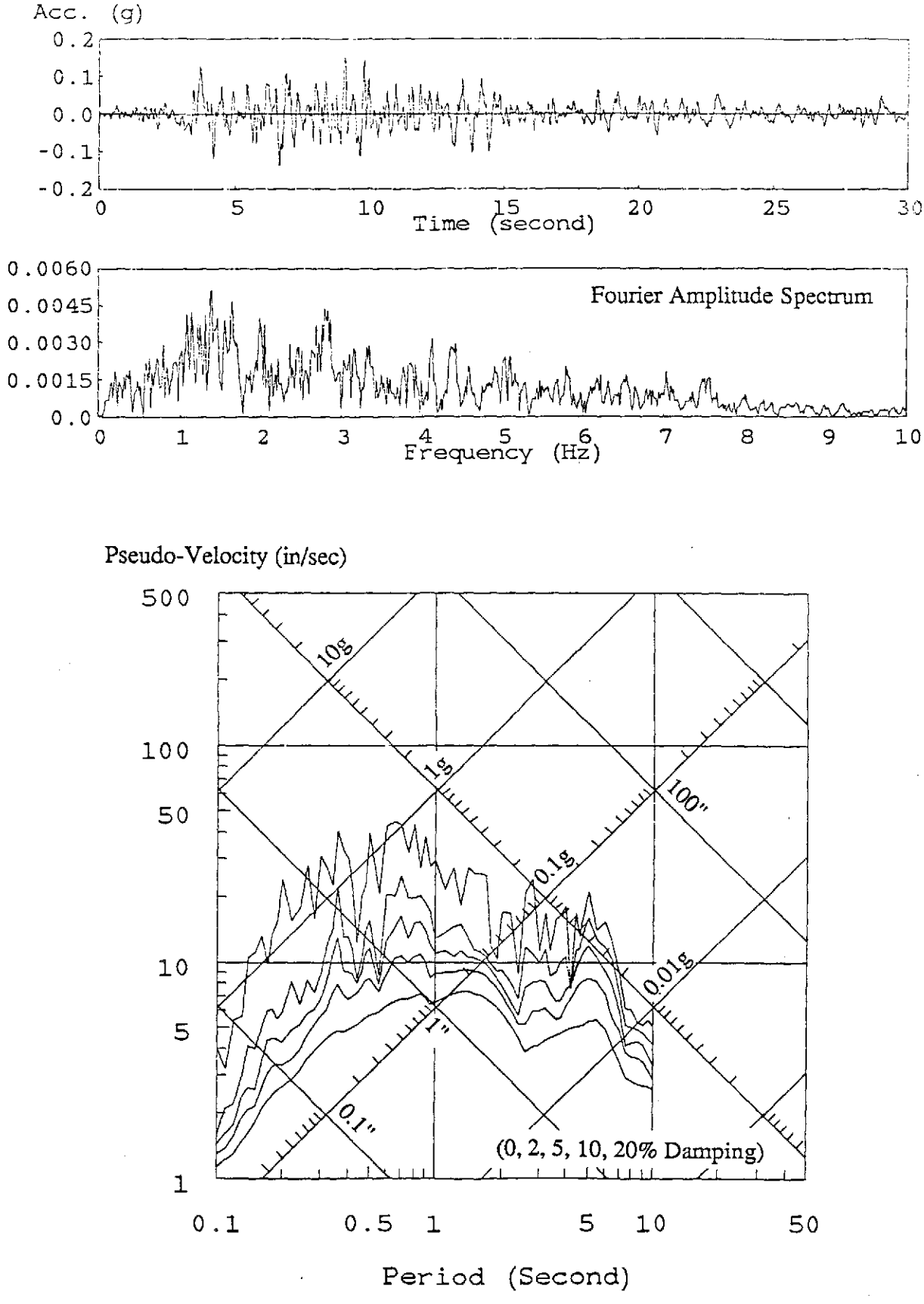

Fig. 2.7 1952 Kern County Earthquake Ground Motion (Taft, N21E)

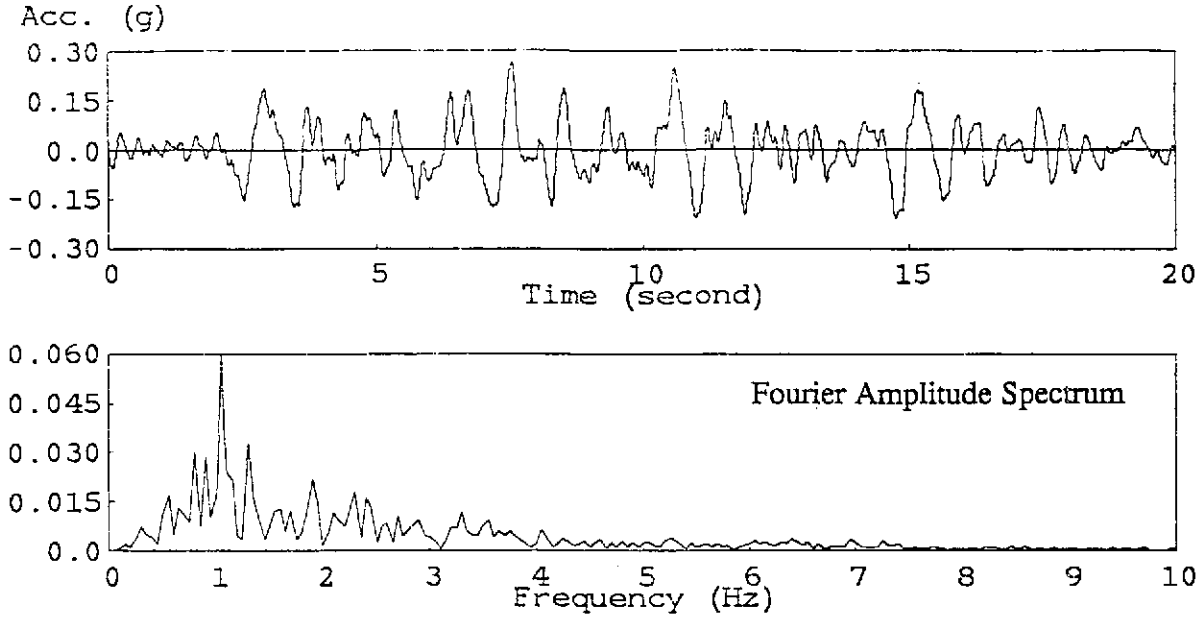

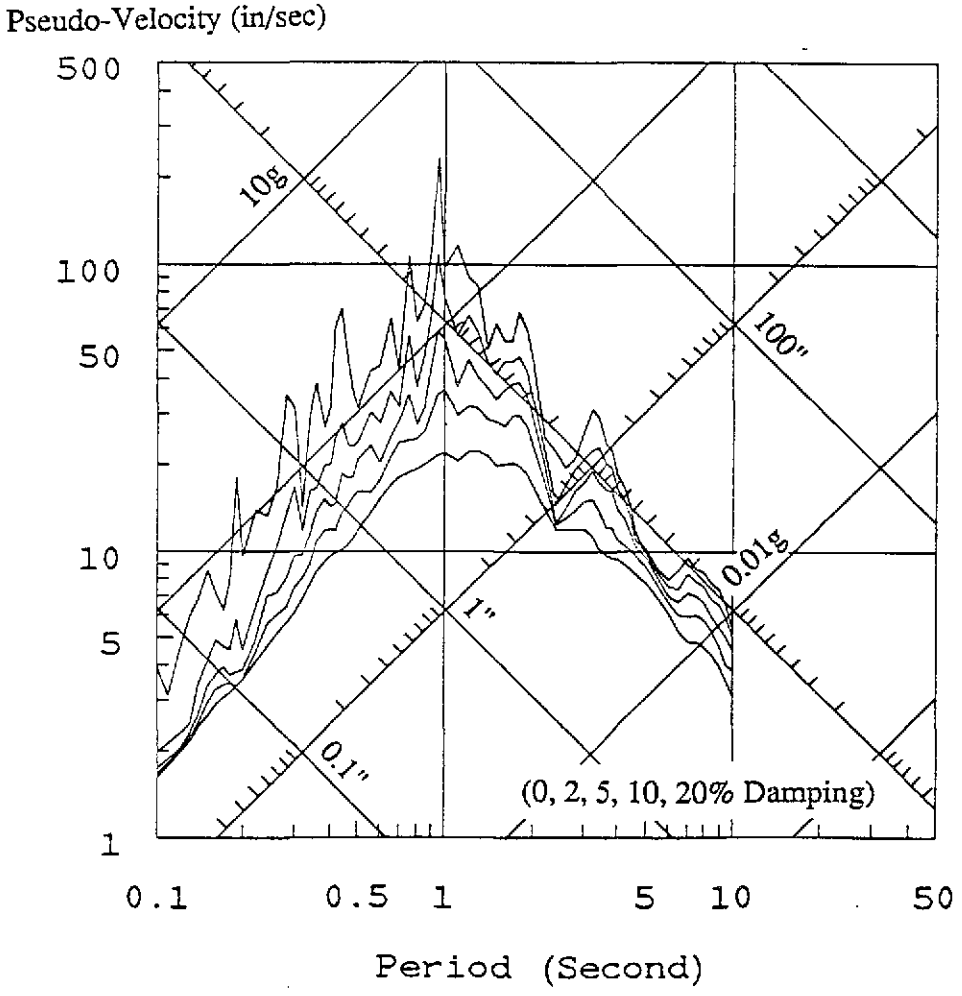

Fig. 2.8 1978 Miyagi-Ken-Oki Earthquake Ground Motion (Tohuku, N00E)

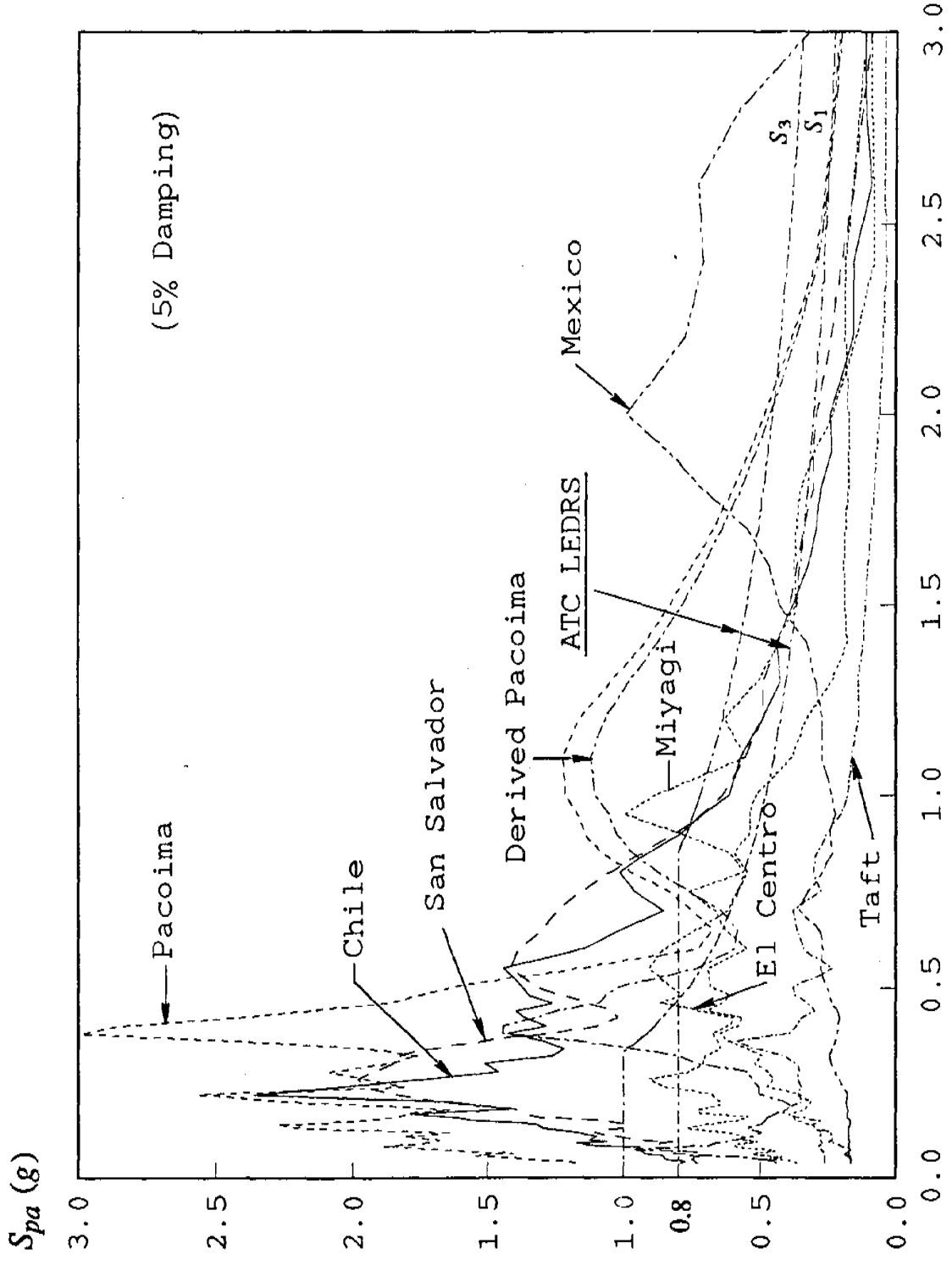

Fig. 2.9a Comparison of Pseudo-Acceleration Response Spectra and ATC LEDRS

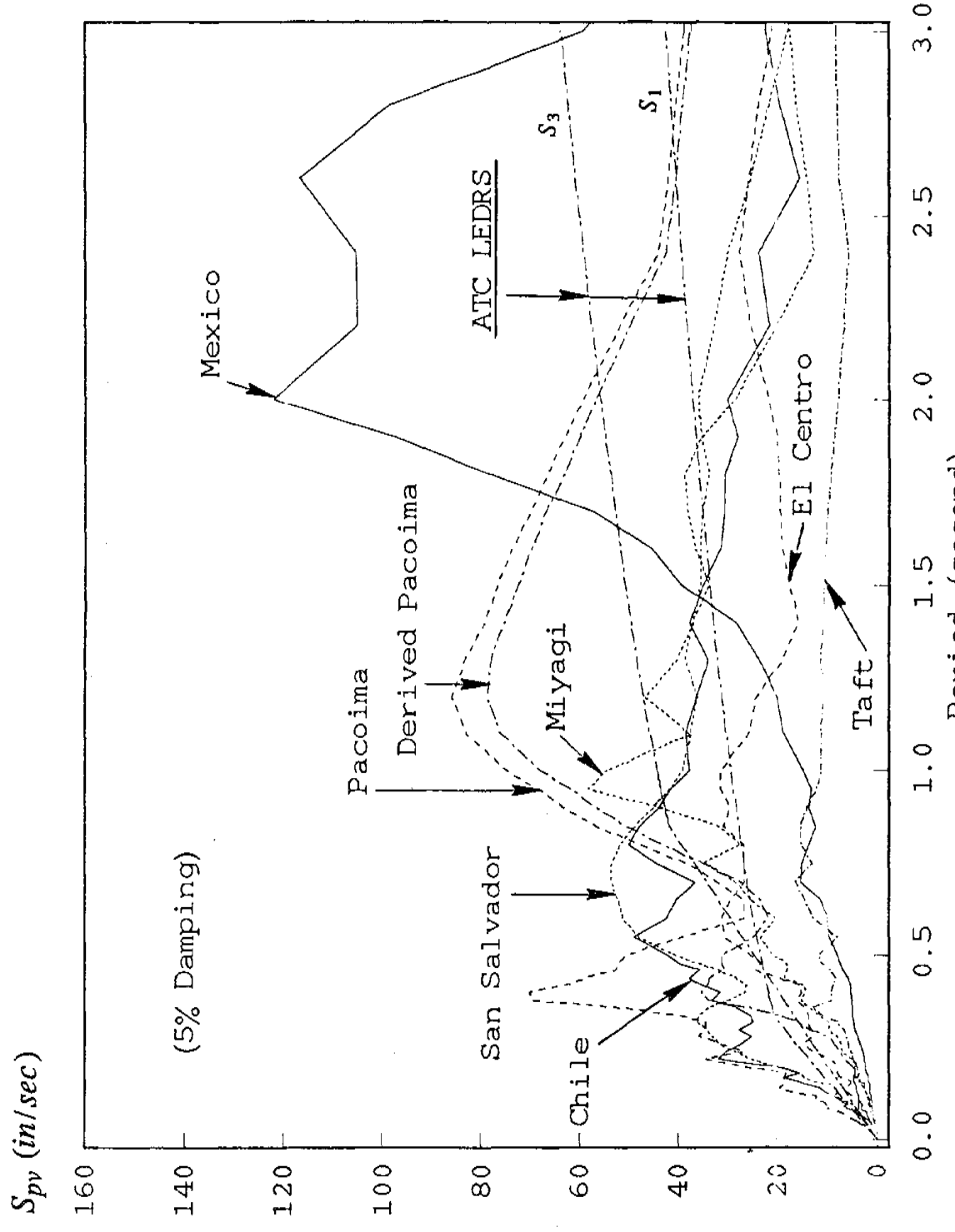

Fig. 2.9b Comparison of Pseudo-Velocity Response Spectra and ATC LEDRS

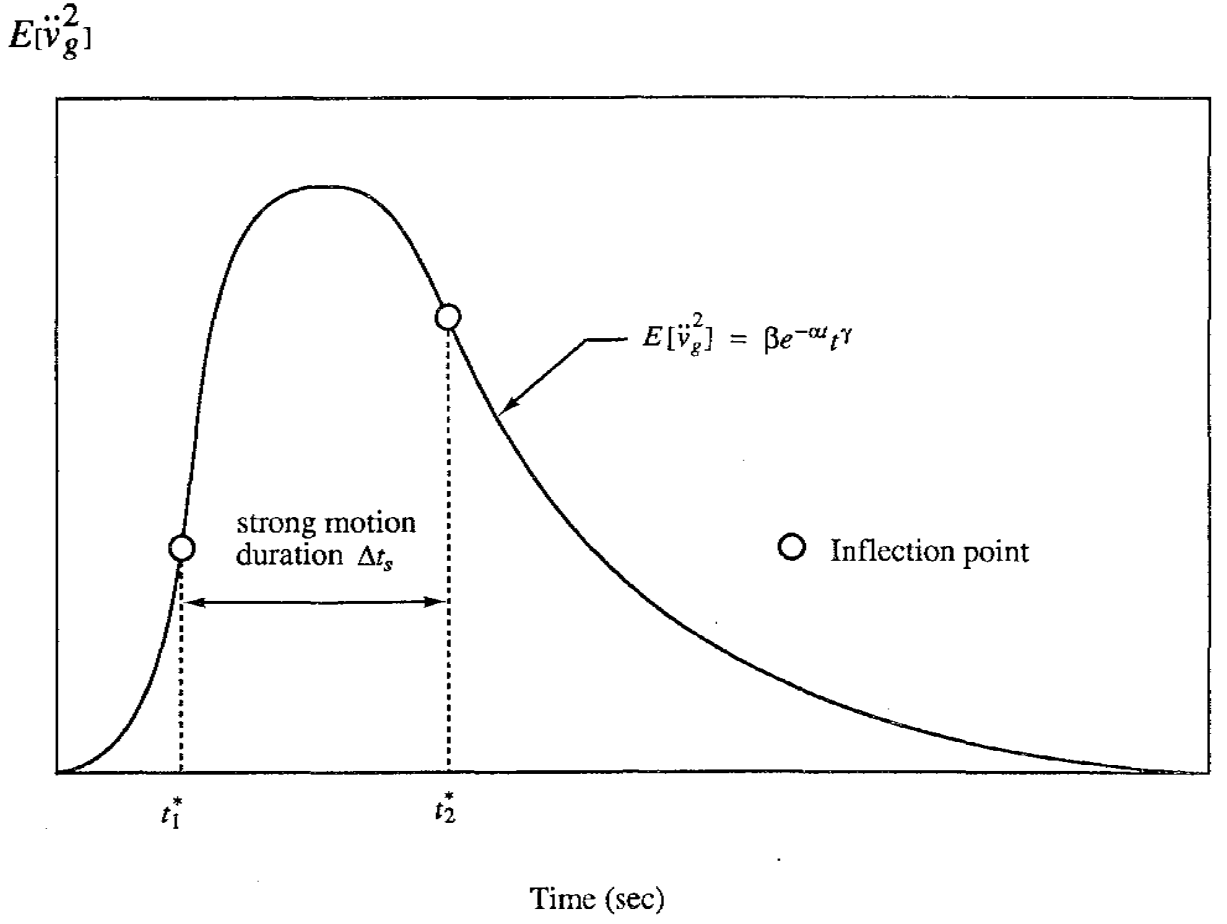

Fig. 2.10 Earthquake Mean-square Acceleration as Represented by Chi-squared Function [7]

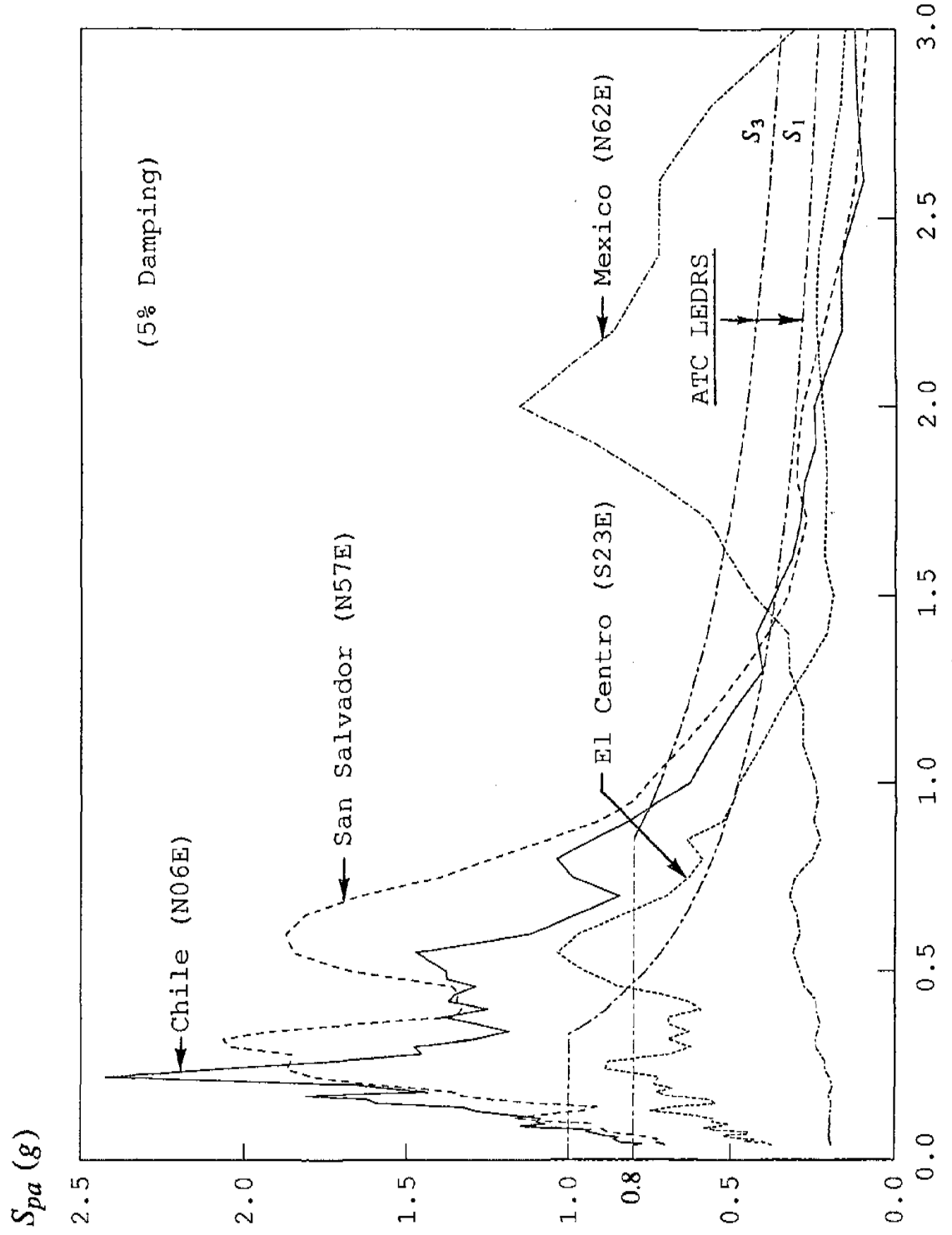

Fig. 2.11a Pseudo-Acceleration Response Spectra and ATC LEDRS (Principal Direction)

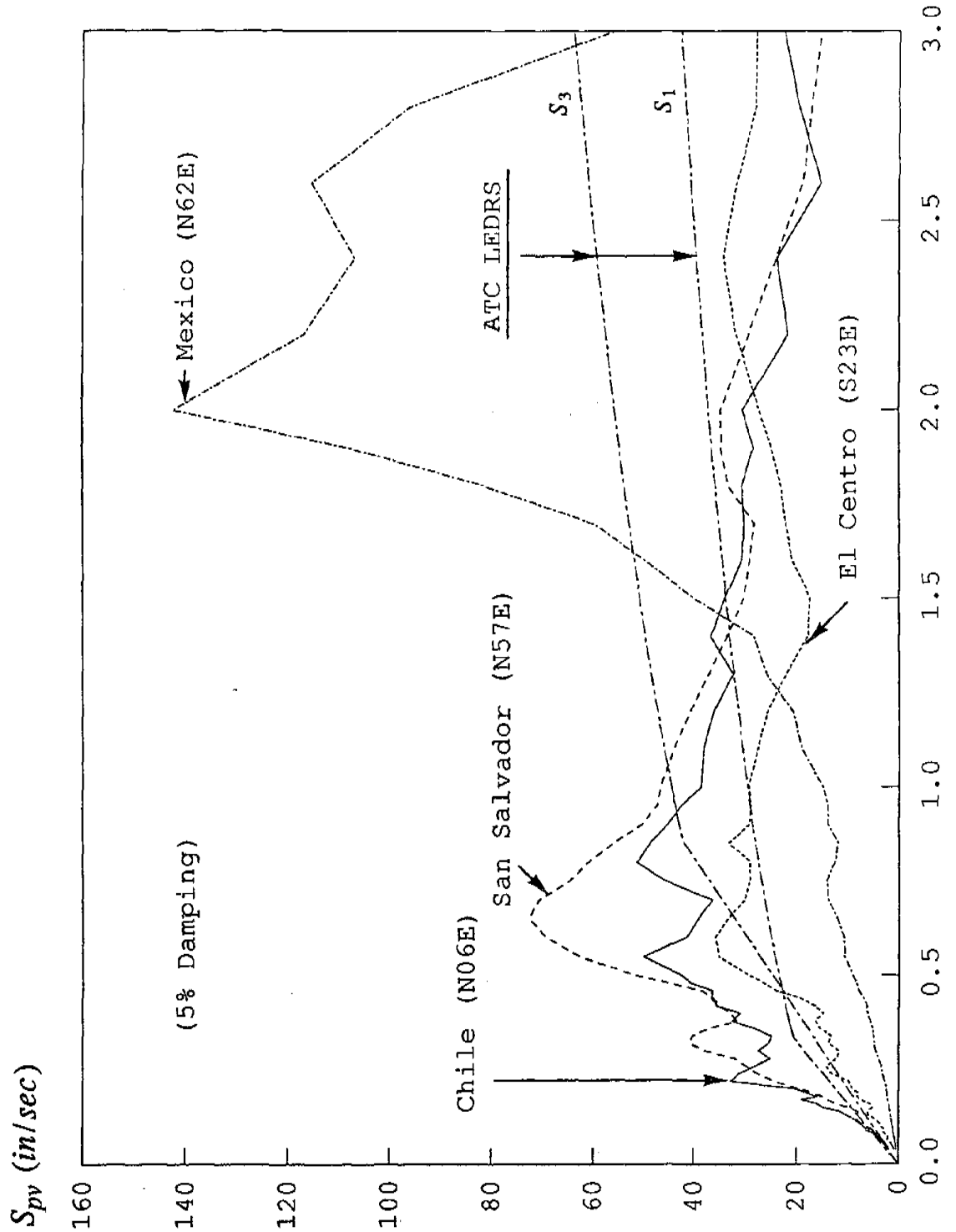

Fig. 2.11b Pseudo-Velocity Response Spectra and ATC LEDRS (Principal Direction)

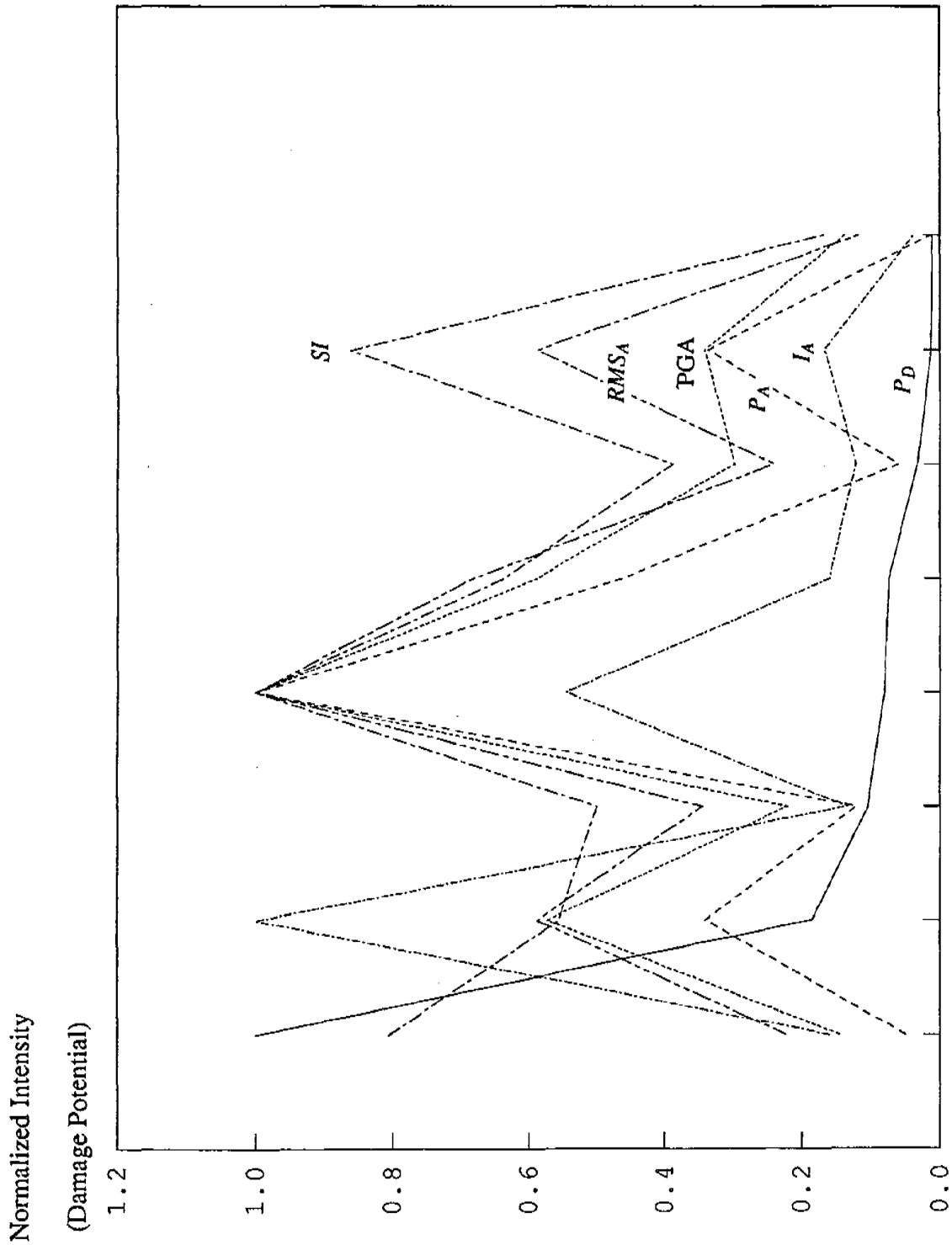

Fig. 2.12 Summary of Normalized Earthquake Ground Motion Parameters

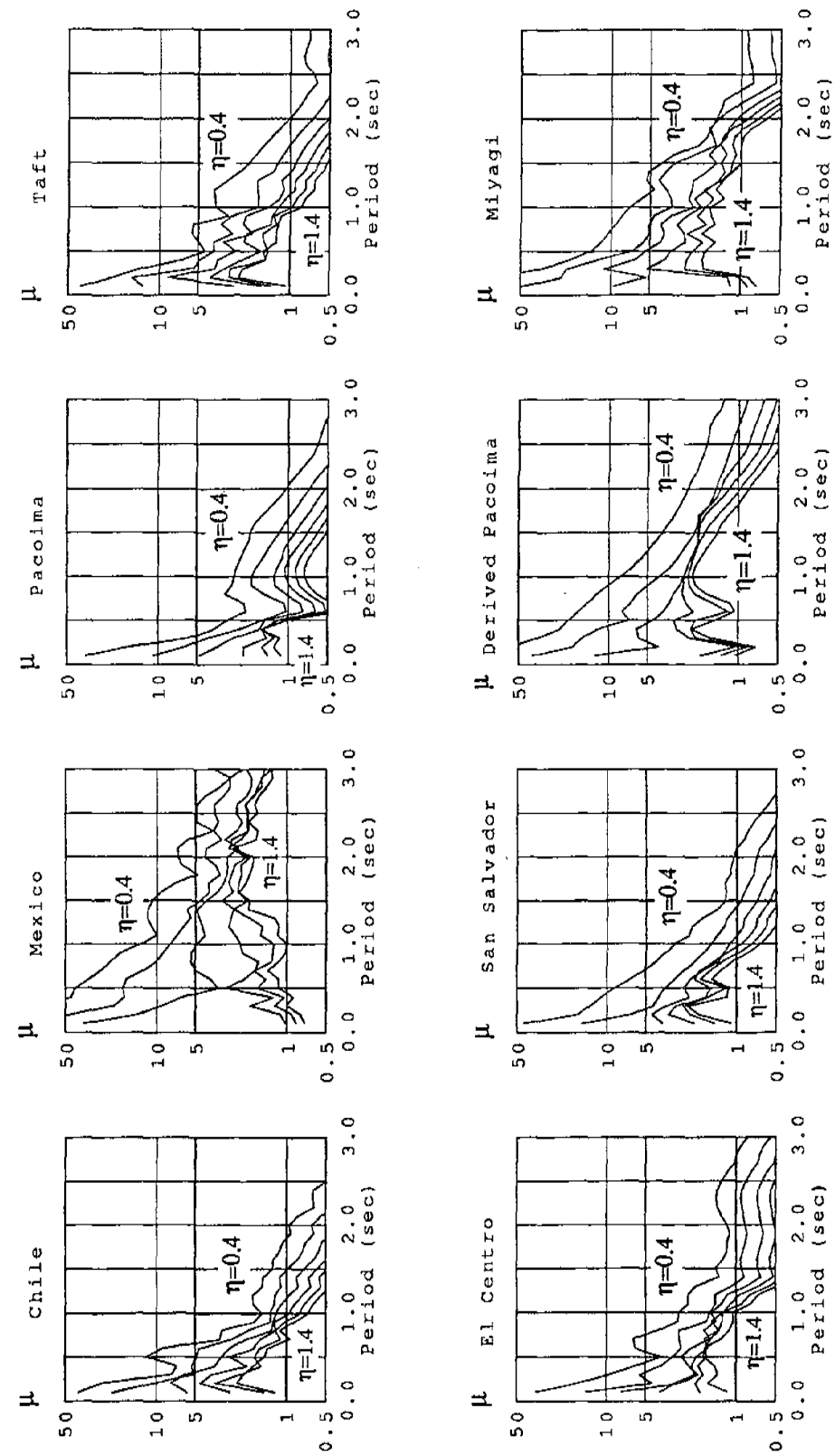

Fig. 3.1 Displacement Ductility Spectra, 5% Damping
(η from 0.4 to 1.4 in 0.2 increment)

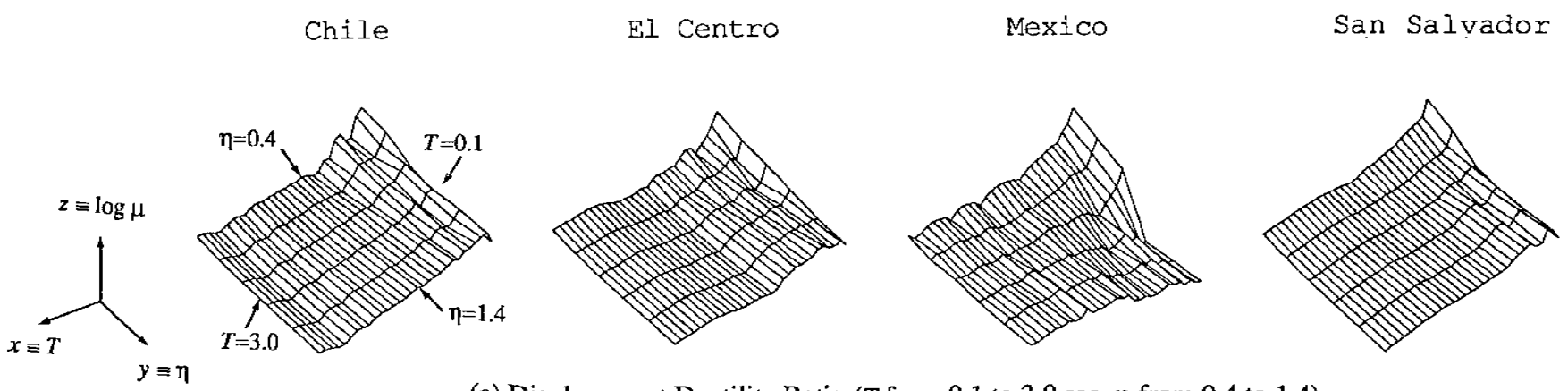

(a) Displacement Ductility Ratio (T from 0.1 to 3.0 sec, η from 0.4 to 1.4)

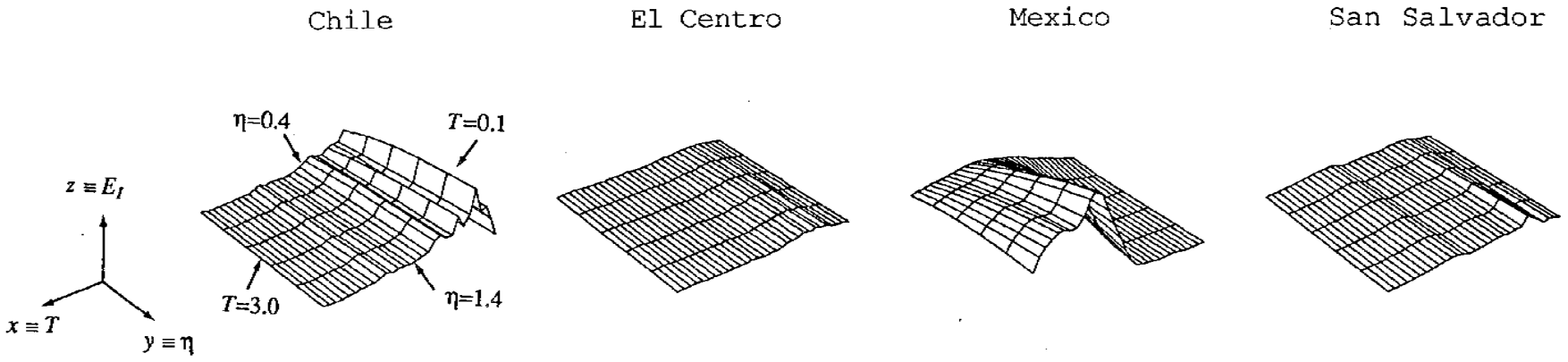

(b) Total Input Energy (T from 0.1 to 3.0 sec, η from 0.4 to 1.4)

Fig. 3.2 Constant Strength Displacement Ductility Ratio and Input Energy Spectra, 5% Damping

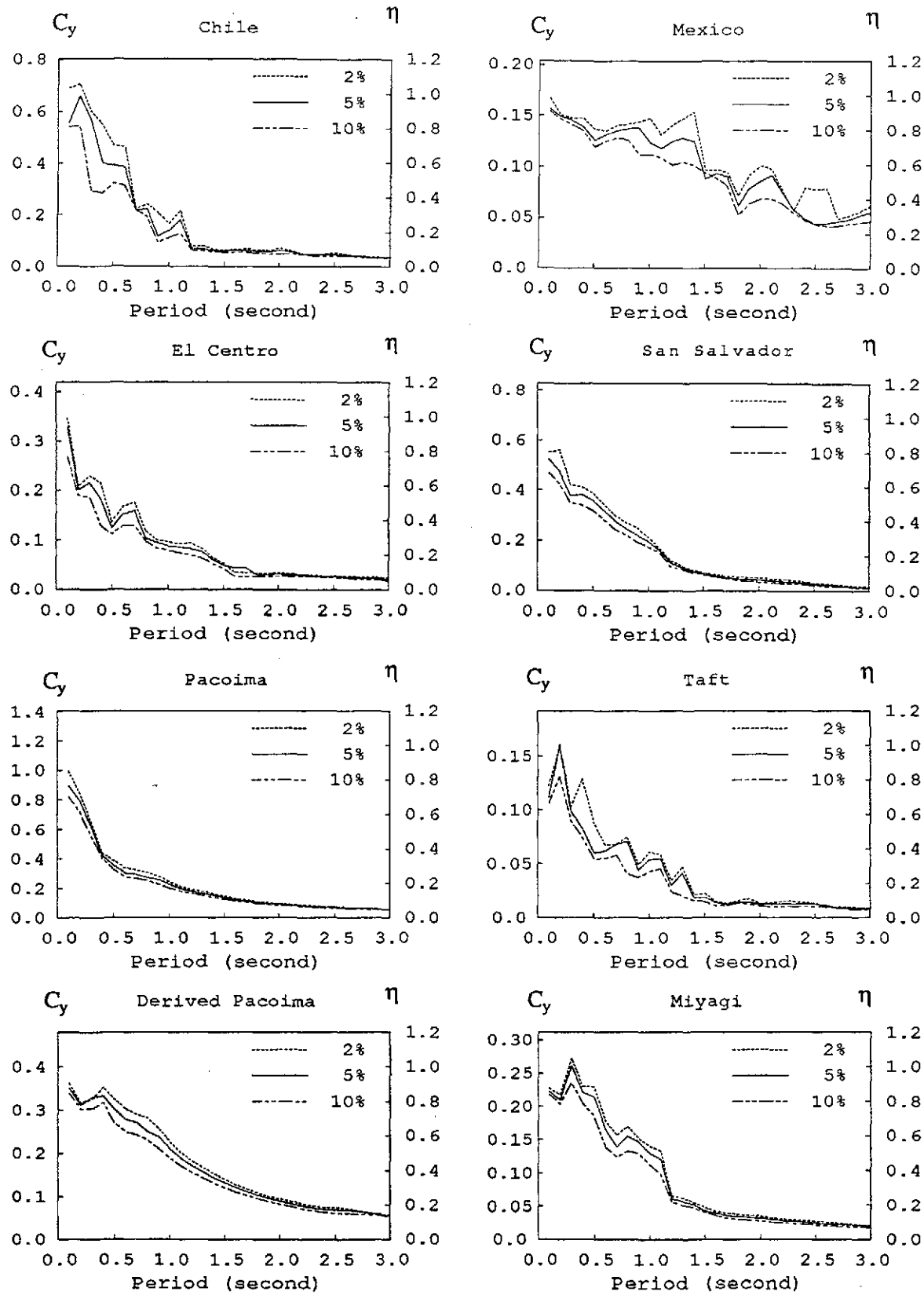

Fig. 3.3 Influence of Damping on Seismic Resistance Coefficient for Ductility 5

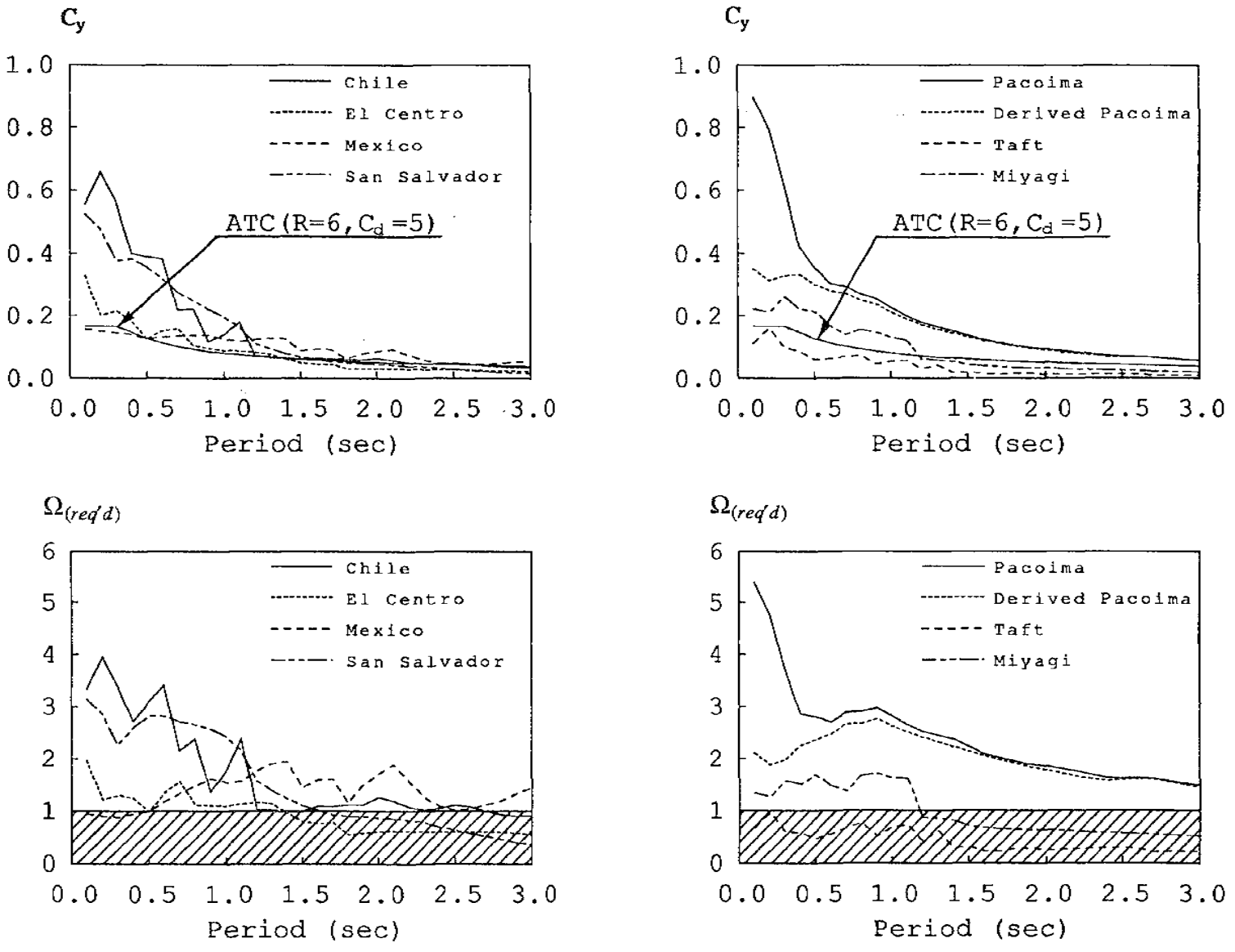

Fig. 3.4a Required Resistance Coefficient and Required Overstrength Factor with Ductility Ratio 5, 5% Damping (ATC Soil Type 1)

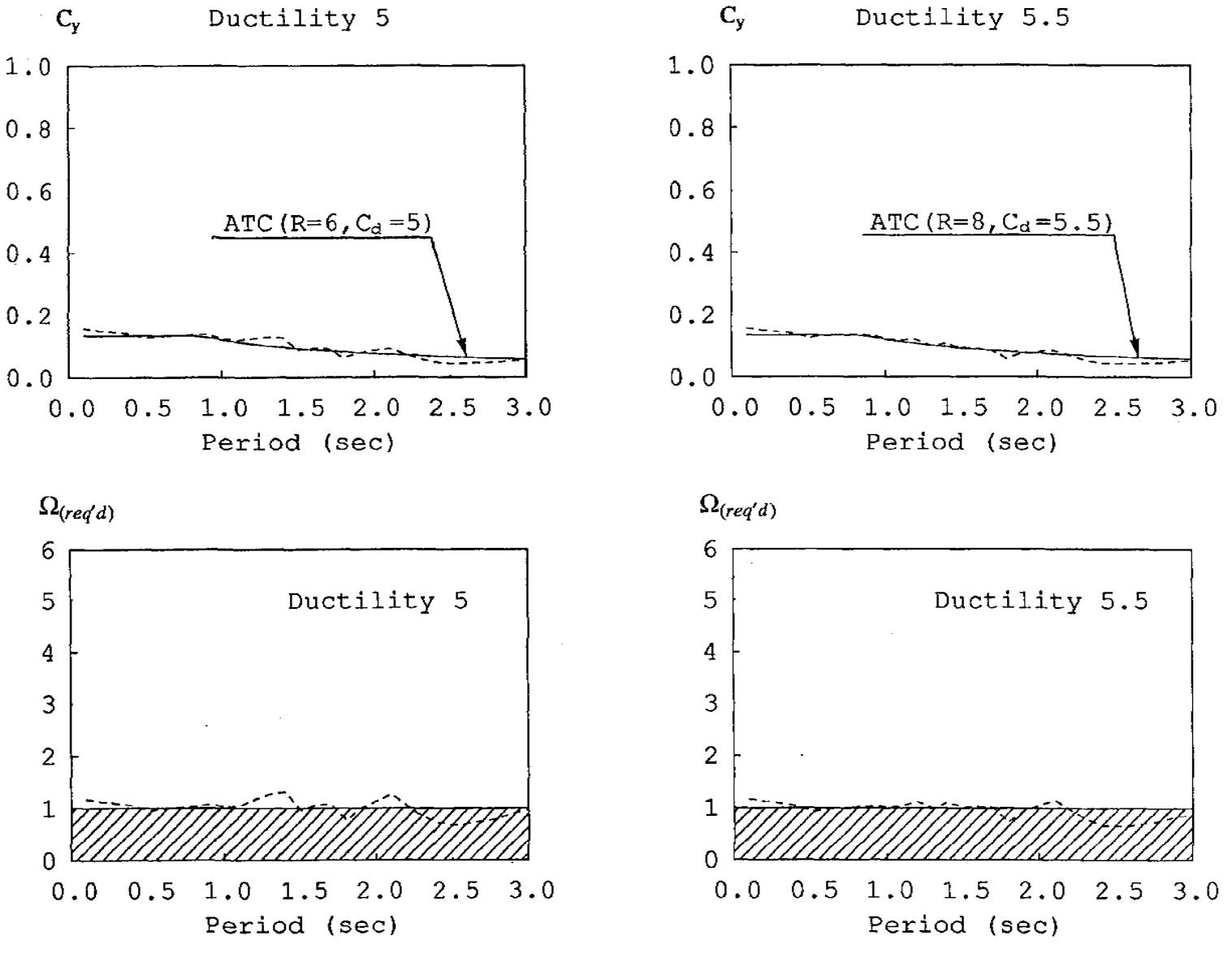

Fig. 3.4b Required Resistance Coefficient and Required Overstrength Factor
5% Damping (1985 Mexico City Earthquake, ATC Soil Type 3)

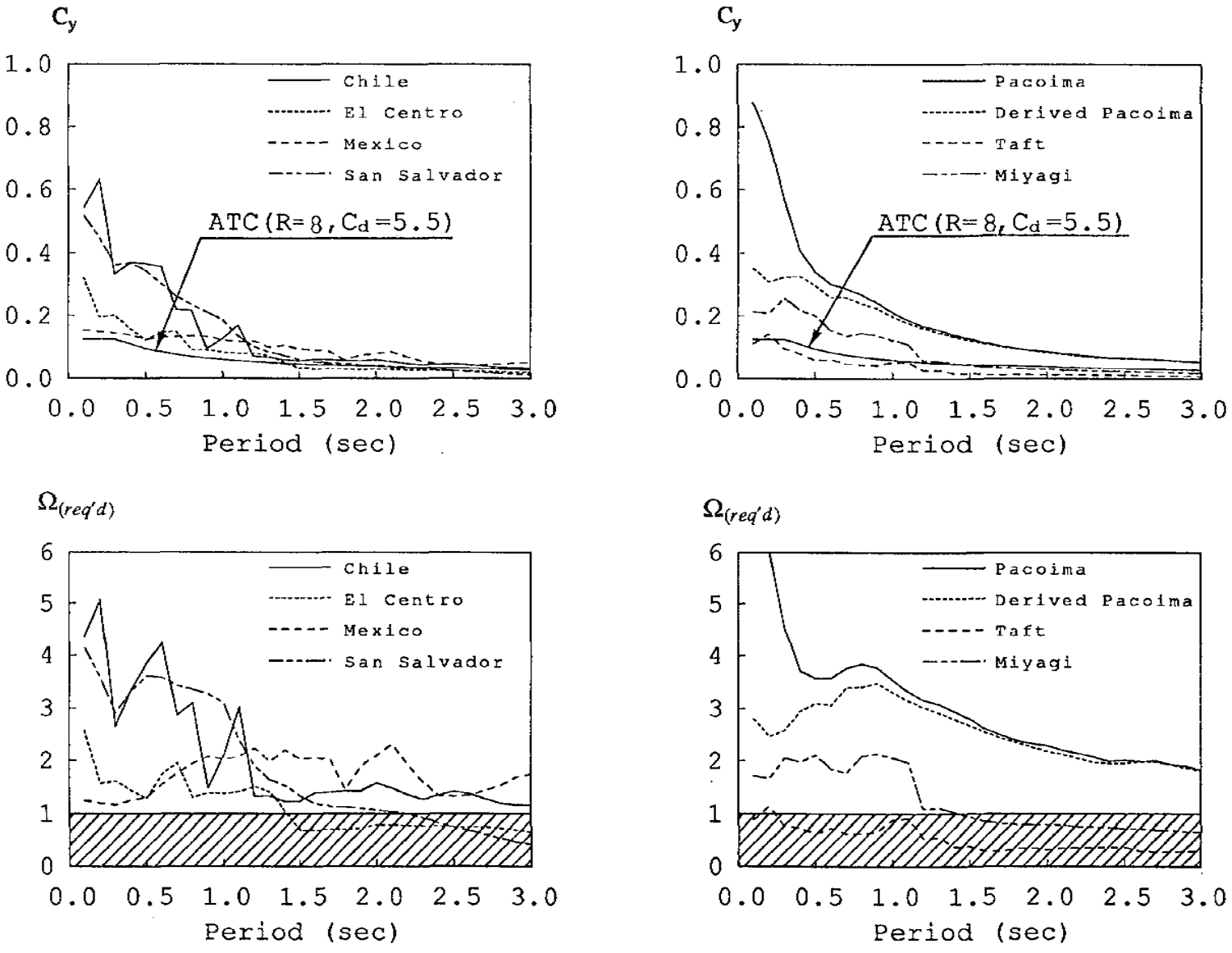

Fig. 3.5 Required Resistance Coefficient and Required Overstrength Factor with Ductility Ratio 5.5, 5% Damping (ATC Soil Type 1)

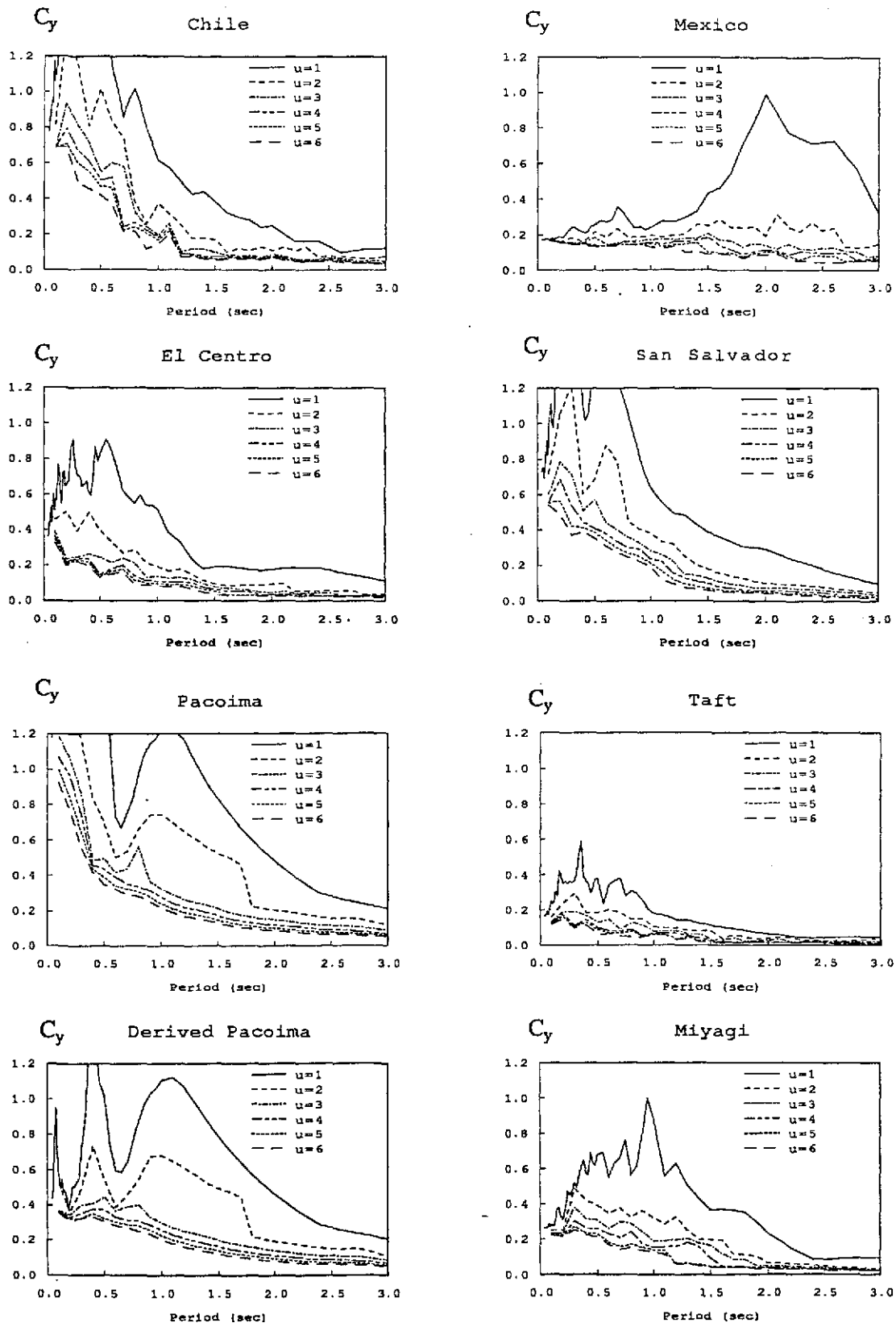

Fig. 3.6 Variation of Resistance Coefficient with Ductility Ratio (5% Damping)

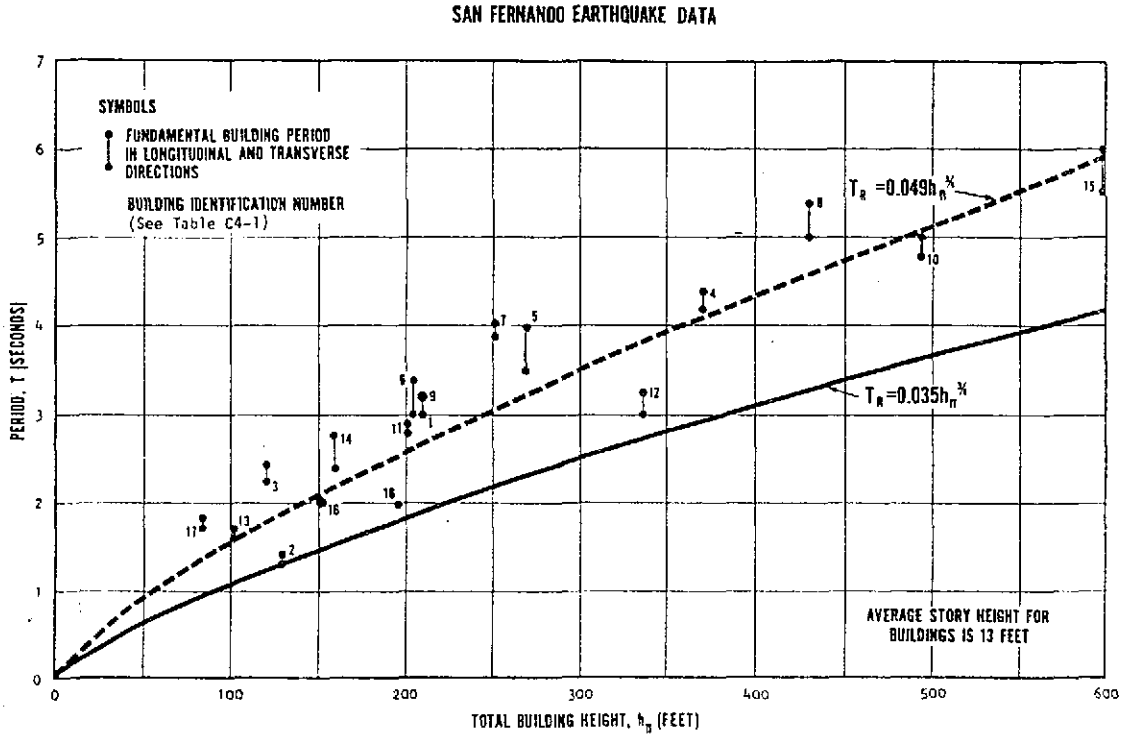

(a) Steel Frames

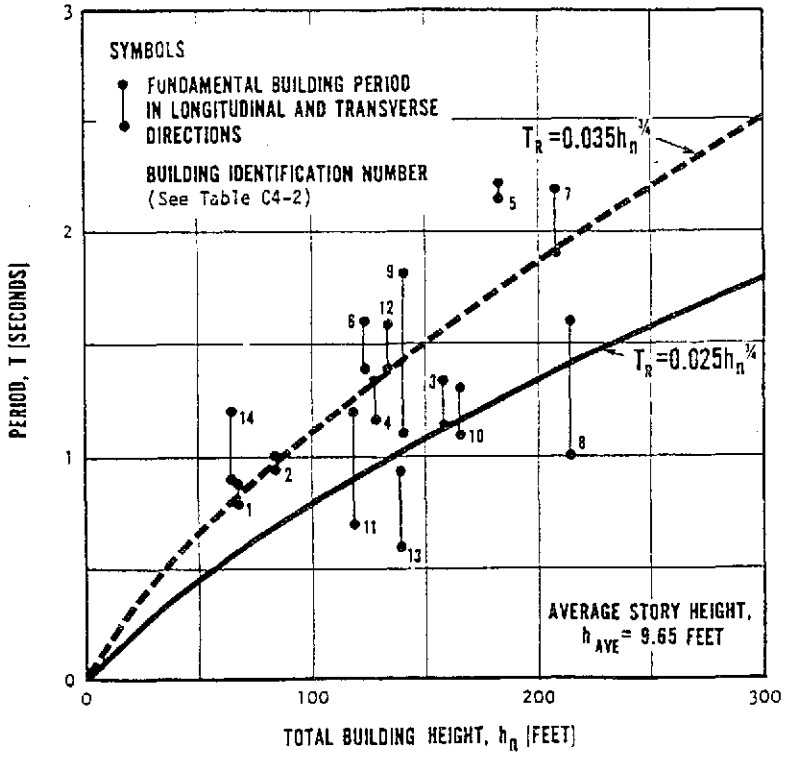

(b) Reinforced Concrete Frames

Fig. 3.7 Measured Fundamental Periods during the 1971 San Fernando Earthquake [11]

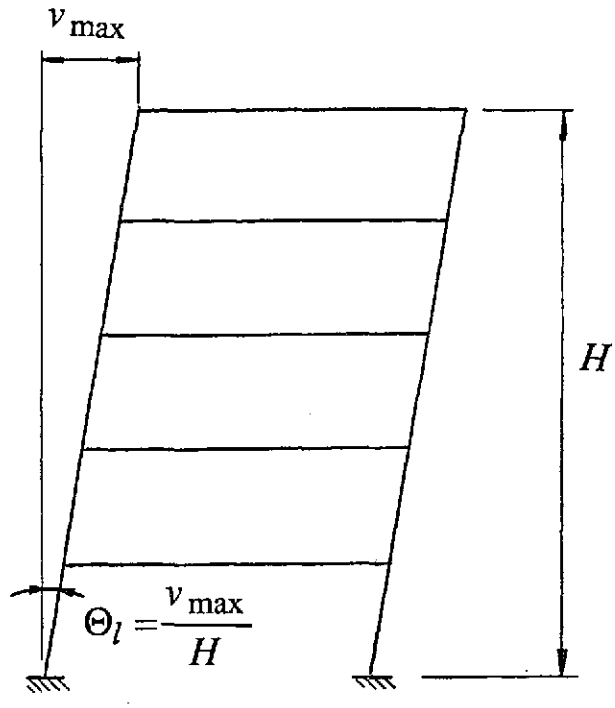

(a) Uniform Drift Index Distribution along Height

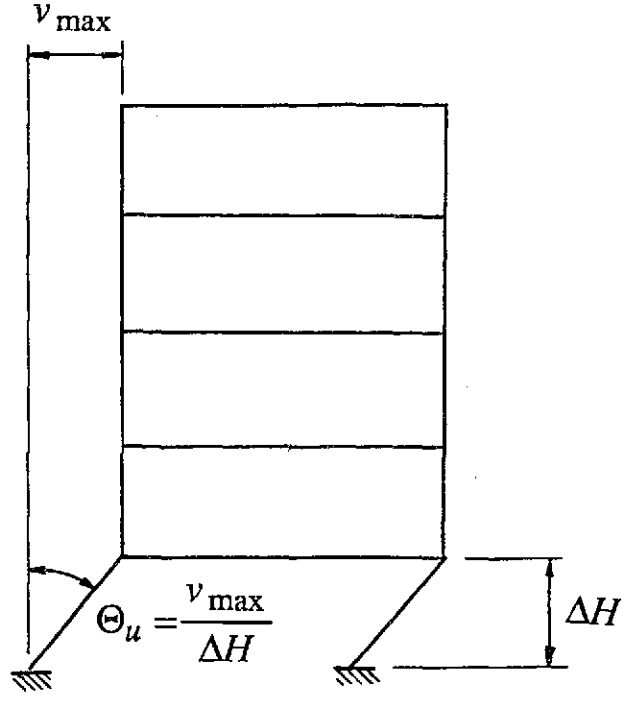

(b) Soft First Story Formation

Fig. 3.8 Calculation of Inter-story Drift Index

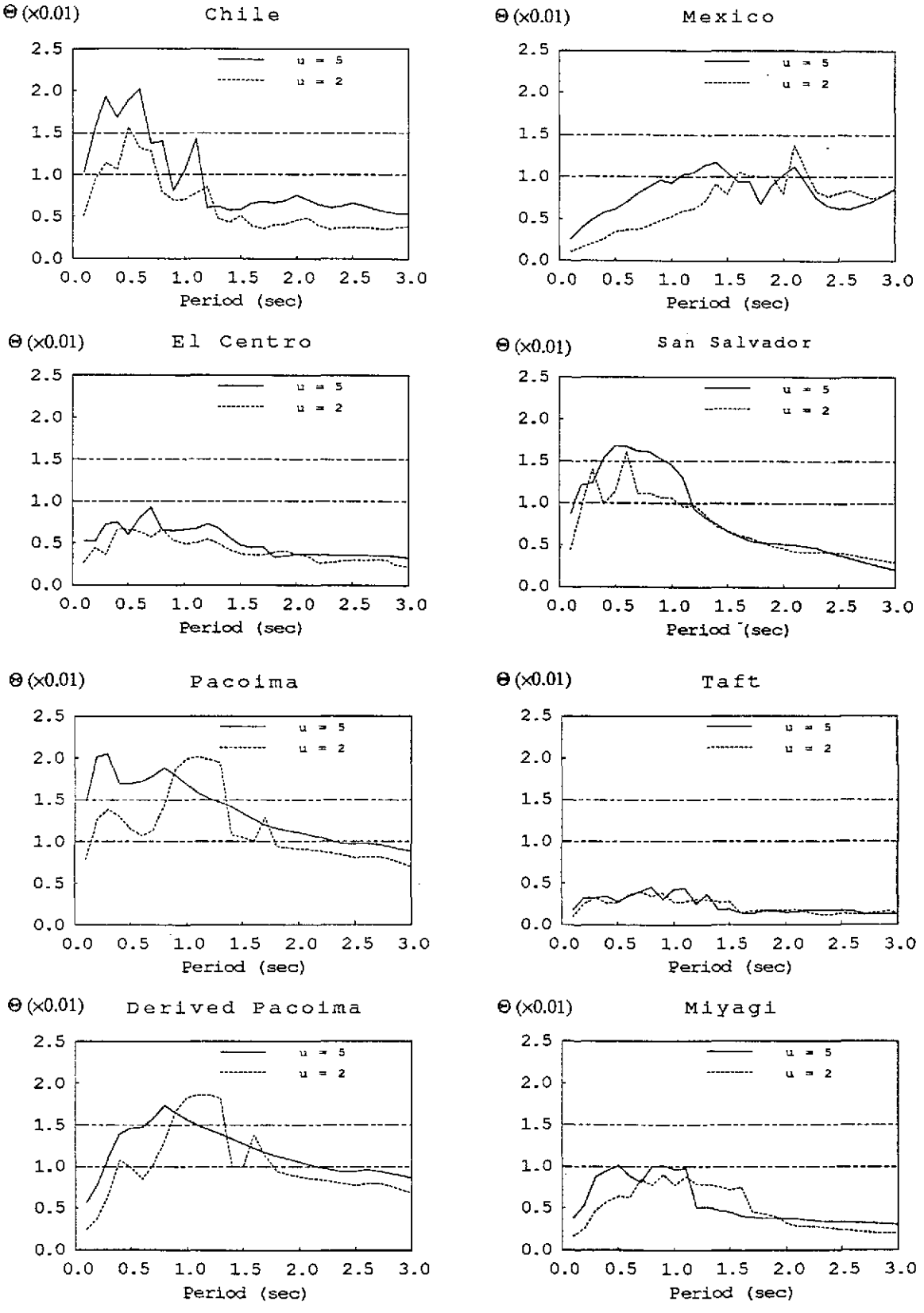

Fig. 3.9a Lower Bound Drift Index Spectra for Ductility Ratios 2 and 5 (5% Damping)

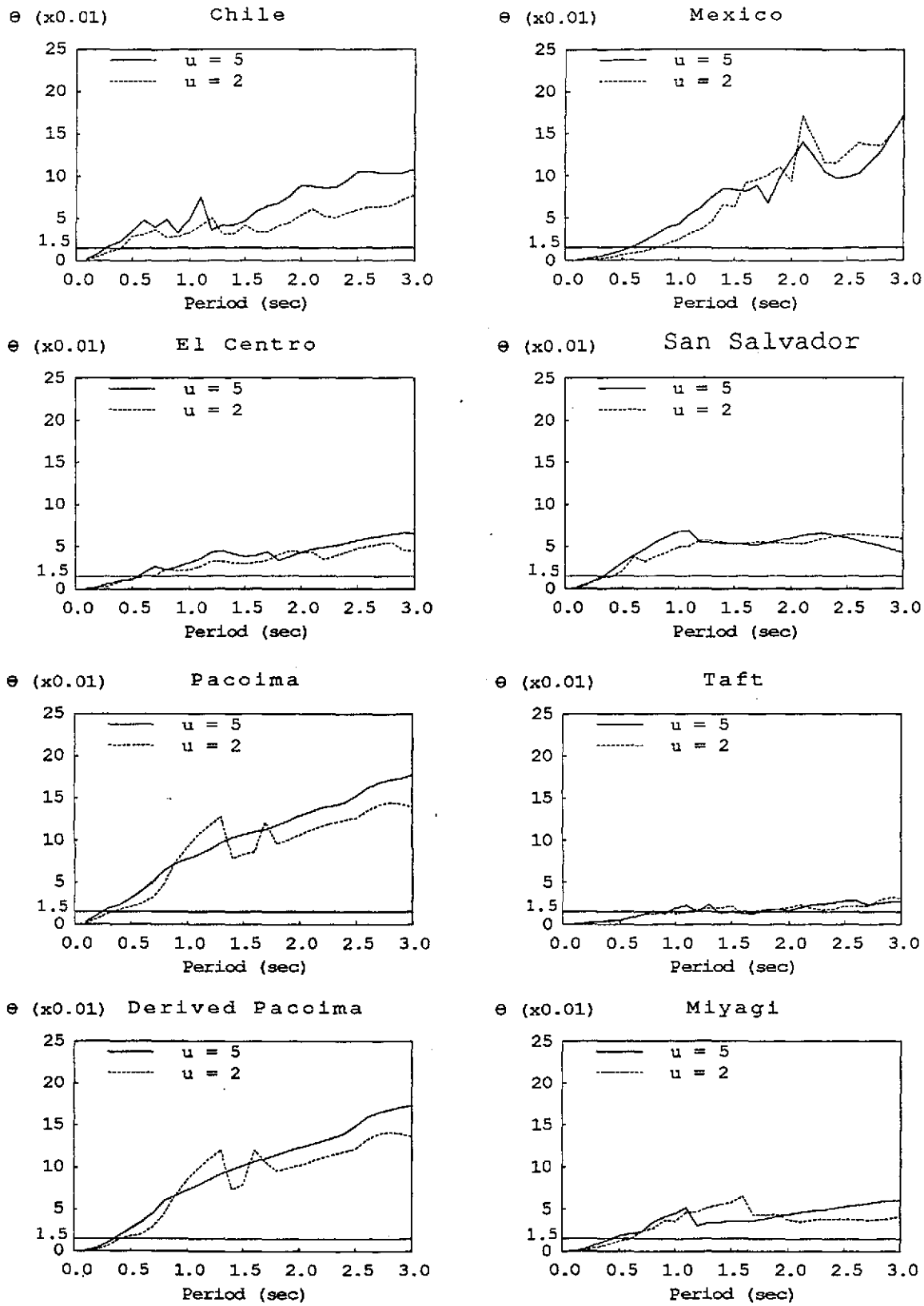

Fig. 3.9b Upper Bound Drift Index Spectra for Ductility Ratios 2 and 5 (5% Damping)

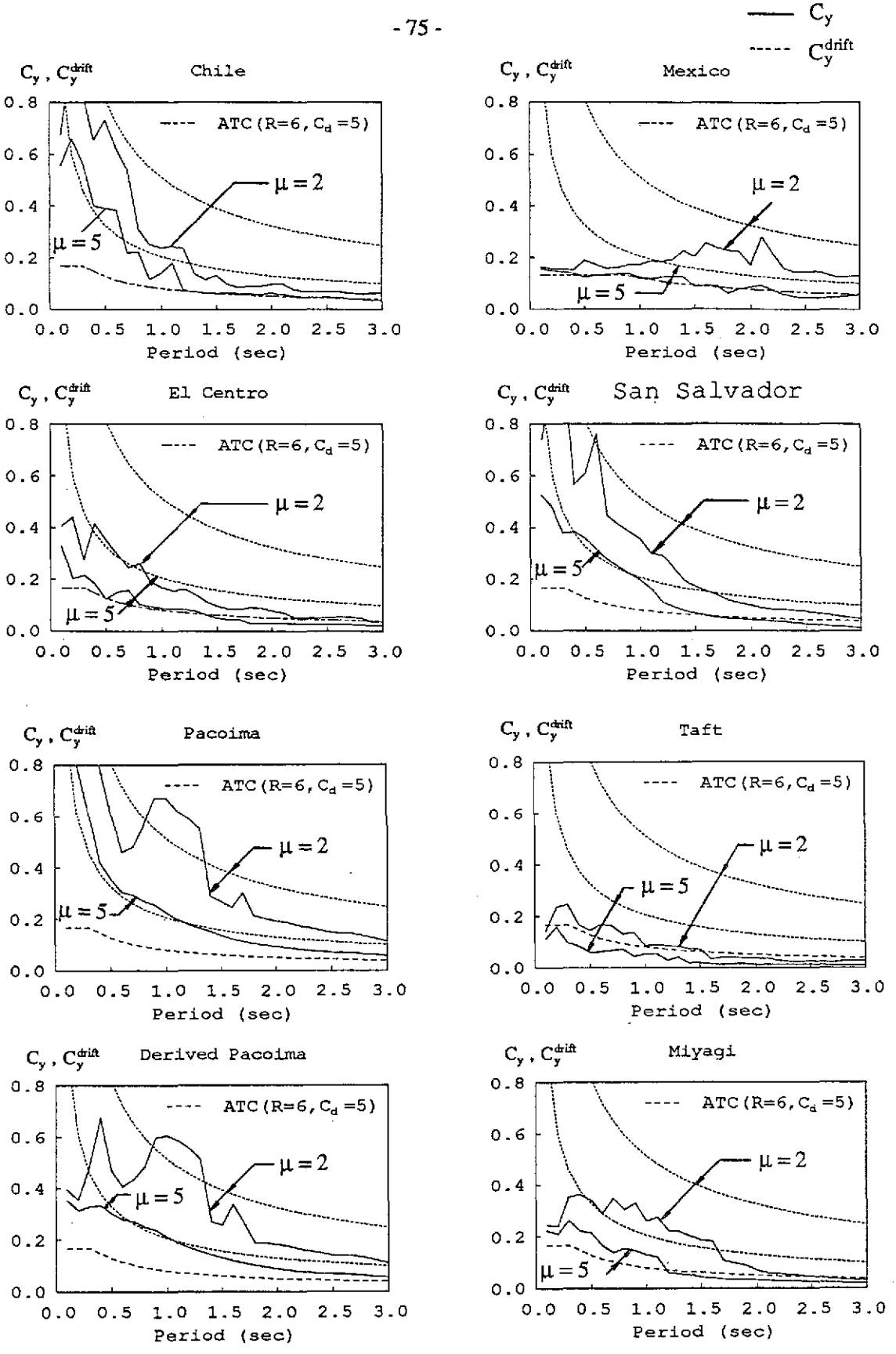

Fig. 3.10 Comparison of C_y and C_y^{drift} Spectra ($\Theta_{max} = 0.015$)

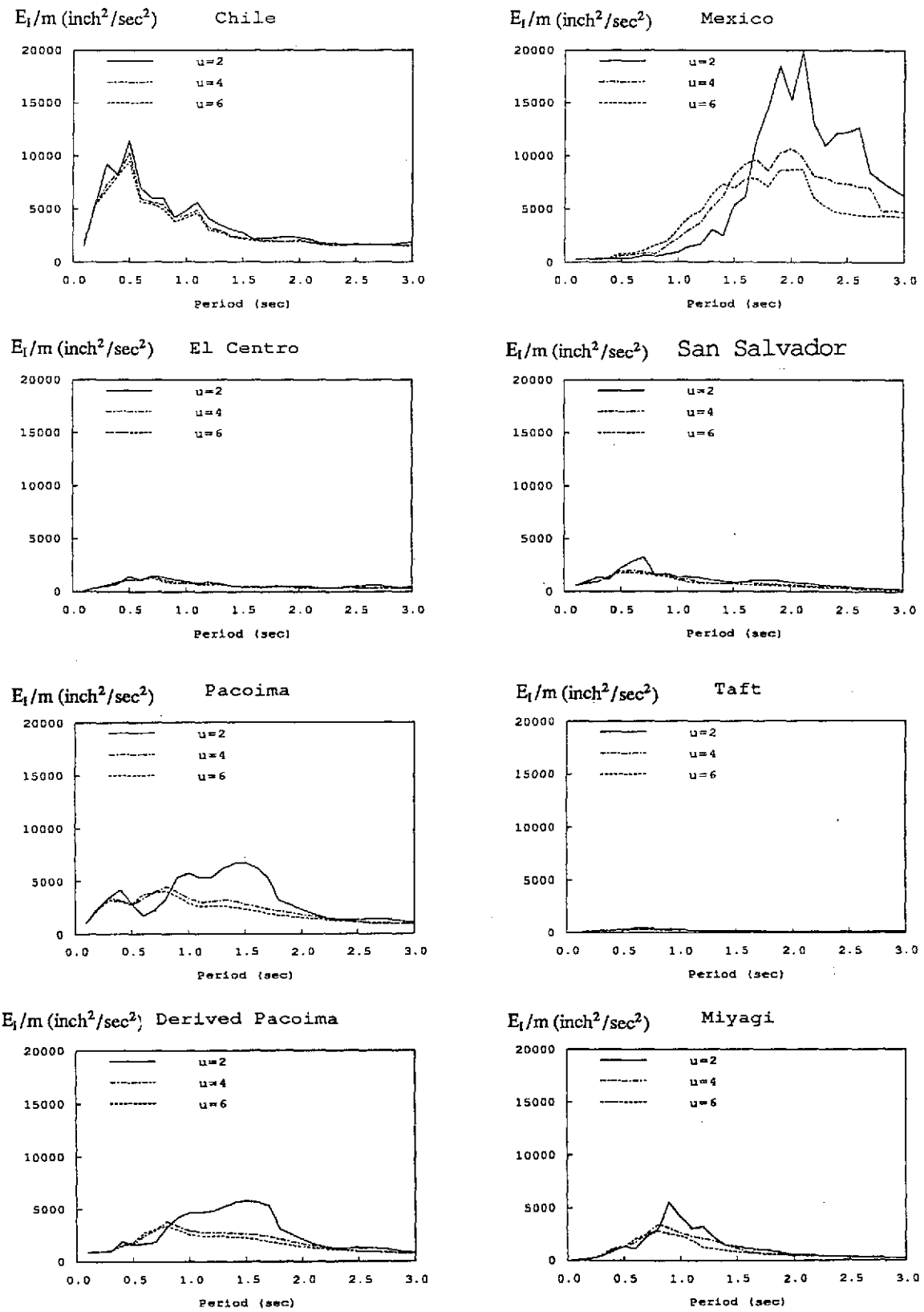

Fig. 3.11 Input Energy Spectra for Ductility Ratios 2,4 and 6 (5% Damping)

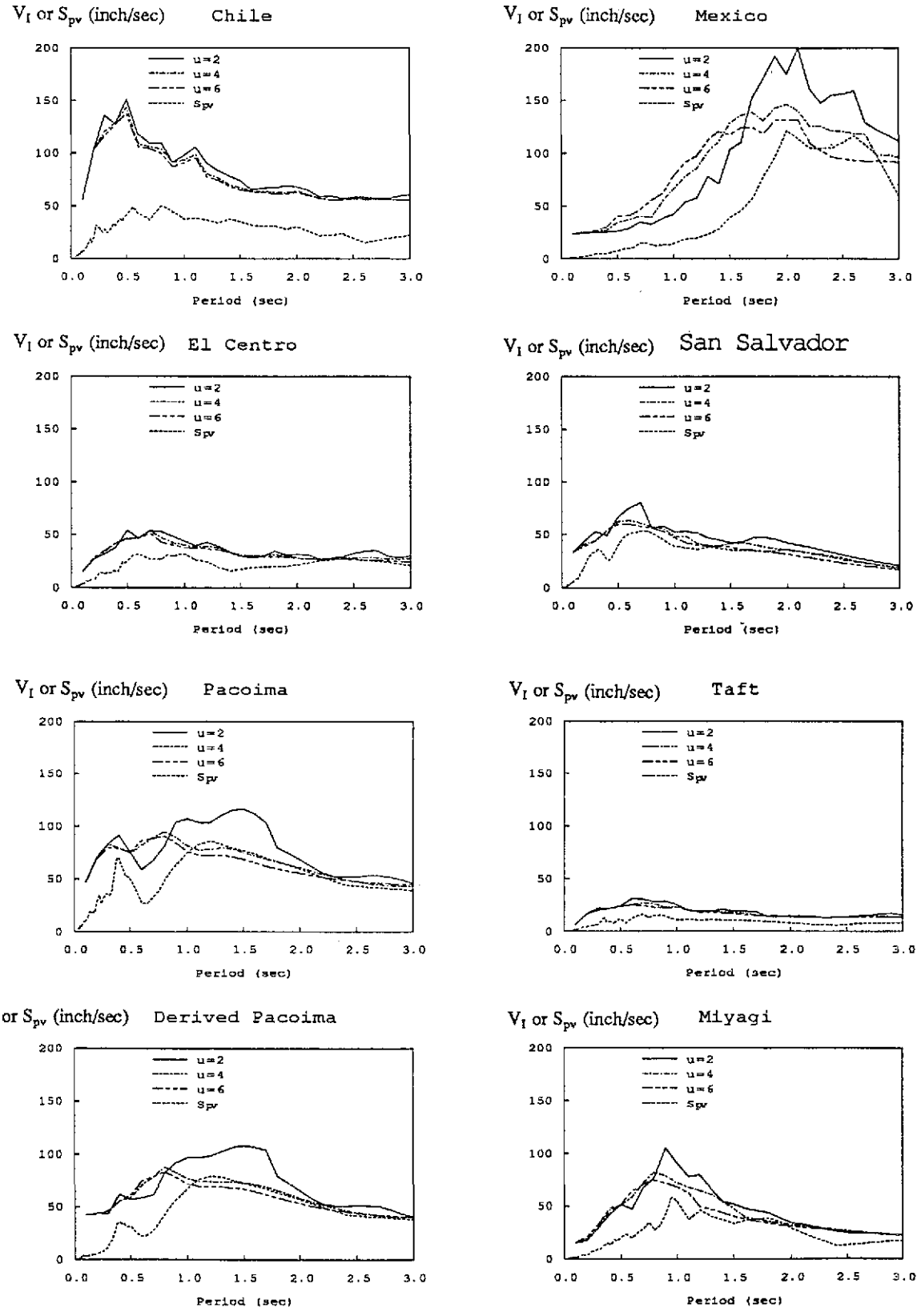

Fig. 3.12 Input Energy Equivalent Velocity V_I and Linear Elastic Pseudo-Velocity S_{pv} Spectra for Ductility Ratios 2,4 and 6 (5% Damping)

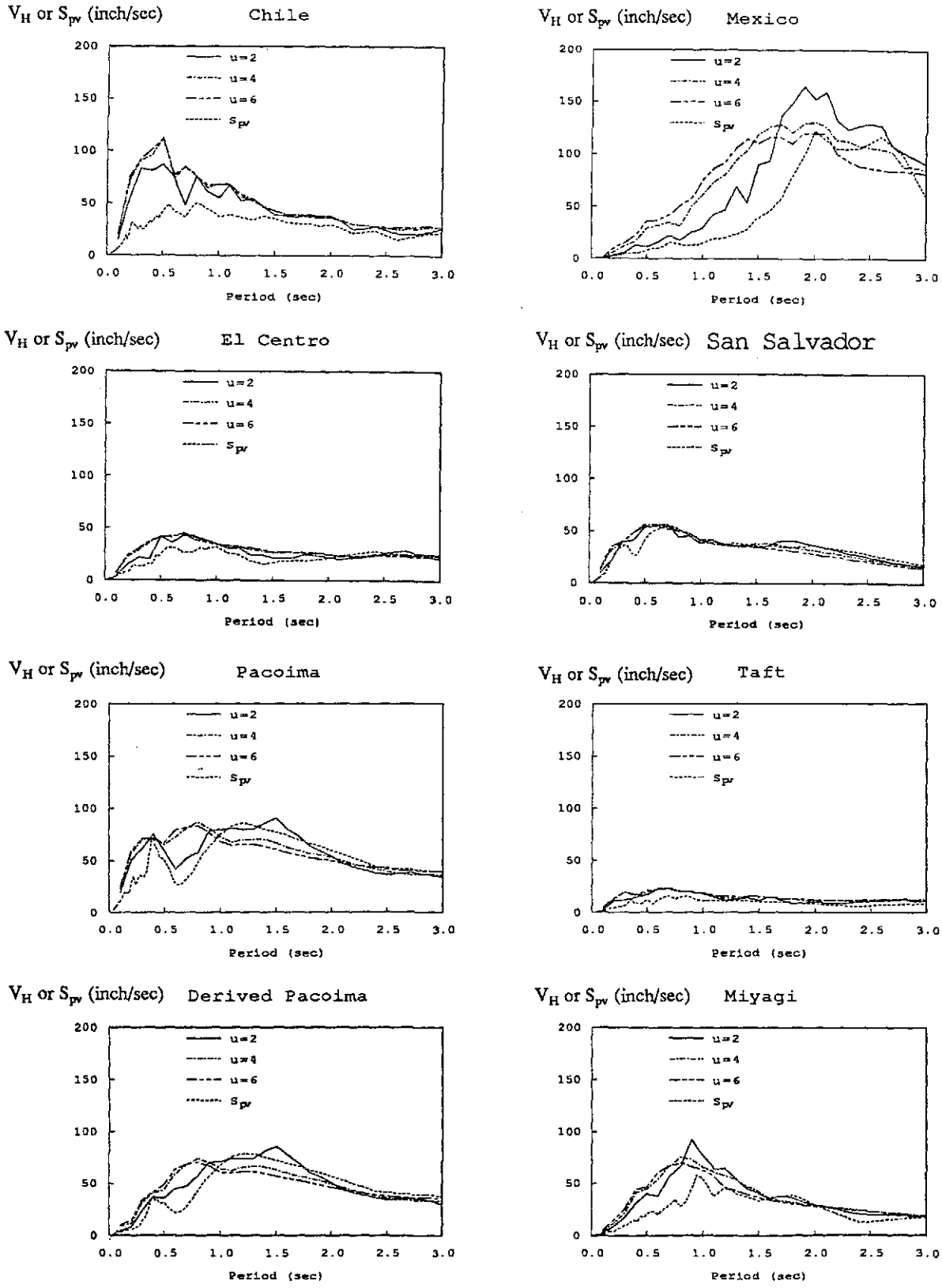

Fig. 3.13 Hysteretic Energy Equivalent Velocity V_H and Linear Elastic Pseudo-Velocity S_{pv} Spectra for Ductility Ratios 2,4 and 6 (5% Damping)

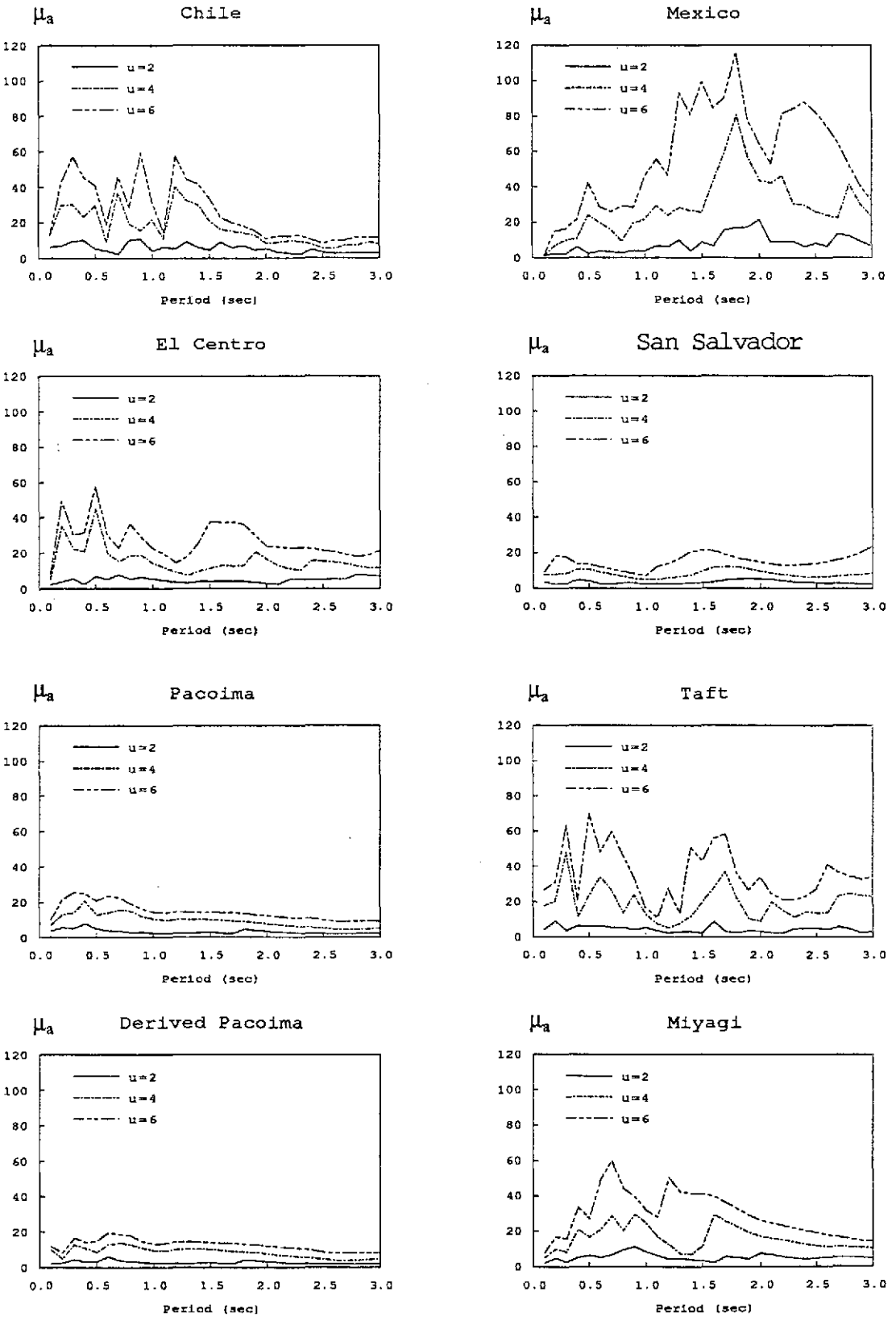

Fig. 3.14 Cumulative Displacement Ductility Ratio Spectra for Ductility Ratios 2,4 and 6 (5% Damping)

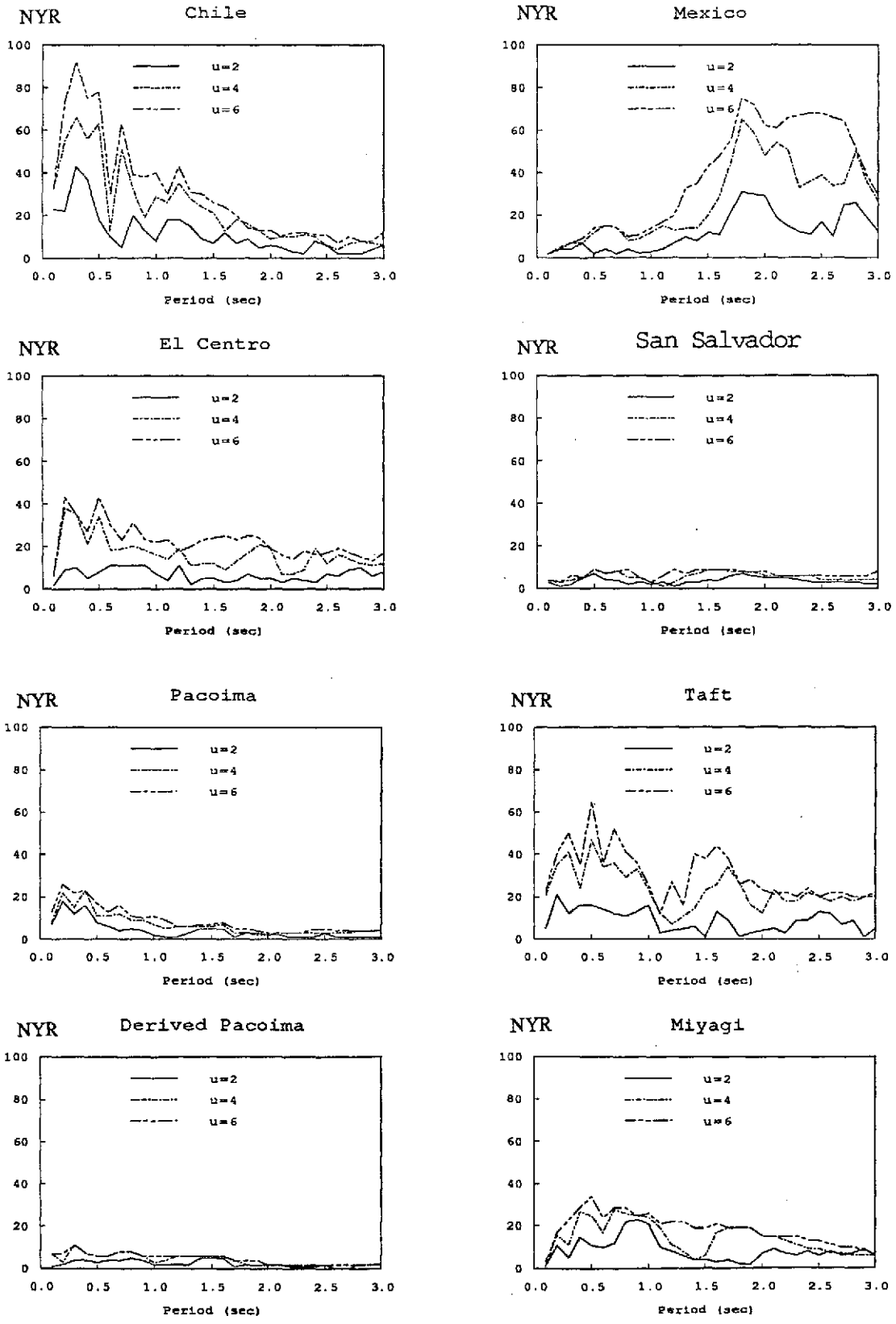

Fig. 3.15 Number of Yield Reversal (NYR) Spectra for Ductility Ratios 2,4 and 6 (5% Damping)

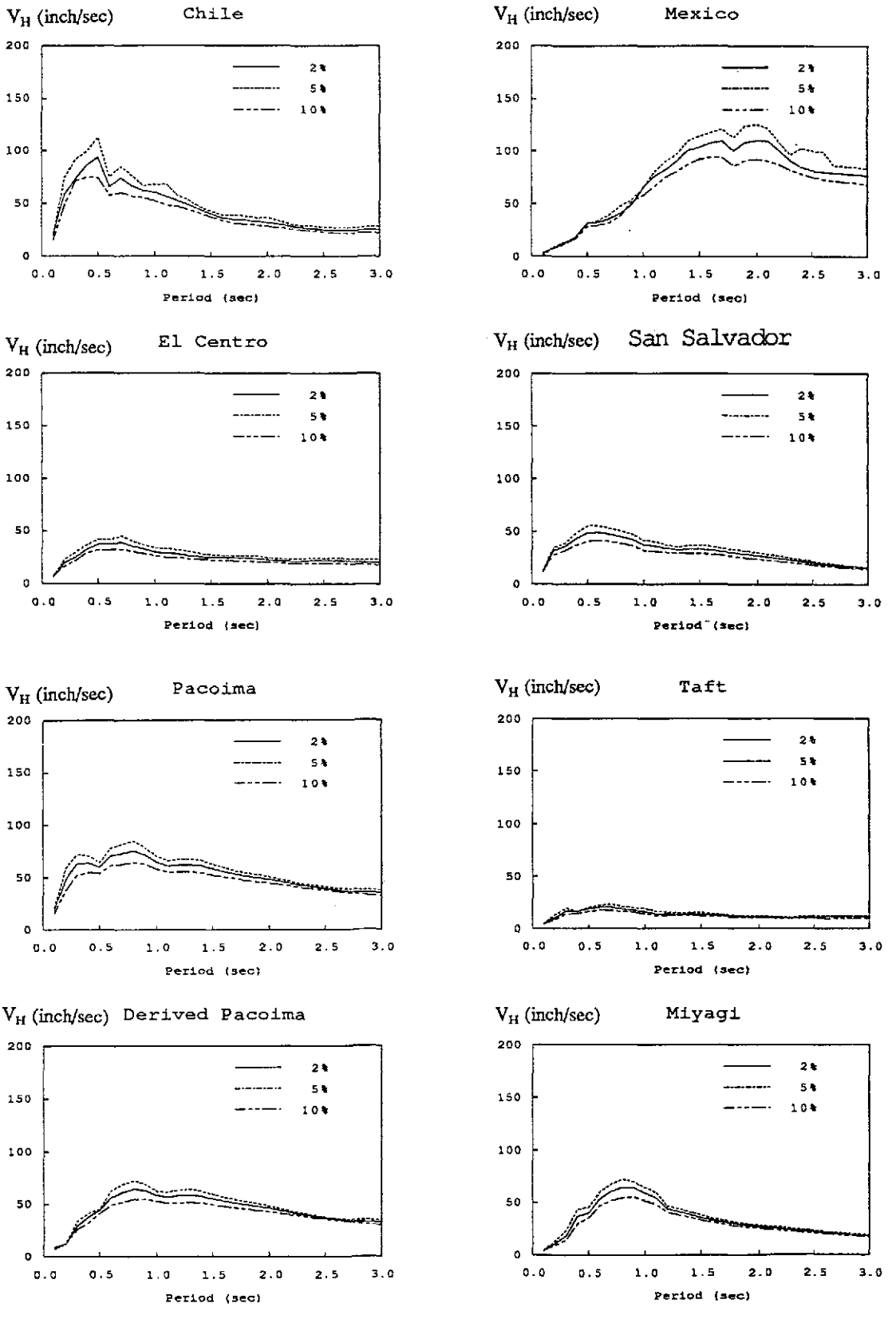

Fig. 3.16 Influence of Damping on Hysteretic Energy Equivalent Velocity V_H for Ductility Ratio 5

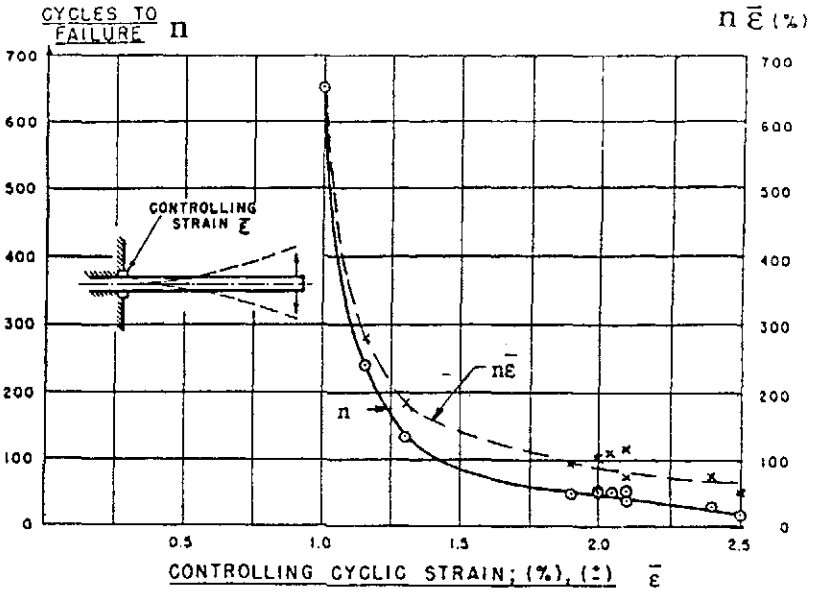

Fig. 3.17 Number of Cycles Required to Attain Fracture as a Function of the Controlling Strain[9]

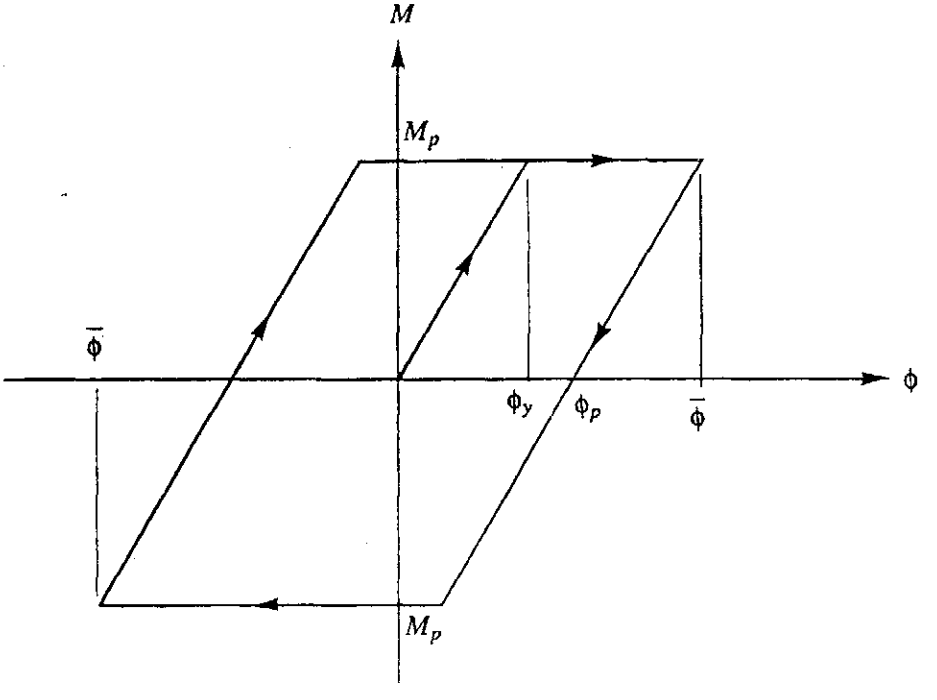

Fig. 3.18 Idealized Moment versus Curvature Relationship

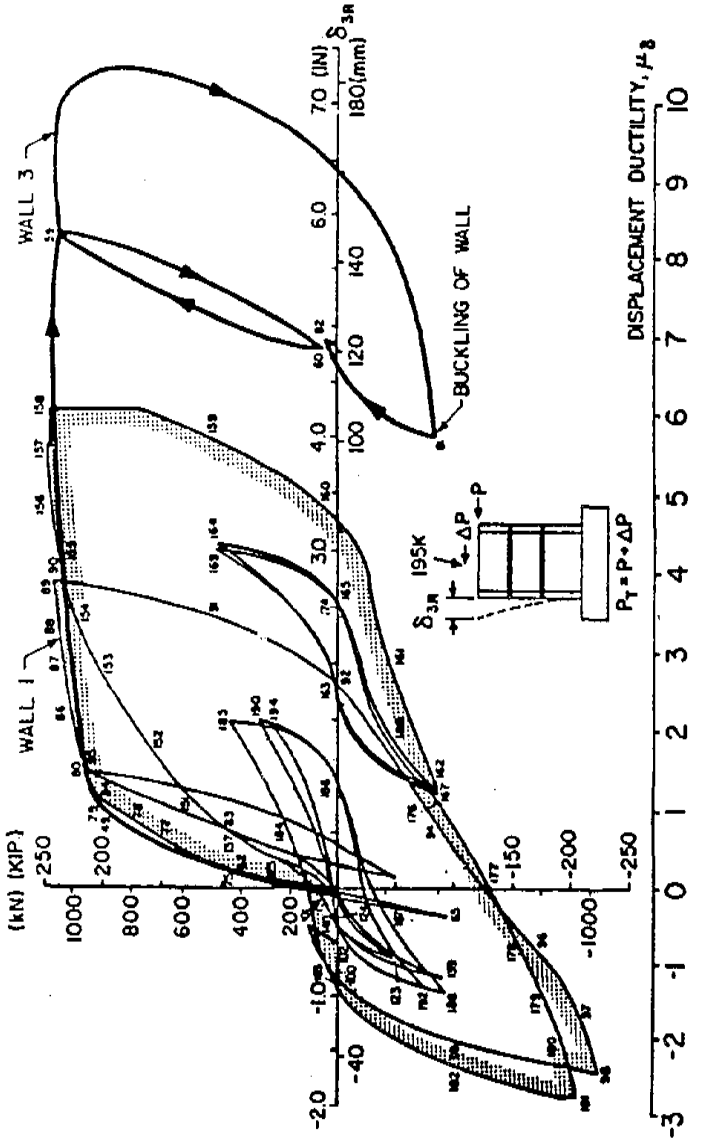

Fig. 3.19 Comparison of Behavior under Monotonic Loading (Wall 3) with Hysteretic Behavior Including Partial Reversals of Displacement (Wall 1)[11]

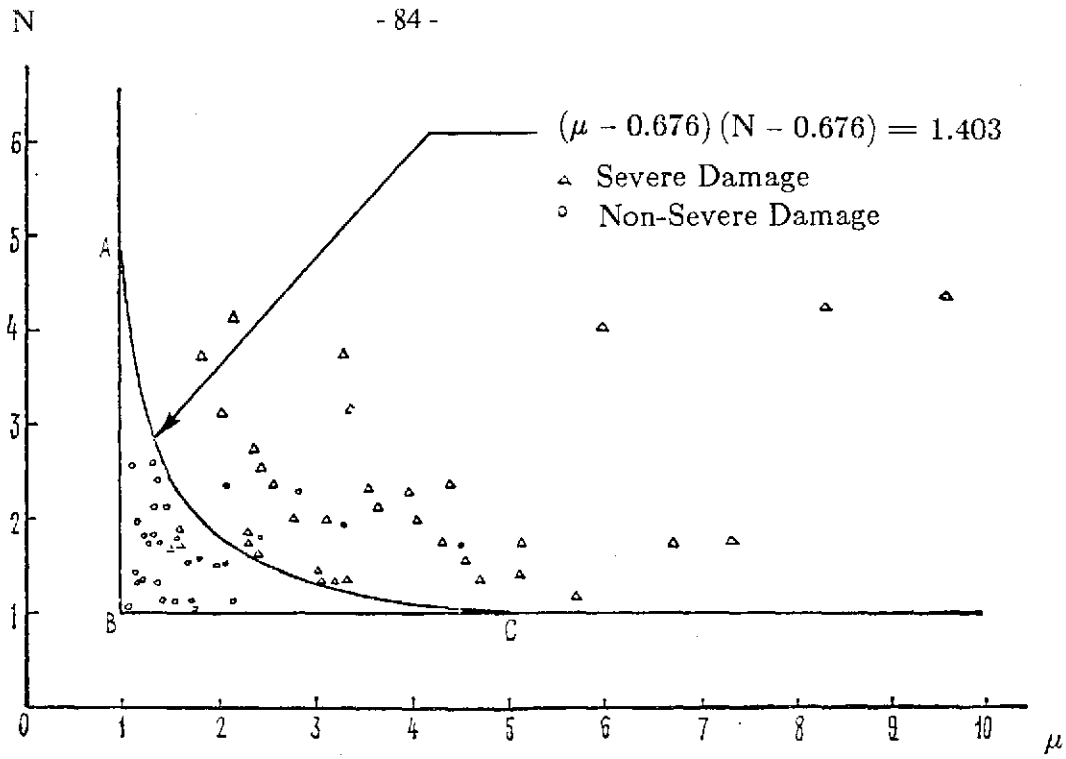

Fig. 3.20 μ — N Relationship of Reinforced Concrete Building Frames[18]

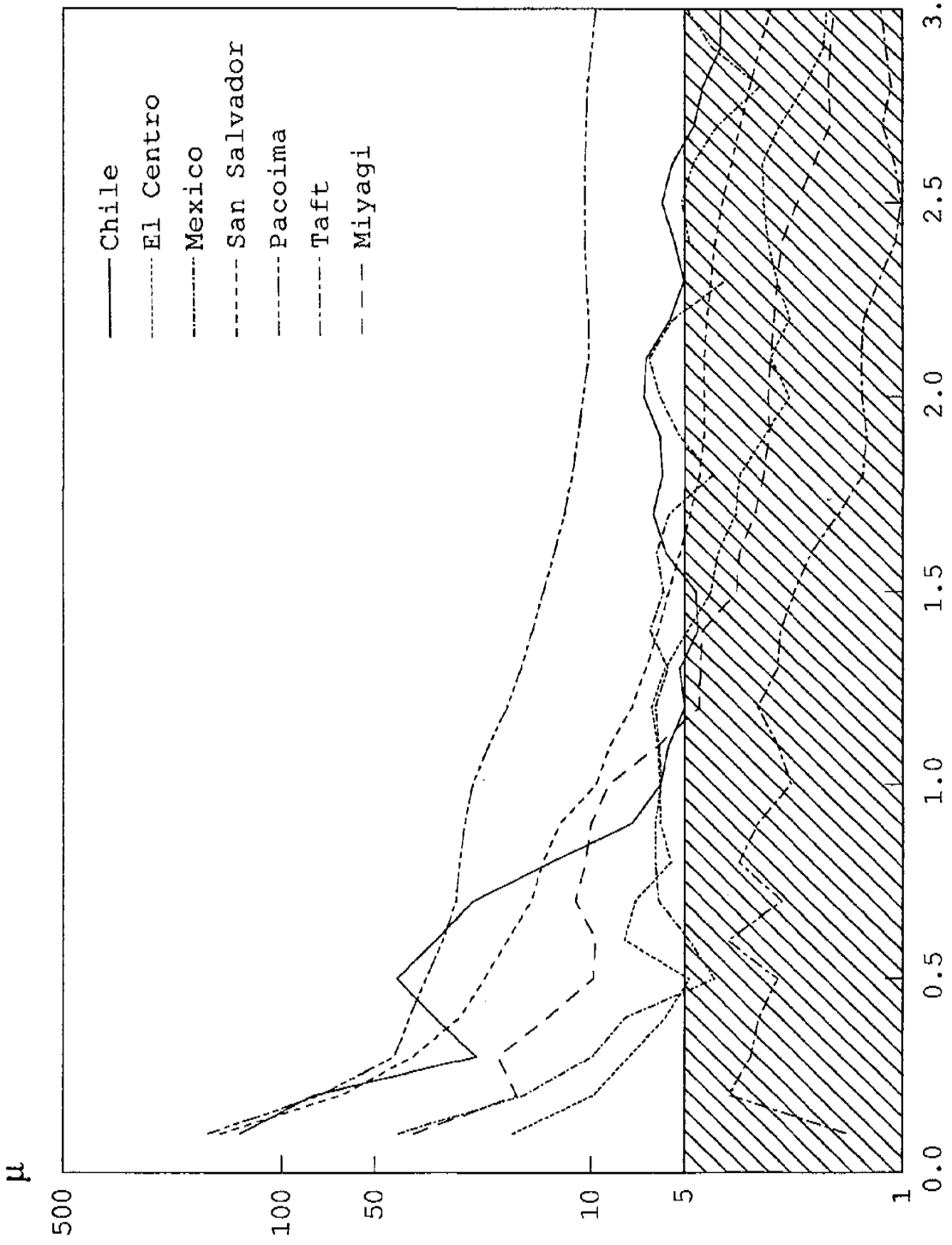

Fig. 4.1 Displacement Ductility Demand for Structures Designed in Compliance with ATC Design Spectra

($R = 6$, $C_d = 5$)

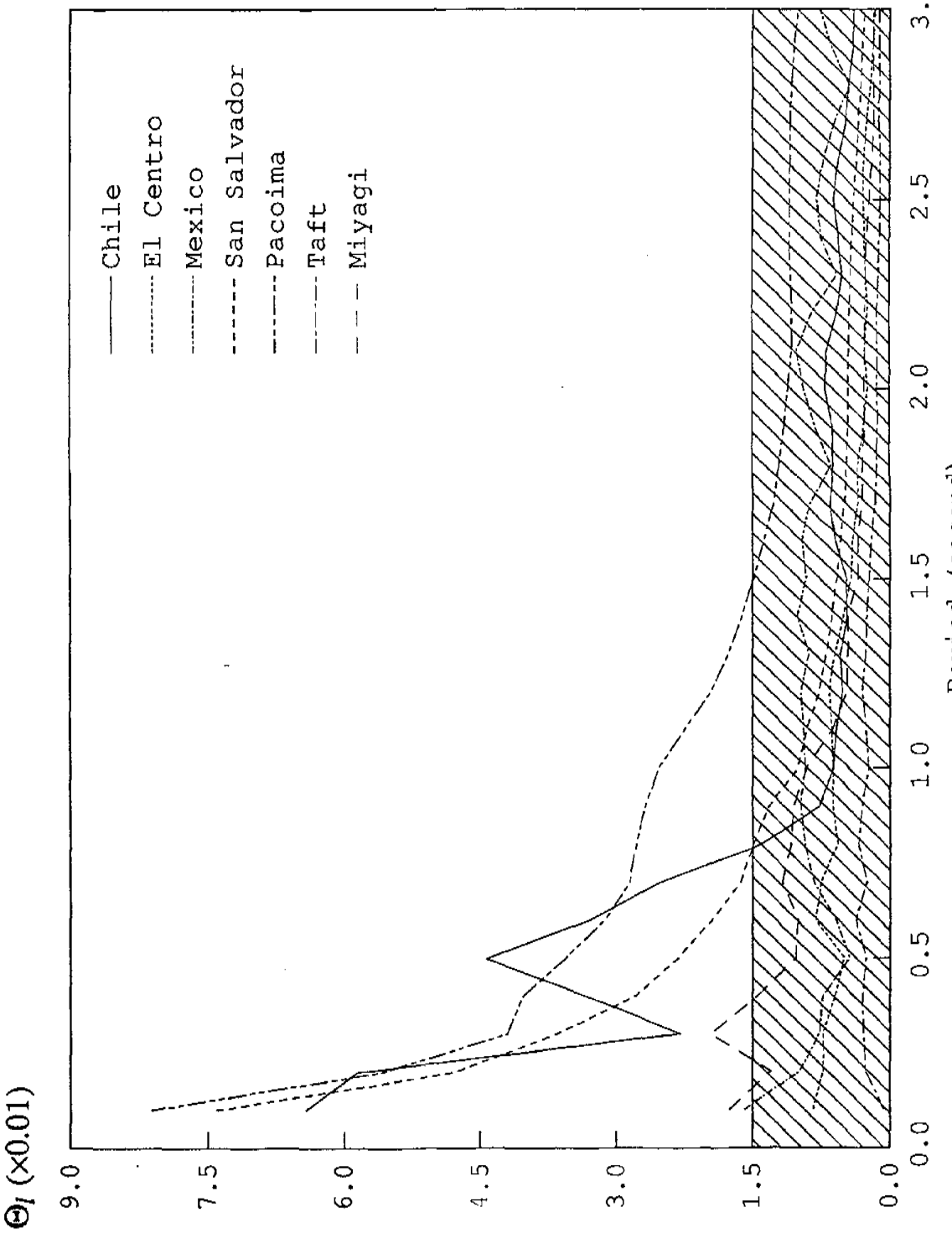

Fig. 4.2 Lower Bound Drift Index Demand for Structures Designed in Compliance with ATC Design Spectra

($R = 6$, $C_d = 5$)

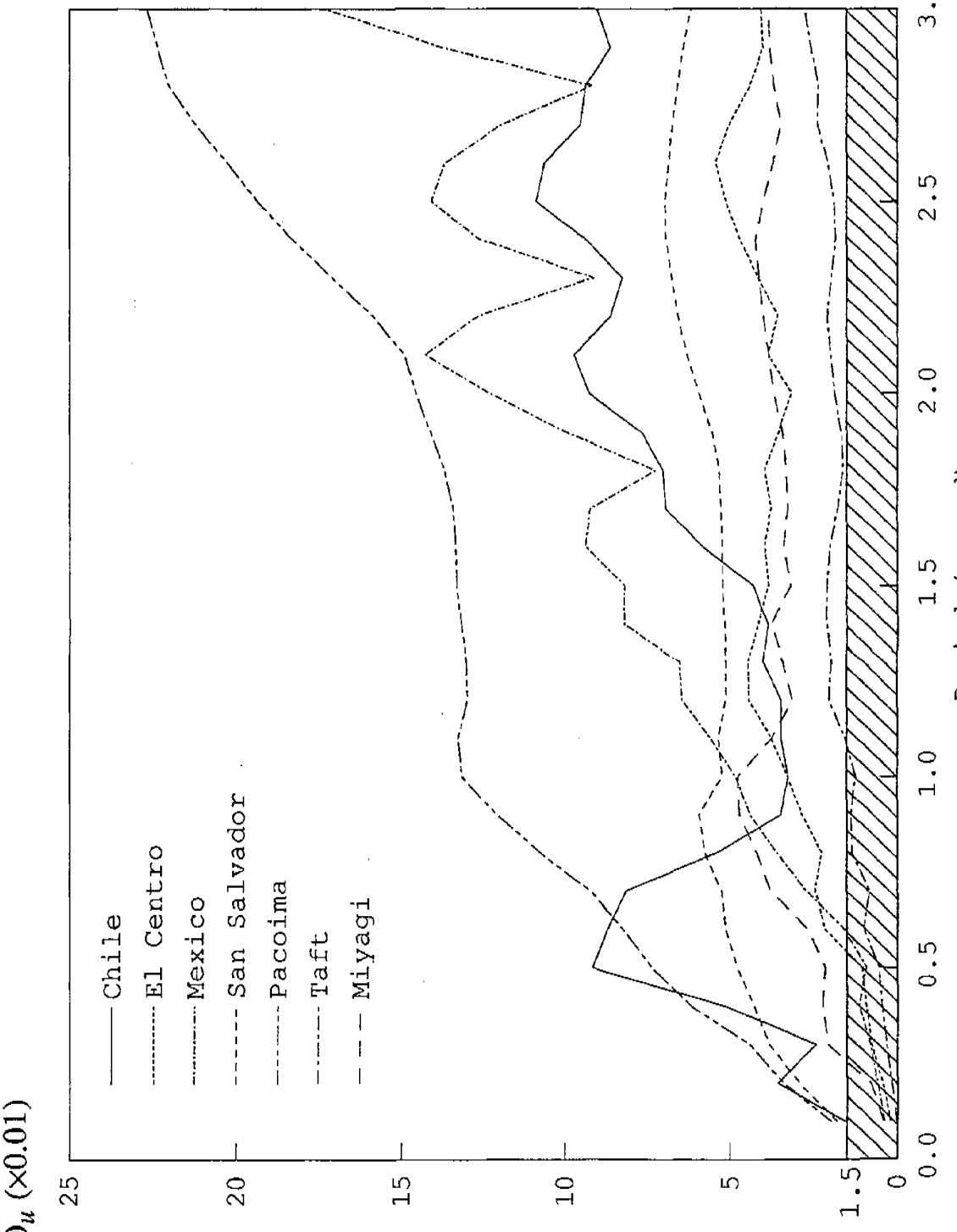

Fig. 4.3 Upper Bound Drift Index Demand for Structures Designed in Compliance with ATC Design Spectra

($R = 6, C_d = 5$)

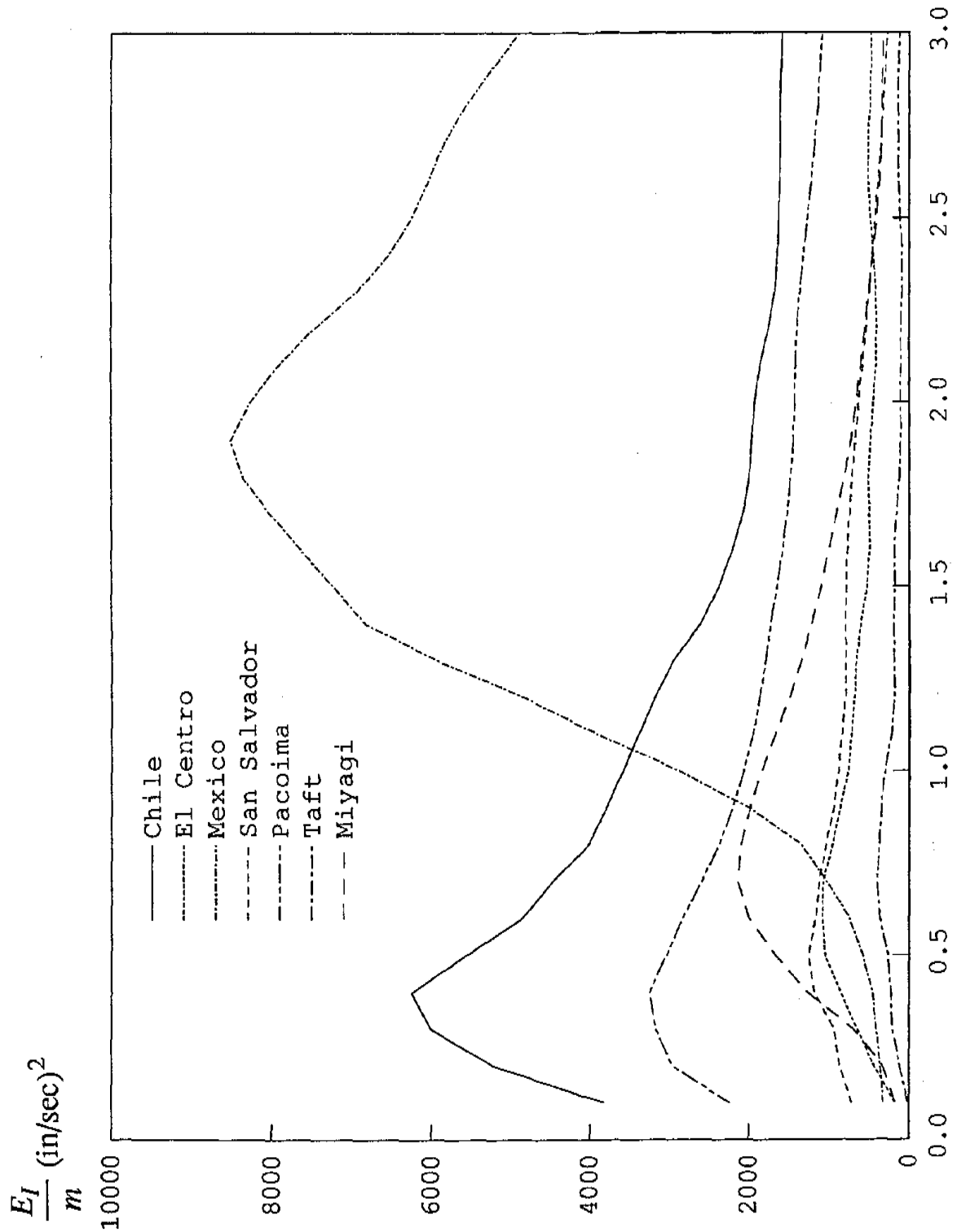

Fig. 4.4 Input Energy Demand for Structures Designed in Compliance with ATC Design Spectra

($R = 6, C_d = 5$)

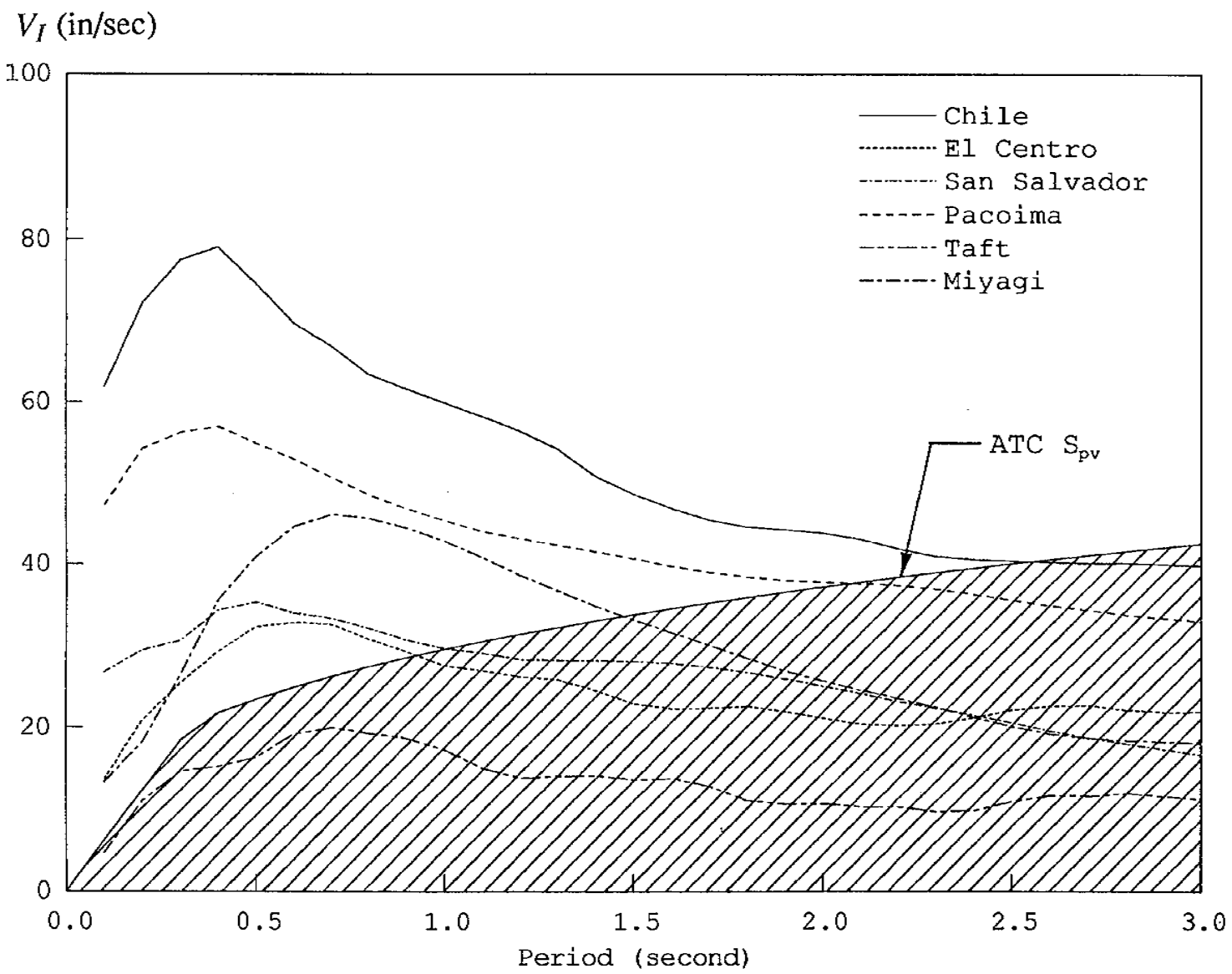

Fig. 4.5a Input Energy Equivalent Velocity Demand for Structures Designed in Compliance with ATC Design Spectra

($R = 6$, $C_d = 5$, Soil Type 1)

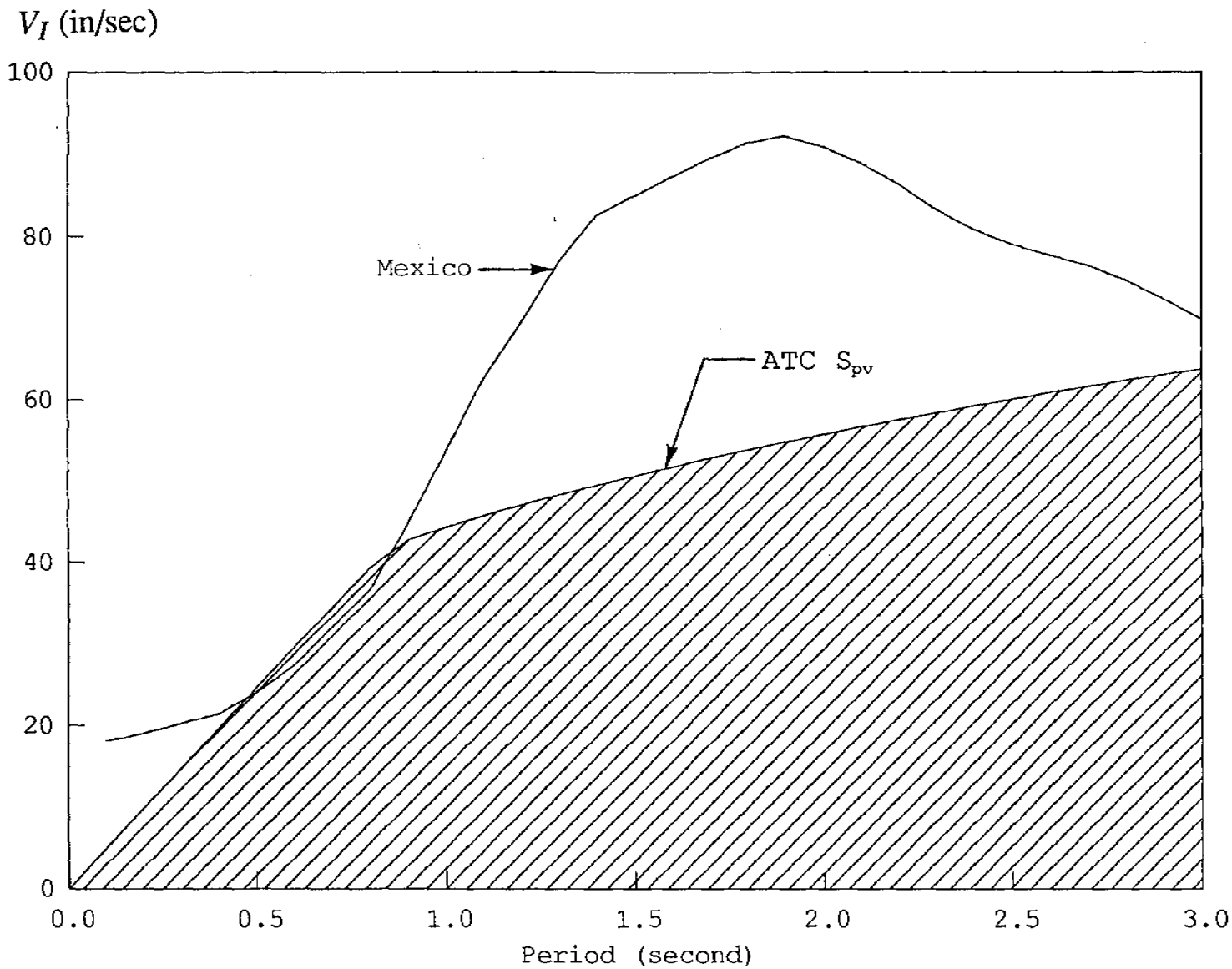

Fig. 4.5b Input Energy Equivalent Velocity Demand for Structures Designed in Compliance with ATC Design Spectra

($R = 6$, $C_d = 5$, Soil Type 3)

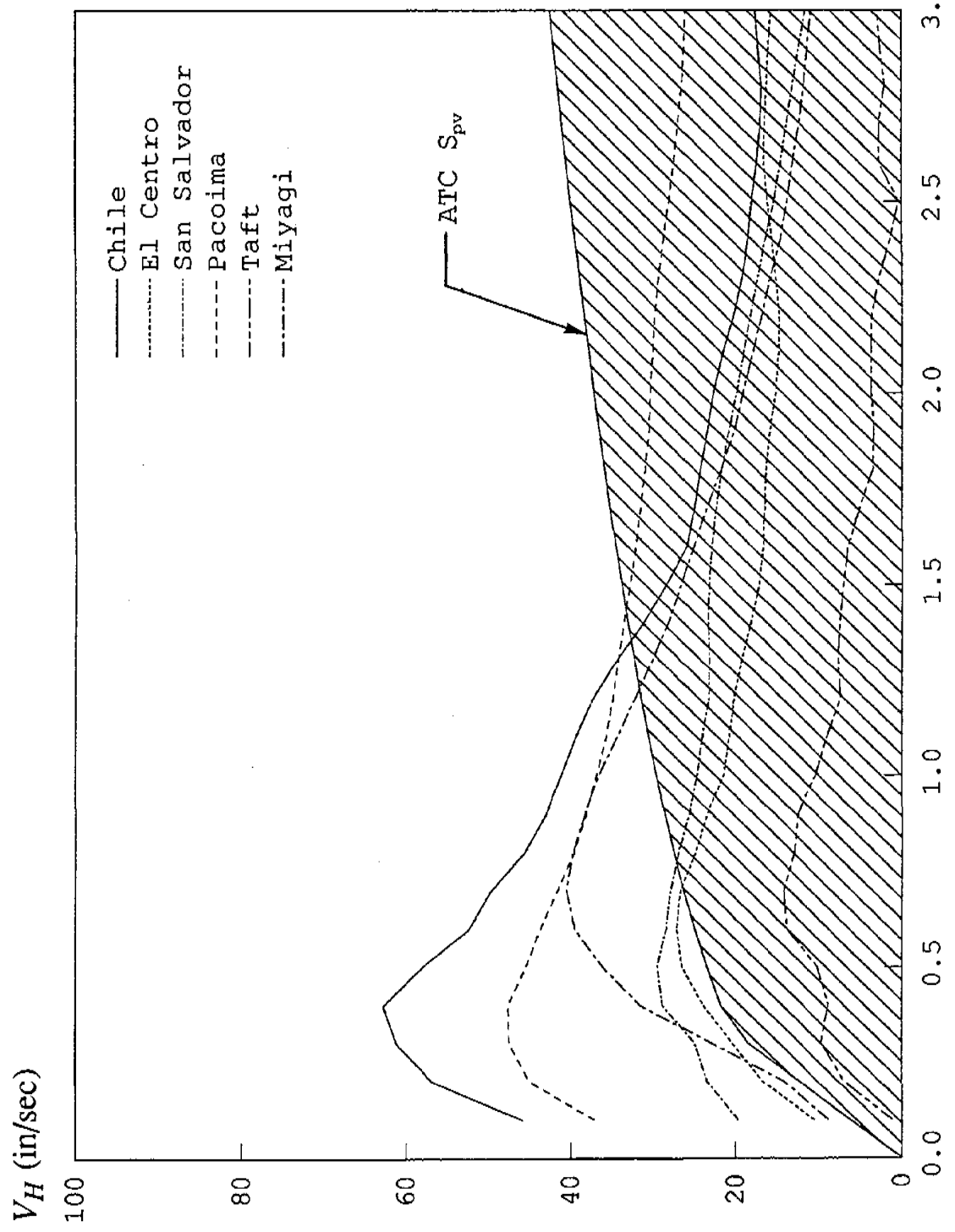

Fig. 4.6a Hysteretic Energy Equivalent Velocity Demand for Structures Designed in Compliance with ATC Design Spectra

($R = 6, C_d = 5$, Soil Type 1)

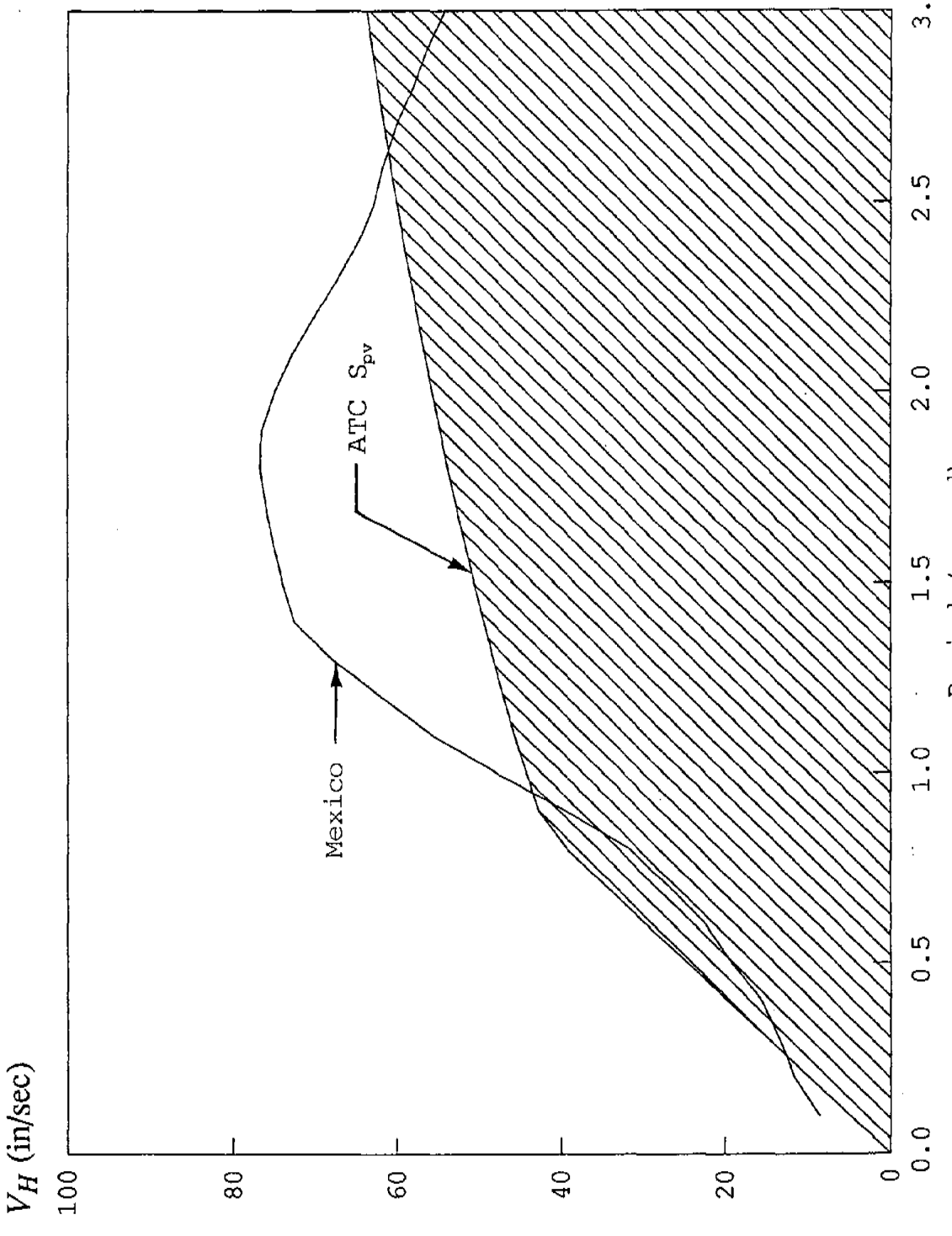

Fig. 4.6b Hysteretic Energy Equivalent Velocity Demand for Structures Designed in Compliance with ATC Design Spectra

($R = 6$, $C_d = 5$, Soil Type 3)

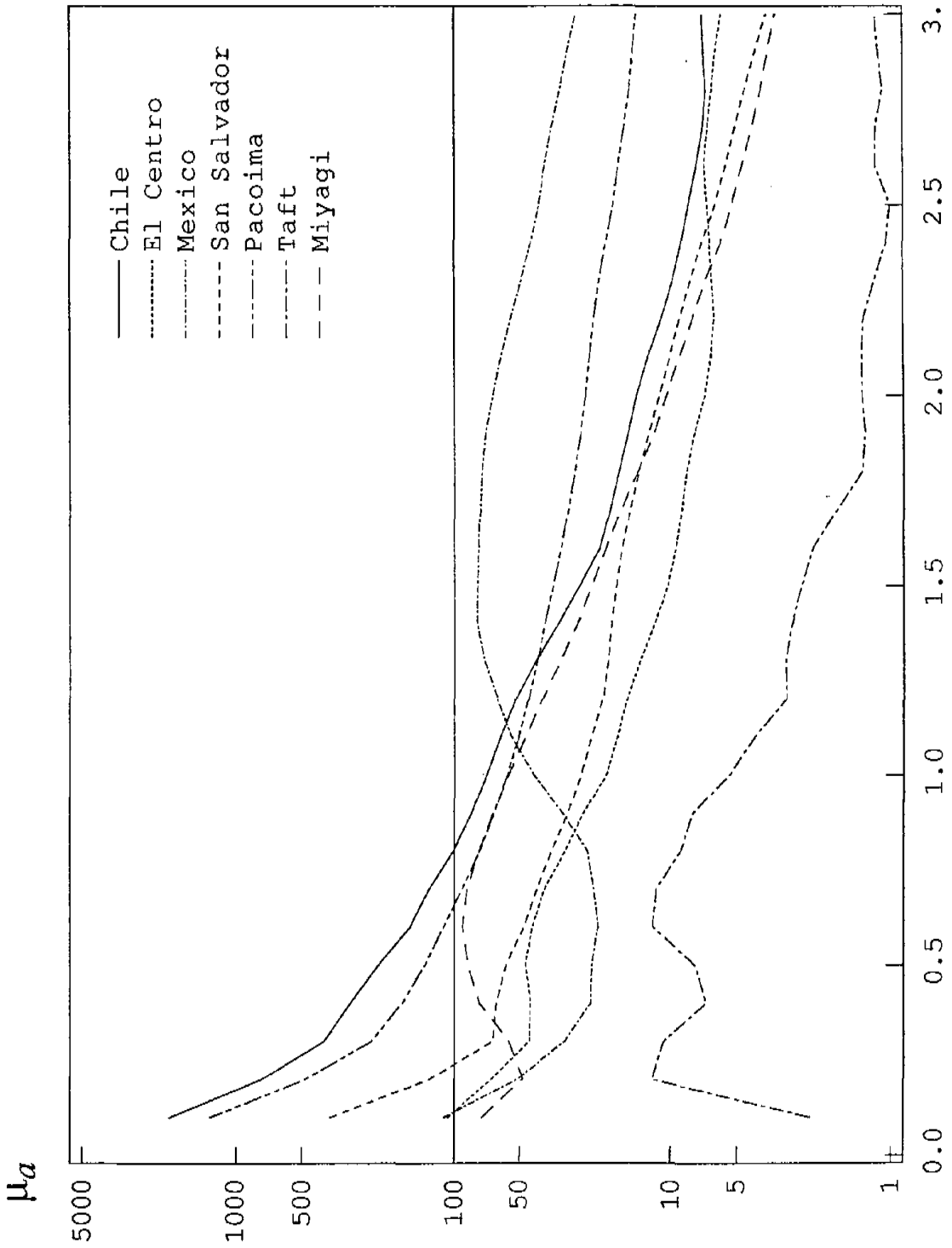

Fig. 4.7 Cumulative Displacement Ductility Demand for Structures Designed in Compliance with ATC Design Spectra

($R = 6, C_d = 5$)

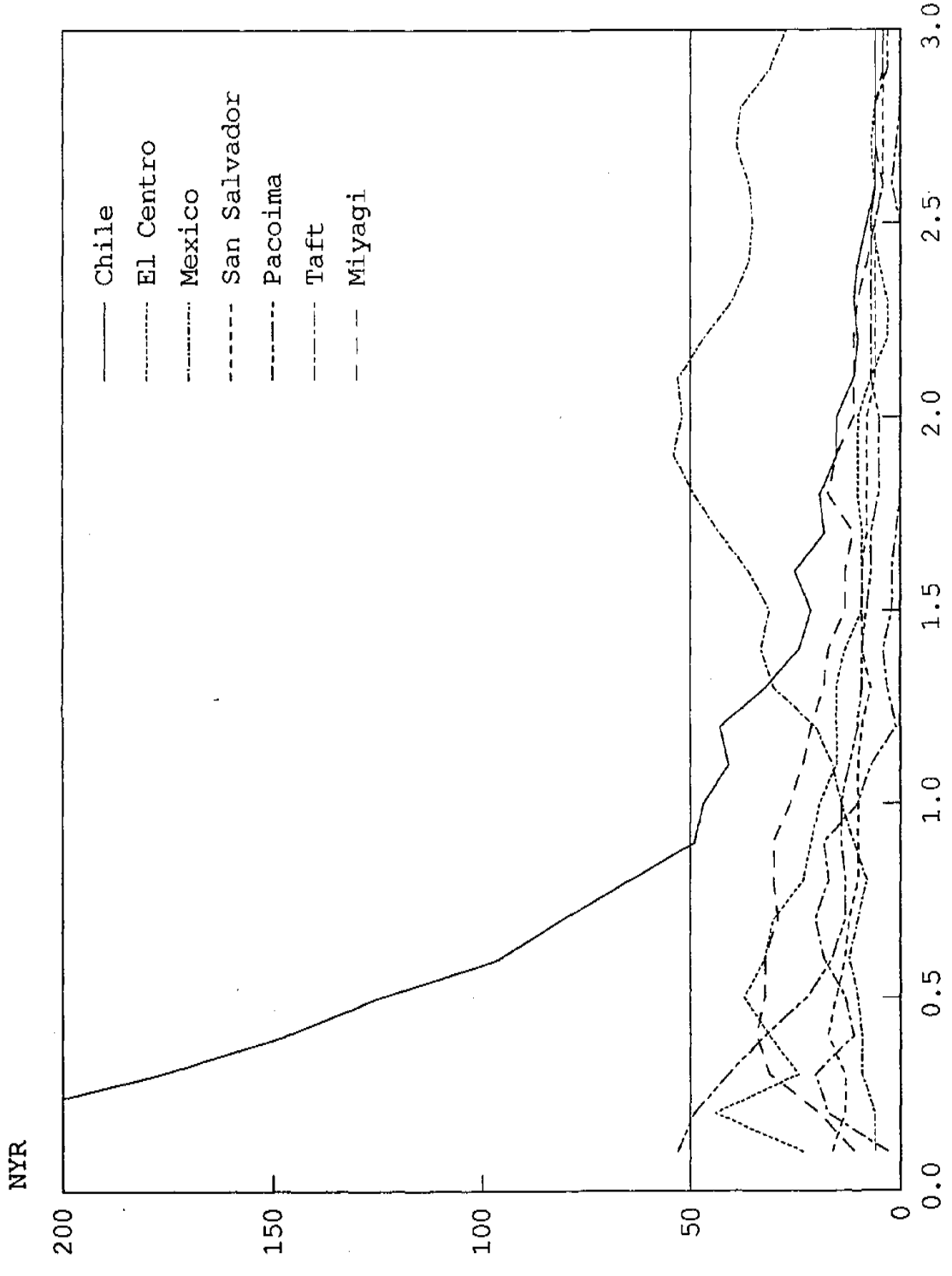

Fig. 4.8 Number of Yield Reversal Demand for Structures Designed in Compliance with ATC Design Spectra

($R = 6$, $C_d = 5$)

EARTHQUAKE ENGINEERING RESEARCH CENTER REPORT SERIES

EERC reports are available from the National Information Service for Earthquake Engineering(NISEE) and from the National Technical Information Service(NTIS). Numbers in parentheses are Accession Numbers assigned by the National Technical Information Service; these are followed by a price code. Contact NTIS, 5285 Port Royal Road, Springfield Virginia, 22161 for more information. Reports without Accession Numbers were not available from NTIS at the time of printing. For a current complete list of EERC reports (from EERC 67-1) and availablity information, please contact University of California, EERC, NISEE, 1301 South 46th Street, Richmond, California 94804.

UCB/EERC-80/01 "Earthquake Response of Concrete Gravity Dams Including Hydrodynamic and Foundation Interaction Effects," by Chopra, A.K., Chakrabarti, P. and Gupta, S., January 1980, (AD-A087297)A10.

UCB/EERC-80/02 "Rocking Response of Rigid Blocks to Earthquakes," by Yim, C.S., Chopra, A.K. and Penzien, J., January 1980, (PB80 166 002)A04.

UCB/EERC-80/03 "Optimum Inelastic Design of Seismic-Resistant Reinforced Concrete Frame Structures," by Zagajeski, S.W. and Bertero, V.V., January 1980, (PB80 164 635)A06.

UCB/EERC-80/04 "Effects of Amount and Arrangement of Wall-Panel Reinforcement on Hysteretic Behavior of Reinforced Concrete Walls," by Iliya, R. and Bertero, V.V., February 1980, (PB81 122 525)A09.

UCB/EERC-80/05 "Shaking Table Research on Concrete Dam Models," by Niwa, A. and Clough, R.W., September 1980, (PB81 122 368)A06.

UCB/EERC-80/06 "The Design of Steel Energy-Absorbing Restrainers and their Incorporation into Nuclear Power Plants for Enhanced Safety (Vol 1a): Piping with Energy Absorbing Restrainers: Parameter Study on Small Systems," by Powell, G.H., Oughourlian, C. and Simons, J., June 1980.

UCB/EERC-80/07 "Inelastic Torsional Response of Structures Subjected to Earthquake Ground Motions," by Yamazaki, Y., April 1980, (PB81 122 327)A08.

UCB/EERC-80/08 "Study of X-Braced Steel Frame Structures under Earthquake Simulation," by Ghanaat, Y., April 1980, (PB81 122 335)A11.

UCB/EERC-80/09 "Hybrid Modelling of Soil-Structure Interaction," by Gupta, S., Lin, T.W. and Penzien, J., May 1980, (PB81 122 319)A07.

UCB/EERC-80/10 "General Applicability of a Nonlinear Model of a One Story Steel Frame," by Sveinsson, B.I. and McNiven, H.D., May 1980, (PB81 124 877)A06.

UCB/EERC-80/11 "A Green-Function Method for Wave Interaction with a Submerged Body," by Kioka, W., April 1980, (PB81 122 269)A07.

UCB/EERC-80/12 "Hydrodynamic Pressure and Added Mass for Axisymmetric Bodies.," by Nilrat, F., May 1980, (PB81 122 343)A08.

UCB/EERC-80/13 "Treatment of Non-Linear Drag Forces Acting on Offshore Platforms," by Dao, B.V. and Penzien, J., May 1980, (PB81 153 413)A07.

UCB/EERC-80/14 "2D Plane/Axisymmetric Solid Element (Type 3-Elastic or Elastic-Perfectly Plastic)for the ANSR-II Program," by Mondkar, D.P. and Powell, G.H., July 1980, (PB81 122 350)A03.

UCB/EERC-80/15 "A Response Spectrum Method for Random Vibrations," by Der Kiureghian, A., June 1981, (PB81 122 301)A03.

UCB/EERC-80/16 "Cyclic Inelastic Buckling of Tubular Steel Braces," by Zayas, V.A., Popov, E.P. and Mahin, S.A., June 1981, (PB81 124 885)A10.

UCB/EERC-80/17 "Dynamic Response of Simple Arch Dams Including Hydrodynamic Interaction," by Porter, C.S. and Chopra, A.K., July 1981, (PB81 124 000)A13.

UCB/EERC-80/18 "Experimental Testing of a Friction Damped Aseismic Base Isolation System with Fail-Safe Characteristics," by Kelly, J.M., Beucke, K.E. and Skinner, M.S., July 1980, (PB81 148 595)A04.

UCB/EERC-80/19 "The Design of Steel Energy-Absorbing Restrainers and their Incorporation into Nuclear Power Plants for Enhanced Safety (Vol.1B): Stochastic Seismic Analyses of Nuclear Power Plant Structures and Piping Systems Subjected to Multiple Supported Excitations," by Lee, M.C. and Penzien, J., June 1980, (PB82 201 872)A08.

UCB/EERC-80/20 "The Design of Steel Energy-Absorbing Restrainers and their Incorporation into Nuclear Power Plants for Enhanced Safety (Vol 1C): Numerical Method for Dynamic Substructure Analysis," by Dickens, J.M. and Wilson, E.L., June 1980.

UCB/EERC-80/21 "The Design of Steel Energy-Absorbing Restrainers and their Incorporation into Nuclear Power Plants for Enhanced Safety (Vol 2): Development and Testing of Restraints for Nuclear Piping Systems," by Kelly, J.M. and Skinner, M.S., June 1980.

UCB/EERC-80/22 "3D Solid Element (Type 4-Elastic or Elastic-Perfectly-Plastic) for the ANSR-II Program," by Mondkar, D.P. and Powell, G.H., July 1980, (PB81 123 242)A03.

UCB/EERC-80/23 "Gap-Friction Element (Type 5) for the Ansr-II Program," by Mondkar, D.P. and Powell, G.H., July 1980, (PB81 122 285)A03.

UCB/EERC-80/24 "U-Bar Restraint Element (Type 11) for the ANSR-II Program," by Oughourlian, C. and Powell, G.H., July 1980, (PB81 122 293)A03.

UCB/EERC-80/25 "Testing of a Natural Rubber Base Isolation System by an Explosively Simulated Earthquake," by Kelly, J.M., August 1980, (PB81 201 360)A04.

UCB/EERC-80/26 "Input Identification from Structural Vibrational Response," by Hu, Y., August 1980, (PB81 152 308)A05.

UCB/EERC-80/27 "Cyclic Inelastic Behavior of Steel Offshore Structures," by Zayas, V.A., Mahin, S.A. and Popov, E.P., August 1980, (PB81 196 180)A15.

UCB/EERC-80/28 "Shaking Table Testing of a Reinforced Concrete Frame with Biaxial Response," by Oliva, M.G., October 1980, (PB81 154 304)A10.

UCB/EERC-80/29 "Dynamic Properties of a Twelve-Story Prefabricated Panel Building," by Bouwkamp, J.G., Kollegger, J.P. and Stephen, R.M., October 1980, (PB82 138 777)A07.

UCB/EERC-80/30 "Dynamic Properties of an Eight-Story Prefabricated Panel Building," by Bouwkamp, J.G., Kollegger, J.P. and Stephen, R.M., October 1980, (PB81 200 313)A05.

UCB/EERC-80/31 "Predictive Dynamic Response of Panel Type Structures under Earthquakes," by Kollegger, J.P. and Bouwkamp, J.G., October 1980, (PB81 152 316)A04.

UCB/EERC-80/32 "The Design of Steel Energy-Absorbing Restrainers and their Incorporation into Nuclear Power Plants for Enhanced Safety (Vol 3): Testing of Commercial Steels in Low-Cycle Torsional Fatigue," by Spanner, P., Parker, E.R., Jongewaard, E. and Dory, M., 1980.

UCB/EERC-80/33 "The Design of Steel Energy-Absorbing Restrainers and their Incorporation into Nuclear Power Plants for Enhanced Safety (Vol 4): Shaking Table Tests of Piping Systems with Energy-Absorbing Restrainers," by Stiemer, S.F. and Godden, W.G., September 1980, (PB82 201 880)A05.

UCB/EERC-80/34 "The Design of Steel Energy-Absorbing Restrainers and their Incorporation into Nuclear Power Plants for Enhanced Safety (Vol 5): Summary Report," by Spencer, P., 1980.

UCB/EERC-80/35 "Experimental Testing of an Energy-Absorbing Base Isolation System," by Kelly, J.M., Skinner, M.S. and Beucke, K.E., October 1980, (PB81 154 072)A04.

UCB/EERC-80/36 "Simulating and Analyzing Artificial Non-Stationary Earth Ground Motions," by Nau, R.F., Oliver, R.M. and Pister, K.S., October 1980, (PB81 153 397)A04.

UCB/EERC-80/37 "Earthquake Engineering at Berkeley - 1980," by , September 1980, (PB81 205 674)A09.

UCB/EERC-80/38 "Inelastic Seismic Analysis of Large Panel Buildings," by Schricker, V. and Powell, G.H., September 1980, (PB81 154 338)A13.

UCB/EERC-80/39 "Dynamic Response of Embankment, Concrete-Gavity and Arch Dams Including Hydrodynamic Interation," by Hall, J.F. and Chopra, A.K., October 1980, (PB81 152 324)A11.

UCB/EERC-80/40 "Inelastic Buckling of Steel Struts under Cyclic Load Reversal.," by Black, R.G., Wenger, W.A. and Popov, E.P., October 1980, (PB81 154 312)A08.

UCB/EERC-80/41 "Influence of Site Characteristics on Buildings Damage during the October 3,1974 Lima Earthquake," by Repetto, P., Arango, I. and Seed, H.B., September 1980, (PB81 161 739)A05.

UCB/EERC-80/42 "Evaluation of a Shaking Table Test Program on Response Behavior of a Two Story Reinforced Concrete Frame," by Blondet, J.M., Clough, R.W. and Mahin, S.A., December 1980, (PB82 196 544)A11.

UCB/EERC-80/43 "Modelling of Soil-Structure Interaction by Finite and Infinite Elements," by Medina, F., December 1980, (PB81 229 270)A04.

UCB/EERC-81/01 "Control of Seismic Response of Piping Systems and Other Structures by Base Isolation," by Kelly, J.M., January 1981, (PB81 200 735)A05.

UCB/EERC-81/02 "OPTNSR- An Interactive Software System for Optimal Design of Statically and Dynamically Loaded Structures with Nonlinear Response," by Bhatti, M.A., Ciampi, V. and Pister, K.S., January 1981, (PB81 218 851)A09.

UCB/EERC-81/03 "Analysis of Local Variations in Free Field Seismic Ground Motions," by Chen, J.-C., Lysmer, J. and Seed, H.B., January 1981, (AD-A099508)A13.

UCB/EERC-81/04 "Inelastic Structural Modeling of Braced Offshore Platforms for Seismic Loading," by Zayas, V.A., Shing, P.-S.B., Mahin, S.A. and Popov, E.P., January 1981, (PB82 138 777)A07.

UCB/EERC-81/05 "Dynamic Response of Light Equipment in Structures," by Der Kiureghian, A., Sackman, J.L. and Nour-Omid, B., April 1981, (PB81 218 497)A04.

UCB/EERC-81/06 "Preliminary Experimental Investigation of a Broad Base Liquid Storage Tank," by Bouwkamp, J.G., Kollegger, J.P. and Stephen, R.M., May 1981, (PB82 140 385)A03.

UCB/EERC-81/07 "The Seismic Resistant Design of Reinforced Concrete Coupled Structural Walls," by Aktan, A.E. and Bertero, V.V., June 1981, (PB82 113 358)A11.

UCB/EERC-81/08 "Unassigned," by Unassigned, 1981.

UCB/EERC-81/09 "Experimental Behavior of a Spatial Piping System with Steel Energy Absorbers Subjected to a Simulated Differential Seismic Input," by Stiemer, S.F., Godden, W.G. and Kelly, J.M., July 1981, (PB82 201 898)A04.

UCB/EERC-81/10 "Evaluation of Seismic Design Provisions for Masonry in the United States," by Sveinsson, B.I., Mayes, R.L. and McNiven, H.D., August 1981, (PB82 166 075)A08.

UCB/EERC-81/11 "Two-Dimensional Hybrid Modelling of Soil-Structure Interaction," by Tzong, T.-J., Gupta, S. and Penzien, J., August 1981, (PB82 142 118)A04.

UCB/EERC-81/12 "Studies on Effects of Infills in Seismic Resistant R/C Construction," by Brokken, S. and Bertero, V.V., October 1981, (PB82 166 190)A09.

UCB/EERC-81/13 "Linear Models to Predict the Nonlinear Seismic Behavior of a One-Story Steel Frame," by Valdimarsson, H., Shah, A.H. and McNiven, H.D., September 1981, (PB82 138 793)A07.

UCB/EERC-81/14 "TLUSH: A Computer Program for the Three-Dimensional Dynamic Analysis of Earth Dams," by Kagawa, T., Mejia, L.H., Seed, H.B. and Lysmer, J., September 1981, (PB82 139 940)A06.

UCB/EERC-81/15 "Three Dimensional Dynamic Response Analysis of Earth Dams," by Mejia, L.H. and Seed, H.B., September 1981, (PB82 137 274)A12.

UCB/EERC-81/16 "Experimental Study of Lead and Elastomeric Dampers for Base Isolation Systems," by Kelly, J.M. and Hodder, S.B., October 1981, (PB82 166 182)A05.

UCB/EERC-81/17 "The Influence of Base Isolation on the Seismic Response of Light Secondary Equipment," by Kelly, J.M., April 1981, (PB82 255 266)A04.

UCB/EERC-81/18 "Studies on Evaluation of Shaking Table Response Analysis Procedures," by Blondet, J. M., November 1981, (PB82 197 278)A10.

UCB/EERC-81/19 "DELIGHT.STRUCT: A Computer-Aided Design Environment for Structural Engineering," by Balling, R.J., Pister, K.S. and Polak, E., December 1981, (PB82 218 496)A07.

UCB/EERC-81/20 "Optimal Design of Seismic-Resistant Planar Steel Frames," by Balling, R.J., Ciampi, V. and Pister, K.S., December 1981, (PB82 220 179)A07.

UCB/EERC-82/01 "Dynamic Behavior of Ground for Seismic Analysis of Lifeline Systems," by Sato, T. and Der Kiureghian, A., January 1982, (PB82 218 926)A05.

UCB/EERC-82/02 "Shaking Table Tests of a Tubular Steel Frame Model," by Ghanaat, Y. and Clough, R.W., January 1982, (PB82 220 161)A07.

UCB/EERC-82/03 "Behavior of a Piping System under Seismic Excitation: Experimental Investigations of a Spatial Piping System supported by Mechanical Shock Arrestors," by Schneider, S., Lee, H.-M. and Godden, W. G., May 1982, (PB83 172 544)A09.

UCB/EERC-82/04 "New Approaches for the Dynamic Analysis of Large Structural Systems," by Wilson, E.L., June 1982, (PB83 148 080)A05.

UCB/EERC-82/05 "Model Study of Effects of Damage on the Vibration Properties of Steel Offshore Platforms," by Shahrivar, F. and Bouwkamp, J.G., June 1982, (PB83 148 742)A10.

UCB/EERC-82/06 "States of the Art and Pratice in the Optimum Seismic Design and Analytical Response Prediction of R/C Frame Wall Structures," by Aktan, A.E. and Bertero, V.V., July 1982, (PB83 147 736)A05.

UCB/EERC-82/07 "Further Study of the Earthquake Response of a Broad Cylindrical Liquid-Storage Tank Model," by Manos, G.C. and Clough, R.W., July 1982, (PB83 147 744)A11.

UCB/EERC-82/08 "An Evaluation of the Design and Analytical Seismic Response of a Seven Story Reinforced Concrete Frame," by Charney, F.A. and Bertero, V.V., July 1982, (PB83 157 628)A09.

UCB/EERC-82/09 "Fluid-Structure Interactions: Added Mass Computations for Incompressible Fluid," by Kuo, J.S.-H., August 1982, (PB83 156 281)A07.

UCB/EERC-82/10 "Joint-Opening Nonlinear Mechanism: Interface Smeared Crack Model," by Kuo, J.S.-H., August 1982, (PB83 149 195)A05.

UCB/EERC-82/11 "Dynamic Response Analysis of Techi Dam," by Clough, R.W., Stephen, R.M. and Kuo, J.S.-H., August 1982, (PB83 147 496)A06.

UCB/EERC-82/12 "Prediction of the Seismic Response of R/C Frame-Coupled Wall Structures," by Aktan, A.E., Bertero, V.V. and Piazzo, M., August 1982, (PB83 149 203)A09.

UCB/EERC-82/13 "Preliminary Report on the Smart 1 Strong Motion Array in Taiwan," by Bolt, B.A., Loh, C.H., Penzien, J. and Tsai, Y.B., August 1982, (PB83 159 400)A10.

UCB/EERC-82/14 "Shaking-Table Studies of an Eccentrically X-Braced Steel Structure," by Yang, M.S., September 1982, (PB83 260 778)A12.

UCB/EERC-82/15 "The Performance of Stairways in Earthquakes," by Roha, C., Axley, J.W. and Bertero, V.V., September 1982, (PB83 157 693)A07.

UCB/EERC-82/16 "The Behavior of Submerged Multiple Bodies in Earthquakes," by Liao, W.-G., September 1982, (PB83 158 709)A07.

UCB/EERC-82/17 "Effects of Concrete Types and Loading Conditions on Local Bond-Slip Relationships," by Cowell, A.D., Popov, E.P. and Bertero, V.V., September 1982, (PB83 153 577)A04.

UCB/EERC-82/18 "Mechanical Behavior of Shear Wall Vertical Boundary Members: An Experimental Investigation," by Wagner, M.T. and Bertero, V.V., October 1982, (PB83 159 764)A05.

UCB/EERC-82/19 "Experimental Studies of Multi-support Seismic Loading on Piping Systems," by Kelly, J.M. and Cowell, A.D., November 1982.

UCB/EERC-82/20 "Generalized Plastic Hinge Concepts for 3D Beam-Column Elements," by Chen, P. F.-S. and Powell, G.H., November 1982, (PB83 247 981)A13.

UCB/EERC-82/21 "ANSR-II: General Computer Program for Nonlinear Structural Analysis," by Oughourlian, C.V. and Powell, G.H., November 1982, (PB83 251 330)A12.

UCB/EERC-82/22 "Solution Strategies for Statically Loaded Nonlinear Structures," by Simons, J.W. and Powell, G.H., November 1982, (PB83 197 970)A06.

UCB/EERC-82/23 "Analytical Model of Deformed Bar Anchorages under Generalized Excitations," by Ciampi, V., Eligehausen, R., Bertero, V.V. and Popov, E.P., November 1982, (PB83 169 532)A06.

UCB/EERC-82/24 "A Mathematical Model for the Response of Masonry Walls to Dynamic Excitations," by Sucuoglu, H., Mengi, Y. and McNiven, H.D., November 1982, (PB83 169 011)A07.

UCB/EERC-82/25 "Earthquake Response Considerations of Broad Liquid Storage Tanks," by Cambra, F.J., November 1982, (PB83 251 215)A09.

UCB/EERC-82/26 "Computational Models for Cyclic Plasticity, Rate Dependence and Creep," by Mosaddad, B. and Powell, G.H., November 1982, (PB83 245 829)A08.

UCB/EERC-82/27 "Inelastic Analysis of Piping and Tubular Structures," by Mahasuverachai, M. and Powell, G.H., November 1982, (PB83 249 987)A07.

UCB/EERC-83/01 "The Economic Feasibility of Seismic Rehabilitation of Buildings by Base Isolation," by Kelly, J.M., January 1983, (PB83 197 988)A05.

UCB/EERC-83/02 "Seismic Moment Connections for Moment-Resisting Steel Frames.," by Popov, E.P., January 1983, (PB83 195 412)A04.

UCB/EERC-83/03 "Design of Links and Beam-to-Column Connections for Eccentrically Braced Steel Frames," by Popov, E.P. and Malley, J.O., January 1983, (PB83 194 811)A04.

UCB/EERC-83/04 "Numerical Techniques for the Evaluation of Soil-Structure Interaction Effects in the Time Domain," by Bayo, E. and Wilson, E.L., February 1983, (PB83 245 605)A09.

UCB/EERC-83/05 "A Transducer for Measuring the Internal Forces in the Columns of a Frame-Wall Reinforced Concrete Structure," by Sause, R. and Bertero, V.V., May 1983, (PB84 119 494)A06.

UCB/EERC-83/06 "Dynamic Interactions Between Floating Ice and Offshore Structures," by Croteau, P., May 1983, (PB84 119 486)A16.

UCB/EERC-83/07 "Dynamic Analysis of Multiply Tuned and Arbitrarily Supported Secondary Systems," by Igusa, T. and Der Kiureghian, A., July 1983, (PB84 118 272)A11.

UCB/EERC-83/08 "A Laboratory Study of Submerged Multi-body Systems in Earthquakes," by Ansari, G.R., June 1983, (PB83 261 842)A17.

UCB/EERC-83/09 "Effects of Transient Foundation Uplift on Earthquake Response of Structures," by Yim, C.-S. and Chopra, A.K., June 1983, (PB83 261 396)A07.

UCB/EERC-83/10 "Optimal Design of Friction-Braced Frames under Seismic Loading," by Austin, M.A. and Pister, K.S., June 1983, (PB84 119 288)A06.

UCB/EERC-83/11 "Shaking Table Study of Single-Story Masonry Houses: Dynamic Performance under Three Component Seismic Input and Recommendations," by Manos, G.C., Clough, R.W. and Mayes, R.L., July 1983, (UCB/EERC-83/11)A08.

UCB/EERC-83/12 "Experimental Error Propagation in Pseudodynamic Testing," by Shiing, P.B. and Mahin, S.A., June 1983, (PB84 119 270)A09.

UCB/EERC-83/13 "Experimental and Analytical Predictions of the Mechanical Characteristics of a 1/5-scale Model of a 7-story R/C Frame-Wall Building Structure," by Aktan, A.E., Bertero, V.V., Chowdhury, A.A. and Nagashima, T., June 1983, (PB84 119 213)A07.

UCB/EERC-83/14 "Shaking Table Tests of Large-Panel Precast Concrete Building System Assemblages," by Oliva, M.G. and Clough, R.W., June 1983, (PB86 110 210/AS)A11.

UCB/EERC-83/15 "Seismic Behavior of Active Beam Links in Eccentrically Braced Frames," by Hjelmstad, K.D. and Popov, E.P., July 1983, (PB84 119 676)A09.

UCB/EERC-83/16 "System Identification of Structures with Joint Rotation," by Dimsdale, J.S., July 1983, (PB84 192 210)A06.

UCB/EERC-83/17 "Construction of Inelastic Response Spectra for Single-Degree-of-Freedom Systems," by Mahin, S. and Lin, J., June 1983, (PB84 208 834)A05.

UCB/EERC-83/18 "Interactive Computer Analysis Methods for Predicting the Inelastic Cyclic Behaviour of Structural Sections," by Kaba, S. and Mahin, S., July 1983, (PB84 192 012)A06.

UCB/EERC-83/19 "Effects of Bond Deterioration on Hysteretic Behavior of Reinforced Concrete Joints," by Filippou, F.C., Popov, E.P. and Bertero, V.V., August 1983, (PB84 192 020)A10.

UCB/EERC-83/20 "Correlation of Analytical and Experimental Responses of Large-Panel Precast Building Systems," by Oliva, M.G., Clough, R.W., Velkov, M. and Gavrilovic, P., May 1988.

UCB/EERC-83/21 "Mechanical Characteristics of Materials Used in a 1/5 Scale Model of a 7-Story Reinforced Concrete Test Structure," by Bertero, V.V., Aktan, A.E., Harris, H.G. and Chowdhury, A.A., October 1983, (PB84 193 697)A05.

UCB/EERC-83/22 "Hybrid Modelling of Soil-Structure Interaction in Layered Media," by Tzong, T.-J. and Penzien, J., October 1983, (PB84 192 178)A08.

UCB/EERC-83/23 "Local Bond Stress-Slip Relationships of Deformed Bars under Generalized Excitations," by Eligehausen, R., Popov, E.P. and Bertero, V.V., October 1983, (PB84 192 848)A09.

UCB/EERC-83/24 "Design Considerations for Shear Links in Eccentrically Braced Frames," by Malley, J.O. and Popov, E.P., November 1983, (PB84 192 186)A07.

UCB/EERC-84/01 "Pseudodynamic Test Method for Seismic Performance Evaluation: Theory and Implementation," by Shing, P.-S.B. and Mahin, S.A., January 1984, (PB84 190 644)A08.

UCB/EERC-84/02 "Dynamic Response Behavior of Kiang Hong Dian Dam," by Clough, R.W., Chang, K.-T., Chen, H.-Q. and Stephen, R.M., April 1984, (PB84 209 402)A08.

UCB/EERC-84/03 "Refined Modelling of Reinforced Concrete Columns for Seismic Analysis," by Kaba, S.A. and Mahin, S.A., April 1984, (PB84 234 384)A06.

UCB/EERC-84/04 "A New Floor Response Spectrum Method for Seismic Analysis of Multiply Supported Secondary Systems," by Asfura, A. and Der Kiureghian, A., June 1984, (PB84 239 417)A06.

UCB/EERC-84/05 "Earthquake Simulation Tests and Associated Studies of a 1/5th-scale Model of a 7-Story R/C Frame-Wall Test Structure," by Bertero, V.V., Aktan, A.E., Charney, F.A. and Sause, R., June 1984, (PB84 239 409)A09.

UCB/EERC-84/06 "R/C Structural Walls: Seismic Design for Shear," by Aktan, A.E. and Bertero, V.V., 1984.

UCB/EERC-84/07 "Behavior of Interior and Exterior Flat-Plate Connections subjected to Inelastic Load Reversals," by Zee, H.L. and Moehle, J.P., August 1984, (PB86 117 629/AS)A07.

UCB/EERC-84/08 "Experimental Study of the Seismic Behavior of a Two-Story Flat-Plate Structure," by Moehle, J.P. and Diebold, J.W., August 1984, (PB86 122 553/AS)A12.

UCB/EERC-84/09 "Phenomenological Modeling of Steel Braces under Cyclic Loading," by Ikeda, K., Mahin, S.A. and Dermitzakis, S.N., May 1984, (PB86 132 198/AS)A08.

UCB/EERC-84/10 "Earthquake Analysis and Response of Concrete Gravity Dams," by Fenves, G. and Chopra, A.K., August 1984, (PB85 193 902/AS)A11.

UCB/EERC-84/11 "EAGD-84: A Computer Program for Earthquake Analysis of Concrete Gravity Dams," by Fenves, G. and Chopra, A.K., August 1984, (PB85 193 613/AS)A05.

UCB/EERC-84/12 "A Refined Physical Theory Model for Predicting the Seismic Behavior of Braced Steel Frames," by Ikeda, K. and Mahin, S.A., July 1984, (PB85 191 450/AS)A09.

UCB/EERC-84/13 "Earthquake Engineering Research at Berkeley - 1984," by , August 1984, (PB85 197 341/AS)A10.

UCB/EERC-84/14 "Moduli and Damping Factors for Dynamic Analyses of Cohesionless Soils," by Seed, H.B., Wong, R.T., Idriss, I.M. and Tokimatsu, K., September 1984, (PB85 191 468/AS)A04.

UCB/EERC-84/15 "The Influence of SPT Procedures in Soil Liquefaction Resistance Evaluations," by Seed, H.B., Tokimatsu, K., Harder, L.F. and Chung, R.M., October 1984, (PB85 191 732/AS)A04.

UCB/EERC-84/16 "Simplified Procedures for the Evaluation of Settlements in Sands Due to Earthquake Shaking," by Tokimatsu, K. and Seed, H.B., October 1984, (PB85 197 887/AS)A03.

UCB/EERC-84/17 "Evaluation of Energy Absorption Characteristics of Bridges under Seismic Conditions," by Imbsen, R.A. and Penzien, J., November 1984.

UCB/EERC-84/18 "Structure-Foundation Interactions under Dynamic Loads," by Liu, W.D. and Penzien, J., November 1984, (PB87 124 889/AS)A11.

UCB/EERC-84/19 "Seismic Modelling of Deep Foundations," by Chen, C.-H. and Penzien, J., November 1984, (PB87 124 798/AS)A07.

UCB/EERC-84/20 "Dynamic Response Behavior of Quan Shui Dam," by Clough, R.W., Chang, K.-T., Chen, H.-Q., Stephen, R.M., Ghanaat, Y. and Qi, J.-H., November 1984, (PB86 115177/AS)A07.

UCB/EERC-85/01 "Simplified Methods of Analysis for Earthquake Resistant Design of Buildings," by Cruz, E.F. and Chopra, A.K., February 1985, (PB86 112299/AS)A12.

UCB/EERC-85/02 "Estimation of Seismic Wave Coherency and Rupture Velocity using the SMART 1 Strong-Motion Array Recordings," by Abrahamson, N.A., March 1985, (PB86 214 343)A07.

UCB/EERC-85/03 "Dynamic Properties of a Thirty Story Condominium Tower Building," by Stephen, R.M., Wilson, E.L. and Stander, N., April 1985, (PB86 118965/AS)A06.

UCB/EERC-85/04 "Development of Substructuring Techniques for On-Line Computer Controlled Seismic Performance Testing," by Dermitzakis, S. and Mahin, S., February 1985, (PB86 132941/AS)A08.

UCB/EERC-85/05 "A Simple Model for Reinforcing Bar Anchorages under Cyclic Excitations," by Filippou, F.C., March 1985, (PB86 112 919/AS)A05.

UCB/EERC-85/06 "Racking Behavior of Wood-framed Gypsum Panels under Dynamic Load," by Oliva, M.G., June 1985.

UCB/EERC-85/07 "Earthquake Analysis and Response of Concrete Arch Dams," by Fok, K.-L. and Chopra, A.K., June 1985, (PB86 139672/AS)A10.

UCB/EERC-85/08 "Effect of Inelastic Behavior on the Analysis and Design of Earthquake Resistant Structures," by Lin, J.P. and Mahin, S.A., June 1985, (PB86 135340/AS)A08.

UCB/EERC-85/09 "Earthquake Simulator Testing of a Base-Isolated Bridge Deck," by Kelly, J.M., Buckle, I.G. and Tsai, H.-C., January 1986, (PB87 124 152/AS)A06.

UCB/EERC-85/10 "Simplified Analysis for Earthquake Resistant Design of Concrete Gravity Dams," by Fenves, G. and Chopra, A.K., June 1986, (PB87 124 160/AS)A08.

UCB/EERC-85/11 "Dynamic Interaction Effects in Arch Dams," by Clough, R.W., Chang, K.-T., Chen, H.-Q. and Ghanaat, Y., October 1985, (PB86 135027/AS)A05.

UCB/EERC-85/12 "Dynamic Response of Long Valley Dam in the Mammoth Lake Earthquake Series of May 25-27, 1980," by Lai, S. and Seed, H.B., November 1985, (PB86 142304/AS)A05.

UCB/EERC-85/13 "A Methodology for Computer-Aided Design of Earthquake-Resistant Steel Structures," by Austin, M.A., Pister, K.S. and Mahin, S.A., December 1985, (PB86 159480/AS)A10 .

UCB/EERC-85/14 "Response of Tension-Leg Platforms to Vertical Seismic Excitations," by Liou, G.-S., Penzien, J. and Yeung, R.W., December 1985, (PB87 124 871/AS)A08.

UCB/EERC-85/15 "Cyclic Loading Tests of Masonry Single Piers: Volume 4 - Additional Tests with Height to Width Ratio of 1," by Sveinsson, B., McNiven, H.D. and Sucuoglu, H., December 1985.

UCB/EERC-85/16 "An Experimental Program for Studying the Dynamic Response of a Steel Frame with a Variety of Infill Partitions," by Yanev, B. and McNiven, H.D., December 1985.

UCB/EERC-86/01 "A Study of Seismically Resistant Eccentrically Braced Steel Frame Systems," by Kasai, K. and Popov, E.P., January 1986, (PB87 124 178/AS)A14.

UCB/EERC-86/02 "Design Problems in Soil Liquefaction," by Seed, H.B., February 1986, (PB87 124 186/AS)A03.

UCB/EERC-86/03 "Implications of Recent Earthquakes and Research on Earthquake-Resistant Design and Construction of Buildings," by Bertero, V.V., March 1986, (PB87 124 194/AS)A05.

UCB/EERC-86/04 "The Use of Load Dependent Vectors for Dynamic and Earthquake Analyses," by Leger, P., Wilson, E.L. and Clough, R.W., March 1986, (PB87 124 202/AS)A12.

UCB/EERC-86/05 "Two Beam-To-Column Web Connections," by Tsai, K.-C. and Popov, E.P., April 1986, (PB87 124 301/AS)A04.

UCB/EERC-86/06 "Determination of Penetration Resistance for Coarse-Grained Soils using the Becker Hammer Drill," by Harder, L.F. and Seed, H.B., May 1986, (PB87 124 210/AS)A07.

UCB/EERC-86/07 "A Mathematical Model for Predicting the Nonlinear Response of Unreinforced Masonry Walls to In-Plane Earthquake Excitations," by Mengi, Y. and McNiven, H.D., May 1986, (PB87 124 780/AS)A06.

UCB/EERC-86/08 "The 19 September 1985 Mexico Earthquake: Building Behavior," by Bertero, V.V., July 1986.

UCB/EERC-86/09 "EACD-3D: A Computer Program for Three-Dimensional Earthquake Analysis of Concrete Dams," by Fok, K.-L., Hall, J.F. and Chopra, A.K., July 1986, (PB87 124 228/AS)A08.

UCB/EERC-86/10 "Earthquake Simulation Tests and Associated Studies of a 0.3-Scale Model of a Six-Story Concentrically Braced Steel Structure," by Uang, C.-M. and Bertero, V.V., December 1986, (PB87 163 564/AS)A17.

UCB/EERC-86/11 "Mechanical Characteristics of Base Isolation Bearings for a Bridge Deck Model Test," by Kelly, J.M., Buckle, I.G. and Koh, C.-G., 1987.

UCB/EERC-86/12 "Effects of Axial Load on Elastomeric Isolation Bearings," by Koh, C.-G. and Kelly, J.M., November 1987.

UCB/EERC-87/01 "The FPS Earthquake Resisting System: Experimental Report," by Zayas, V.A., Low, S.S. and Mahin, S.A., June 1987.

UCB/EERC-87/02 "Earthquake Simulator Tests and Associated Studies of a 0.3-Scale Model of a Six-Story Eccentrically Braced Steel Structure," by Whittaker, A., Uang, C.-M. and Bertero, V.V., July 1987.

UCB/EERC-87/03 "A Displacement Control and Uplift Restraint Device for Base-Isolated Structures," by Kelly, J.M., Griffith, M.C. and Aiken, I.D., April 1987.

UCB/EERC-87/04 "Earthquake Simulator Testing of a Combined Sliding Bearing and Rubber Bearing Isolation System," by Kelly, J.M. and Chalhoub, M.S., 1987.

UCB/EERC-87/05 "Three-Dimensional Inelastic Analysis of Reinforced Concrete Frame-Wall Structures," by Moazzami, S. and Bertero, V.V., May 1987.

UCB/EERC-87/06 "Experiments on Eccentrically Braced Frames with Composite Floors," by Ricles, J. and Popov, E., June 1987.

UCB/EERC-87/07 "Dynamic Analysis of Seismically Resistant Eccentrically Braced Frames," by Ricles, J. and Popov, E., June 1987.

UCB/EERC-87/08 "Undrained Cyclic Triaxial Testing of Gravels-The Effect of Membrane Compliance," by Evans, M.D. and Seed, H.B., July 1987.

UCB/EERC-87/09 "Hybrid Solution Techniques for Generalized Pseudo-Dynamic Testing," by Thewalt, C. and Mahin, S.A., July 1987.

UCB/EERC-87/10 "Ultimate Behavior of Butt Welded Splices in Heavy Rolled Steel Sections," by Bruneau, M., Mahin, S.A. and Popov, E.P., July 1987.

UCB/EERC-87/11 "Residual Strength of Sand from Dam Failures in the Chilean Earthquake of March 3, 1985," by De Alba, P., Seed, H.B., Retamal, E. and Seed, R.B., September 1987.

UCB/EERC-87/12 "Inelastic Seismic Response of Structures with Mass or Stiffness Eccentricities in Plan," by Bruneau, M. and Mahin, S.A., September 1987.

UCB/EERC-87/13 "CSTRUCT: An Interactive Computer Environment for the Design and Analysis of Earthquake Resistant Steel Structures," by Austin, M.A., Mahin, S.A. and Pister, K.S., September 1987.

UCB/EERC-87/14 "Experimental Study of Reinforced Concrete Columns Subjected to Multi-Axial Loading," by Low, S.S. and Moehle, J.P., September 1987.

UCB/EERC-87/15 "Relationships between Soil Conditions and Earthquake Ground Motions in Mexico City in the Earthquake of Sept. 19, 1985," by Seed, H.B., Romo, M.P., Sun, J., Jaime, A. and Lysmer, J., October 1987.

UCB/EERC-87/16 "Experimental Study of Seismic Response of R. C. Setback Buildings," by Shahrooz, B.M. and Moehle, J.P., October 1987.

UCB/EERC-87/17 "The Effect of Slabs on the Flexural Behavior of Beams," by Pantazopoulou, S.J. and Moehle, J.P., October 1987.

UCB/EERC-87/18 "Design Procedure for R-FBI Bearings," by Mostaghel, N. and Kelly, J.M., November 1987.

UCB/EERC-87/19 "Analytical Models for Predicting the Lateral Response of R C Shear Walls: Evaluation of their Reliability," by Vulcano, A. and Bertero, V.V., November 1987.

UCB/EERC-87/20 "Earthquake Response of Torsionally-Coupled Buildings," by Hejal, R. and Chopra, A.K., December 1987.

UCB/EERC-87/21 "Dynamic Reservoir Interaction with Monticello Dam," by Clough, R.W., Ghanaat, Y. and Qiu, X-F., December 1987.

UCB/EERC-87/22 "Strength Evaluation of Coarse-Grained Soils," by Siddiqi, F.H., Seed, R.B., Chan, C.K., Seed, H.B. and Pyke, R.M., December 1987.

UCB/EERC-88/01 "Seismic Behavior of Concentrically Braced Steel Frames," by Khatib, I., Mahin, S.A. and Pister, K.S., January 1988.

UCB/EERC-88/02 "Experimental Evaluation of Seismic Isolation of Medium-Rise Structures Subject to Uplift," by Griffith, M.C., Kelly, J.M., Coveney, V.A. and Koh, C.G., January 1988.

UCB/EERC-88/03 "Cyclic Behavior of Steel Double Angle Connections," by Astaneh-Asl, A. and Nader, M.N., January 1988.

UCB/EERC-88/04 "Re-evaluation of the Slide in the Lower San Fernando Dam in the Earthquake of Feb. 9, 1971," by Seed, H.B., Seed, R.B., Harder, L.F. and Jong, H.-L., April 1988.

UCB/EERC-88/05 "Experimental Evaluation of Seismic Isolation of a Nine-Story Braced Steel Frame Subject to Uplift," by Griffith, M.C., Kelly, J.M. and Aiken, I.D., May 1988.

UCB/EERC-88/06 "DRAIN-2DX User Guide.," by Allahabadi, R. and Powell, G.H., March 1988.

UCB/EERC-88/07 "Cylindrical Fluid Containers in Base-Isolated Structures," by Chalhoub, M.S. and Kelly, J.M. , April 1988.

UCB/EERC-88/08 "Analysis of Near-Source Waves: Separation of Wave Types using Strong Motion Array Recordings," by Darragh, R.B., June 1988.

UCB/EERC-88/09 "Alternatives to Standard Mode Superposition for Analysis of Non-Classically Damped Systems," by Kusainov, A.A. and Clough, R.W., June 1988.

UCB/EERC-88/10 "The Landslide at the Port of Nice on October 16, 1979," by Seed, H.B., Seed, R.B., Schlosser, F., Blondeau, F. and Juran, I., June 1988.

UCB/EERC-88/11 "Liquefaction Potential of Sand Deposits Under Low Levels of Excitation," by Carter, D.P. and Seed, H.B., August 1988.

UCB/EERC-88/12 "Nonlinear Analysis of Reinforced Concrete Frames Under Cyclic Load Reversals," by Filippou, F.C. and Issa, A., September 1988.

UCB/EERC-88/13 "Implications of Recorded Earthquake Ground Motions in Seismic Design of Building Structures," by Uang, C.-M. and Bertero, V.V., November 1988.

increase proportionally with increasing displacement ductility ratio (Fig. 3.6.)

(3) Estimates of upper and lower bounds for the drift index for multi-story buildings have been derived for a constant displacement ductility ratio. The lower bound for the drift index (corresponding to a uniform drift index distribution) may control the design of structures in the short period range. The upper bound for the drift index (corresponding to the formation of a soft bottom story) becomes increasingly critical with increasing period.

(4) An upper bound has been derived for C_y on the basis of constant displacement ductility and code drift limits. Drift limit usually does not control the design for long period structures ($T > 1.5$ sec) if soft story mechanisms can be avoided. For short period structures subjected to earthquakes with severe accceleration pulses (i.e., pulses with large peak ground acceleration, say in excess of 0.4g, and long duration) the ductility ratio that can be used should be limited. In this case, the use of a large ductility ratio to reduce seismic design forces leads to excessive drift indices. The use of a constant displacement ductility ratio to construct design spectra cannot be justified from the viewpoint of drift control.

(5) One significant disadvantage of seismic resistance (C_y) spectra is that the effect of strong motion duration is not considered. The energy demands associated with a long duration earthquake record may be very large and a design based only on C_y may not be conservative. A study of this conventional way of constructing an inelastic design response spectrum suggests that other controlling factors must be considered.

(6) While the linear elastic pseudo-velocity spectra S_{pv} can be used to obtain a lower bound to the equivalent input energy V_I spectra, they may significantly underestimate the true energy input.

(7) Although the equivalent hysteretic energy V_H spectra are in general in close agreement with the S_{pv} spectra, the S_{pv} spectra may significantly underestimate the V_H spectra in the case of long duration strong ground shaking such as CH and MX.

(8) While a variation in the value of damping ratio affects the response of linear elastic structures considerably, this variation has only minor effects on the required yielding strength C_y as well as on the hysteretic energy of yielding structures.

3.10. Possible Parameters to Construct Inelastic Spectra

In the previous sections all the inelastic response spectra were calculated on the basis of a constant displacement ductility ratio. The use of displacement ductility as a damage criterion is reasonable from two perspectives: (i) it not only allows the structural damage to be controlled, but it also allows damage to deformation-sensitive nonstructural components to be controlled; and (ii) it allows the undesirable effects of geometric nonlinearities to be controlled. However, using seismic resistance spectra (C_y spectra) based on a constant ductility ratio for design purposes may be inadequate because other failure modes may control. Damage criteria should ideally reflect the following important parameters:

(1) The energy dissipation capacity of both the structural members and the entire structural systems;

(2) Cyclic ductility demand due to repeated bursts of large energy input in an earthquake record.

Use of these parameters to establish damage criteria requires identification of the acceptable levels of hysteretic energy dissipation capacity and cyclic ductility of structural elements, structural systems, and of entire soil-foundation-superstructure and non-structural component system.

The high hysteretic energy demanded by MX (Fig. 3.13), based on a constant ductility ratio, is a good example to demonstrate the need for establishing damage criteria that include energy dissipation demand.

Previous researchers [5,22] have proposed that the energy dissipation capacity of a structure under cyclic excitation be estimated directly from its response under monotonic loading. The energy dissipation capacity of a structure under monotonic loading is usually well defined.[12,20] Other researchers have found that energy dissipation capacity is not constant and varies with the amplitudes of the inelastic deformation and loading or deformation paths as shown by the following results obtained by Bertero *et al.*;[9] Fig. 3.17 shows results of steel beams tested under yielding reversals. By ignoring strain hardening and Bauschinger effects, the moment-curvature curve under cyclic loading can be idealized as shown in Fig. 3.18; these two factors tend to compensate each other from the standpoint of energy dissipation. The dissipated energy per unit length, e_d, is the area enclosed by the hysteresis loop: